TRPV4 IN VENTILATOR-INDUCED LUNG INJURY

–

MECHANISMS OF ENDOTHELIAL MECHANOTRANSDUCTION AND BARRIER REGULATION IN THE LUNG

Dissertation to obtain the academic degree

Doctor rerum naturalium (Dr. rer. nat.)

Submitted to the Department of Biology, Chemistry and Pharmacy

of the Freie Universität Berlin

by

Laura Michalick

from Bautzen

2016

This work has been prepared in the period from March 2011 to December 2016 under supervision of Prof. Dr. Wolfgang M. Kübler.

1st reviewer: Prof. Dr. Wolfgang M. Kübler,

Charité – Universitätsmedizin Berlin

2nd reviewer: Prof. Dr. Petra Knaus,

Freie Universität Berlin

Disputation on 12.05.2017

INDEX

LIST OF FIGURES

LIST OF TABLES

LIST OF ACRONYMS

4αPDD	4α-phorbol 12,13-didecanoate
AIP4	E3 ubiquitin-protein ligase
ANK	Ankyrin repeats
AKAP79/150	A-kinase anchor protein 79/150
ARDS	Acute respiratry distress syndrom
AT1aR	Angiotensin II receptor subtype 1a
BALF	Bronchoalveolar lavage fluid
BK	Big Ca^{2+}-activated K^+ channel
bw	Body weight
$[Ca^{2+}]_i$	Intracellular calcium
CaM	Calmodulin
CaMBD	Calmodulin binding domain
$CPAP_{high}$	High continious positive airway pressure
$CPAP_{low}$	Low continious positive airway pressure
c-Src kinase	Cellular sarcoma kinase
DAPI	4',6-Diamidino-2-phenylindole
EETs	Epoxyeicosatrienoic acids
EMP	Endothelial-derived microparticles
ENaC	Epithelial Na^+ channel
Fura2-AM	Fura-2-acetoxymethyl ester
HSA	Human serum albumin
HETEs	Hydroxyeicosatetraenoic acid
HV_T	High tidal volume
IK	Intermediate Ca^{2+}-activated K^+ channel
IP_3	Inositol trisphosphate
KO	Knockout
LV_T	Low tidal volume
MLC-2	Myosin regulatory light-chain type 2
MLCK	Myosin light-chain kinase
MLCP	Myosin light-chain phosphatase
MP	Microparticles
NFκB	nuclear factor kappa-light-chain-enhancer of activated B-cells
NGF	Nerve growth factor
NLS	Nuclear localization sequence

ORAI1	Calcium release-activated calcium channel protein 1
OS-9	Osteosarcoma amplified 9/endoplasmic reticulum lectin
PACSIN-3	Protein kinase C and casein kinase substrate in neurons protein 3
PBS	Phosphate-buffered saline
PC	phosphatidylcholine
PDK1	Pyruvate dehydrogenase kinase 1
PE	phosphatidylethanolamine
$PI(4,5)P_2$	Phosphatidylinositol 4,5-bisphosphate
PIBS	$PI(4,5)P_2$ binding site
PLA	Proximity ligation assay
PRD	Proline-rich domain
PS	phosphatidylserine
RGD	Arg-Gly-Asp amino acid sequence
RIPA	Radioimmunoprecipitation assay
ROMK	Renal Outer Medullary Potassium K^+ channel
SGK1	Serum glucocorticoid-regulated kinase 1
SK	Small Ca^{2+}-activated K^+ channel
STIM1	Stromal interaction molecule 1
TBS	Tris-buffered saline
TRPV1	Transient receptor potential vanilloid type 1 channel
TRPV4	Transient receptor potential vanilloid type 4 channel
VE-cadherin	Vascular endothelial cadherin
VILI	Ventilator-induced lung injury
WNK1	With-no-lysine kinase 1
WNK4	With-no-lysine kinase 4
WT	Wild type

1 ABSTRACT

Acute respiratory failure (ARDS) represents a serious health problem in the western civilization with a high incidence and mortality. In ARDS, mechanical ventilation is the only life-saving treatment. However, long term mechanical ventilation can cause adverse side effects and resulting mechanical forces at the parenchymal level, respectively, can damage the lung by causing alveolar-capillary barrier failure and edema formation. Yet, the exact mechanisms underlying the transduction of these mechanical forces at the microvascular barrier are at present still unclear. The Ca^{2+} permeable, mechanosensitive transient receptor potential vanilloid 4 (TRPV4) cation channel presents a particularly attractive candidate in transmission of mechanical forces into inflammatory or apoptotic cell responses.

The current work provides a new insight into the cellular mechanotransduction cascade that underlies, in that TRPV4 acting as the central mechanosensor in this scenario, is activated by mechanical stretch and concomitant by phosphorylation through serum glucocorticoid-regulated kinase 1 (SGK1). As a consequence of TRPV4-mediated Ca^{2+} influx, the elevated levels of intracellular Ca^{2+} lead to opening of Ca^{2+}-activated K^+ channels, followed by hyperpolarization of the plasma membrane. In my thesis, I could further show that inhibition of Ca^{2+}-activated K^+ channels leads to less Ca^{2+} influx and stabilizes the endothelial barrier, suggesting a positive feedback on TRPV4 activity by membrane hyperpolarization. In addition, I provide in this work evidence for the existence of a new heteromeric TRP channel complex consisting of TRPV4 and TRPV1 in which TRPV1 is an amplifier of the endothelial Ca^{2+} response to mechanical stress. Furthermore, I found that release of endothelial microparticles is induced by strong cyclic stretch, and in turn could be attenuated by inhibition of the SGK1/TRPV4 and TRPV1/TRPV4 signaling axes.

My findings focus attention on TRPV4-dependent and mechanosensitive dysregulation of endothelial barrier integrity in response to excessive mechanical stretch. TRPV4 is supposed to be the direct and central mediator of ventilator-induced lung injury, and its upstream and downstream effectors may present novel targets in pharmacological approaches to reduce the risk for developing lung injury and systemic organ failure in mechanically ventilated patients.

KURZFASSUNG

Das Syndrom des akuten Lungenversagens (ARDS) stellt durch hohe Inzidenz und Mortalität ein schwerwiegendes Gesundheitsproblem der westlichen Zivilisation dar. Hierbei stellt mechanische Beatmung die einzige lebensrettende Behandlung dar. Eine längerfristige mechanische Beatmung kann jedoch zu unerwünschten Nebenwirkungen führen, insofern als die entstehenden mechanischen Kräfte auf parenchymaler Ebene zum Versagen der alveolar-kapillären Barriere und Ödembildung und damit zu einer schwerwiegenden Schädigung der Lunge führen können. Die genauen Mechanismen, die dieser Transduktion von mechanischen Kräften an der mikrovaskulären Barriere zugrunde liegen, sind derzeit noch unklar. Der Ca^{2+} permeable, mechanosensitive „Transient Receptor Potential Vanilloid-4“ (TRPV4) Kationenkanal stellt einen besonders attraktiven Kandidaten bei der Übertragung mechanischer Kräfte in entzündliche oder apoptotische zelluläre Antworten dar.

Die aktuelle Arbeit offenbart einen neuen Einblick in die zelluläre Mechanotransduktionskaskade beim Beatmungs-induzierten Lungenschaden, in der TRPV4, der zentrale Mechanosensor in diesem Szenario, durch mechanische Dehnung und gleichzeitige Phosphorylierung via Serum Glukokortikoid-regulierter Kinase 1 (SGK1) aktiviert wird. Als Folge des TRPV4-vermittelten Ca^{2+} Einstroms führen die erhöhten Konzentrationen an intrazellulärem Ca^{2+} zur Öffnung von Ca^{2+}-aktivierten K^+ Kanälen, was wiederum zu einer Hyperpolarisation der Plasmamembran führt. In der vorliegenden Arbeit konnte ich ferner zeigen, dass die Hemmung von Ca^{2+}-aktivierten K^+ Kanälen zu weniger Ca^{2+} Einstrom und zu einer Stabilisierung der Endothelbarriere führt, was auf ein positives Feedback auf die Aktivität von TRPV4 durch eine Membranhyperpolarisation hindeutet. Darüber hinaus liefere ich in dieser Arbeit Hinweise auf die Existenz eines neuen heteromeren TRP Kanalkomplexes bestehend aus TRPV4 und TRPV1, in dem TRPV1 als Verstärker der Ca^{2+}-Antwort auf mechanischen Stress fungiert. Zudem konnte ich nachweisen, dass durch starke zyklische Dehnung die Freisetzung von endothelialen Mikropartikeln angeregt wird, die wiederum durch die Hemmung der SGK1/TRPV4 und TRPV1/TRPV4 Signalachsen vermindert wird.

Meine Ergebnisse lenken den Fokus auf die TRPV4-abhängige und mechanosensitive Dysregulation der endothelialen Barriere-Integrität als Antwort auf exzessive mechanische Dehnung. TRPV4 wird als der direkte und zentrale Regulator des beatmungsinduzierten Lungenschadens identifiziert, und seine stromaufwärts und -abwärts gelegenen Effektoren könnten neue Ziele für pharmakologische Ansätze darstellen, die das Risiko für mechanisch-beatmete Patienten, einen Lungenschaden und systemisches Organversagen zu entwickeln, vermindern könnten.

2 INTRODUCTION

2.1 MECHANICAL VENTILATION

Acute respiratory distress syndrome (ARDS) is defined as acute and diffuse inflammatory lung injury, which leads to increased pulmonary vascular permeability, increased lung weight, bilateral radiographic opacities and cumulating in a loss of aerated lung tissue by increased physiological dead space, hypoxemia and decreased lung compliance (ARDS Definition Task Force et al., 2012). In 1967 Ashbaugh and colleagues first described the acute respiratory distress syndrome (ARDS) as manifestation of hypoxemia, loss of compliance, bilateral alveolar infiltrates, interstitial and intra-alveolar hemorrhages, increased levels of alveolar macrophages, and edema (Ashbaugh et al., 1967). ARDS can be caused by several direct and indirect risk factors like pneumonia, aspiration of gastric contents or multiple trauma. In acute respiratory failure (ARDS) mechanical ventilation is the only life-saving treatment. However, long term mechanical ventilation has also critical adverse effects, in that, it can cause vascular barrier dysfunction, fluid extravasation, edema formation, leukocyte recruitment, impaired pulmonary gas exchange, local inflammation and systemic release of pro-inflammatory cytokines, which ultimately lead to dysfunction of distal organs and multiple organ failure (Figure 1) (Ricard and Dreyfuss, 2001; Ricard et al., 2002; Volpin et al., 2014), and is described as ventilator-induced lung injury (VILI).

VILI was initially thought to be a result of excessive volumes and pressures, which occur locally during mechanical ventilation and leads to the rupture of the lung parenchyma. This rupture by excessive volumes or pressures is described as volu- or barotrauma (Dreyfuss and Saumon, 1998; Mead et al., 1970). Over the past decades, it has become clear that within the limits of clinically relevant ventilation pressures and tidal volumes, VILI is mainly the consequence of activation pro-inflammatory and mechanosensitve signaling cascades at the alveolo-capillary barrier. In ventilated patients, the global tidal volumes do normally not exceed values of 10 mL/kg, but in contrast, regional tidal volumes surpass values of 20 mL/kg body weight and result in a massive lung overdistension of these areas (Bone, 1993). This heterogenous distribution of the inspired tidal volumes is caused by alveolar collapse and fluid extravasation in the injured regions, which in turn only receive a small fraction of the total tidal volume and the majority of the tidal volume will be delivered to the non-injured areas with relatively normal (lower compared to injured areas) compliance. For this reason, the actual ventilated lung volume of lungs of ARDS patients has shown to be small as described by Gattinoni and Pesenti in their "baby lung concept" (Gattinoni and Pesenti, 2005). A recent study confirmed this concept by showing that the volume increase during recruitment maneuvers by holding the breath for 30 sec at 40 cmH_2O was one third of the predicted lung volume (Beitler et al., 2016). This indicates that two thirds of the predicted lung volume are not ventilated during mechanical ventilation, and the residual one third is ventilated a volume three-fold higher as intended. Based on these findings, the

effective tidal volume in the ventilated lung areas will be approximately 20 mL/kg, based on the most common ventilation strategy of 7 mL/kg body weight (Bellani et al., 2016). The resulting biotrauma (Slutsky, 2005) is defined by failure of the alveolo-capillary barrier and an inflammatory response that comprises the infiltration of immune cells and the release of cytokines and damage-associated molecular patterns (DAMPs) into the circulating blood (Tremblay et al., 1997; Ricard and Dreyfuss, 2001; Stüber et al., 2002; Volpin et al., 2014), which then again drive the systemic propagation of the injury that ultimately cumulates in multiple organ failure. ARDS is associated with an considerable mortality that correlates with disease severity (35% among those with mild ARDS, 40% for those with moderate disease and 46% for patients with severe ARDS, as recently reported by (Bellani et al., 2016). Currently, there are several approaches to minimize the burden of long-term ventilation in ICU clinical trials, like diminishing of the inflated tidal volume or inspiratory pressure (ARDSNetwork, 2000), recruitment maneuvers to ensure an "open lung" (Meade et al., 2008) and prone-positioning instead of supine-positioning (Broccard et al., 2000; Guérin et al., 2013; Park et al., 2015). In spite of this well characterized pathology, the exact mechanisms underlying mechanotransduction at the alveolo-capillary barrier in VILI remain still unclear.

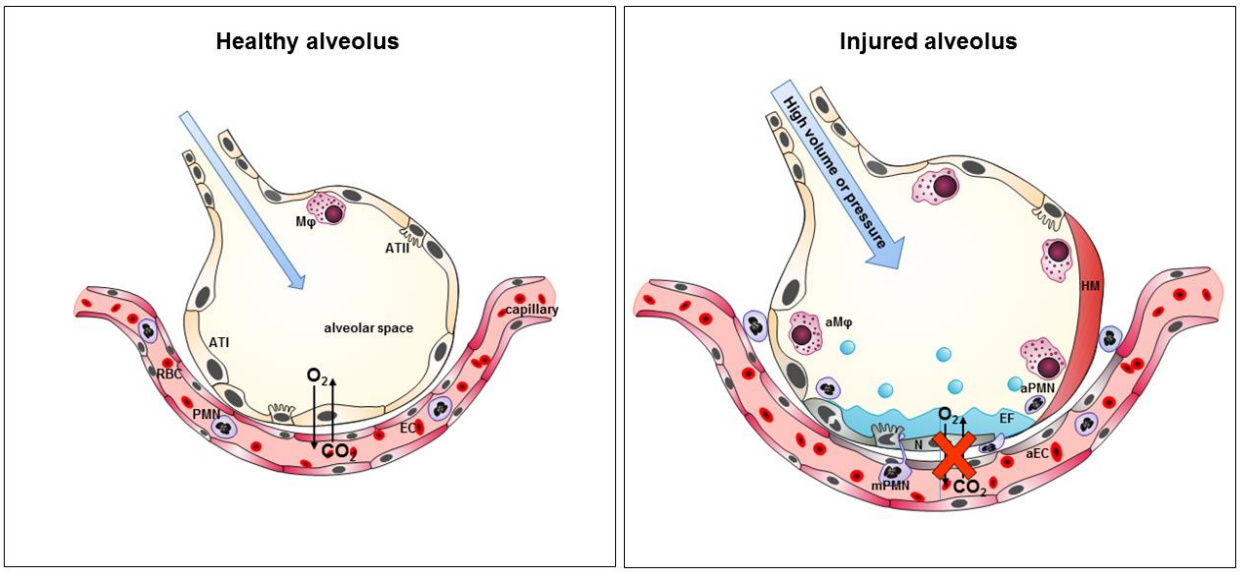

Figure 1: Scheme of alveolar-capillary function and dysfunction in response to mechanical stimuli such as ventilation with high volumes or pressures leading to impaired gas exchange. Abbreviations (left): ATI = alveolar type 1 cells; ATII = alveolar type 2 cells, EC = endothelial cells; Mφ = macrophages; PMN = neutrophils; RBCs = red blood cells. Abbreviations (right): aEC = activated endothelial cells; aMφ = activated macrophages; EF = edema fluid; HM = hyaline membranes; mPMN = migrating neutrophils; N = necrotic cells and tissue.

2.2 THE ENDOTHELIAL BARRIER

The endothelial barrier is composed of a monolayer of vascular endothelial cells separating the luminal from the abluminal space. The critical properties of the endothelial barrier are the maintenance of the trans-endothelial fluid balance as well as the regulation of protein extravasation and migration of immune cells between intra- and extravascular space. This regulation is a fine-tuned machinery of vesicular transcytosis, cell-cell junctions, focal adhesions, and the cytoskeleton (Yuan and Rigor, 2010). First, endothelial barrier function is regulated through transcellular transport of water and macromolecules via transcytosis, which combines endo- and exocytotic processes. These endo- and exocytosis processes are located in hotspots and are endothelial-selective lipid raft domains, which form cave-like invaginations of the plasma membrane – the caveolae (Predescu and Palade, 1993; Simons and Ikonen, 1997; Predescu et al., 2007). At the apical plasmamembrane, caveolae can endocytose substantial volumes of water and macromolecules such as albumin which – following their transcellular transport - are in turn exocytosed at the basolateral site. Series of partially fused caveolae are capable to form transcellular pores, the vesiculo-vacuolar organelles (Dvorak et al., 1996; Predescu et al., 2007). Additionally, endothelial cells express aquaporins, which support transendothelial water transport (Effros et al., 1997; Verkman et al., 2000).

Second, the endothelial barrier function can be regulated through inter-endothelial junctions consisting of gap junctions, adherens and tight junctions (Mehta and Malik, 2006; Komarova et al., 2007; Komarova and Malik, 2010). Gap junctions are intercellular transmembane pores, which consist of six connexin subuntits and serve as mediators of intercellular signal transduction, allowing rapid transmission of small signaling molecules like Ca^{2+} (Koval and Bhattacharya, 2005). Gap junctions are not contributing directly to endothelial barrier function. They are rather indirect actors by regulation of intercellular communication and Ca^{2+} signaling. Adherens junctions, e.g. VE-cadherin, interconnect endothelial cells to a width of approximately 3 nm and as such, make it impermanent for albumin (Simionescu et al., 1978; Mehta and Malik, 2006). Interestingly, in a recent study, VE-Cadherin was shown to get internalized by c-Src-kinase phosphorylation, which ultimately reduces endothelial barrier integrity (Gavard and Gutkind, 2006; Benn et al., 2016). Tight junctions (e.g. ZO-1), which are mainly expressed in microvascular endothelial cells, mediate additional barrier function by preventing the extravasation of much smaller molecules right (< 1 kDa) up to inorganic ions, like Na^{+} (Curry, 2005). The endothelial barrier integrity varies with the tissue-specific composition of cell-cell junctions as well as moment-to-moment changes like reorganization, internalization, cytoskeletal interactions in response to mechanical stimuli, and therewith correlates with endothelial permeability.

Endothelial barrier integrity does not only depend on the tightness of the intercellular connections but also on the interaction of endothelial abluminal plasma membrane with the extracellular matrix

surrounding the microvascular wall (Wu, 2005). To this end, focal adhesions and connecting components (RGD proteins) of the extracellular matrix (ECM) connect the intracellular cytoskeleton via integrins to the extracellular matrix, whereby the binding strength is dependent on the composition of matrix proteins (Albelda et al., 1989; Luscinskas and Lawler, 1994). Integrins are localized in the plasma membrane of endothelial cells and are essential to establish and stabilize the endothelial barrier (del Zoppo and Milner, 2006). Moreover, integrins are critical mediators of endothelial mechanotransduction and modulators of vascular permeability (Ingber, 2002; Chien et al., 2005; Haase et al., 2014; Humphrey et al., 2014). Moment-to-moment changes of integrin properties induced by e.g. shear stress can reduce the focal adhesion strength and increase vascular hyperpermeability (Wu, 2005; Humphrey et al., 2014). These changes can activate on the one hand an inside-out signaling, but on the other hand also outside-in signaling, which defines the activation of intracellular pathways and recruitment of kinases like Src kinases through binding of integrins to RGD proteins (Piccardoni et al., 2004; Destaing et al., 2011). For instance, the Src-kinase PTK modulates the effect of Serum glucocorticoid-reguated Kinase 1 (SGK1) and With-no-lysine kinase 4 (WNK4) on the renal outer medullary K^+ channel (ROMK) (D.-H. Lin et al., 2015; Yue et al., 2009).

Focal adhesions are intracellularly connected to the cytoskeleton, which is composed of microtubules, intermediate filaments and actin filaments, whereby intermediate filaments such as vimentin serve as connective scaffold proteins between focal adhesions and actin cytoskeleton (McGillem and Garcia, 2005; Prasain and Stevens, 2009; Shen et al., 2009). The moment-to-moment changes of cytoskeletal structures determine cell morphology, adhesion and barrier function, according to the dynamic changes by polymerization and depolymerization. The most important structural mediator of endothelial barrier integrity and vascular hyperpermeability is actin. Under physiological conditions actin is distributed throughout the intracellular space as short filaments and diffuse actin monomers and peripheral cortical actin (Birukov, 2009; Prasain and Stevens, 2009). Under pathophysiological conditions like mechanical stretch, cytoskeletal reorganization like stress fiber formation and activation of the contractile machinery acts directly as cytoskeletal tension force on focal adhesions (inside-out signaling) and cell-cell junctions, and thereby ultimately diminishes endothelial barrier function (Birukov, 2009; Shen et al., 2009). This is controlled by the activity of myosin light chain kinase (MLCK) and its corresponding phosphatase MLCP (Garcia et al., 1995; Goeckeler and Wysolmerski, 1995). Mechanical stress elevates cytosolic calcium concentrations and thereby increases the activity of MLCK and in turn inhibits MLCP activity, which leads to an enhanced phosphorylation of Myosin light chain-2 (MLC-2) and endothelial permeability (Sheldon et al., 1993; Shen et al., 2010; Rigor et al., 2013; Kása et al., 2015). These findings are based on *in vitro* experiments from cultured endothelial cells. Cultured endothelial cells are losing their heterogeneity by losing their specific vascular beds. Under the currently prevailing cell culture conditions, endothelial cells show fundamental differences compared to *in situ* equivalents by a lack of the typical glycocalyx, differential

expression of surface proteins or loss of caveolae *in vitro* (Uhlig et al., 2014). Under *in situ* or *in vivo* conditions calcium is the major driving force of endothelial barrier regulation (Hamanaka et al., 2007; Yin et al., 2008; Samapati et al., 2012).

The microtubular system is primary responsible for mitosis, cell morphology and intracellular trafficking, but also affects the endothelial permeability by its interaction with actin filaments (McGillem and Garcia, 2005; Prasain and Stevens, 2009). The stabilization of microtubules by capping or other posttranslational modifications has been shown to protect the endothelial cells against stress fiber formation and vascular hyperpermeability (Birukova et al., 2004b; Shivanna and Srinivas, 2009). Additionally, stabilization of microtubules by cAMP, or activation of protein kinase A (PKA) has barrier protective effects by preventing stress fiber formation (Birukova et al., 2004a; Shivanna and Srinivas, 2009). Although, the exact mechanisms are well described *in vitro*, these mechanisms seem to play a minor role. *In vivo*, calcium is the only and central factor, which has been verified to regulate endothelial barrier function, suggesting that mechanosensitive calcium channels may play a major role in the regulation of endothelial barrier function (Hamanaka et al., 2007; Yin et al., 2008; Michalick et al., 2017).

2.3 THE ROLE OF TRANSIENT RECEPTOR POTENTIAL VANILLOID 4 (TRPV4) CATION CHANNEL IN VENTILATOR-INDUCED LUNG INJURY (VILI) AND ENDOTHELIAL BARRIER FAILURE

The transient receptor potential vanilloid 4 (TRPV4) cation channel is a particularly promising candidate in VILI, as it is known to be mechanosensitive and has previously been shown to be a crucial regulator in stretch-induced vascular hyperpermeability in isolated and perfused lungs (Hamanaka et al., 2007; Jian et al., 2008; Yin et al., 2008). TRPV4 is ubiquitously expressed in different pulmonary cell types, such as alveolar macrophages (Hamanaka et al., 2010; Groot-Kormelink et al., 2012), neutrophils (Yin et al., 2016), smooth muscle cells (Jia et al., 2004; Goldenberg et al., 2015b), fibroblasts (Rahaman et al., 2014; Rahman et al., 2016), epithelial cells (Nayak et al., 2015) and particularly endothelial cells (Alvarez et al., 2006), where its activation is implicated to induce inflammatory pathways in both parenchymal and immune cells (Nayak et al., 2015; Zhao et al., 2015; Yin et al., 2016). Additionally, a critical role of TRPV4 has been linked to the cellular transduction of mechanical forces, as it gets activated by cell swelling (Liedtke and Friedman, 2003a; Strotmann et al., 2003; Vriens et al., 2004; O'Neil and Heller, 2005; Wu et al., 2007; Jo et al., 2015) or surface expansion (Shin et al., 2012).

In endothelial cells, it has been shown that TRPV4 is activated by mechanical stimuli such as uniaxial and circumferential stretch or shear stress, and mediates Ca^{2+} influx into the endothelium (Hartmannsgruber et al., 2007; Loukin et al., 2010; Song et al., 2014). Following the binding to calmodulin, the increase in cytosolic Ca^{2+} concentration ($[Ca^{2+}]_i$) can increase endothelial permeability (Hamanaka et al., 2007; Yin et al., 2008; Balakrishna et al., 2014) via activation of endothelial MLCK (Parker et al., 2013). Furthermore, several studies reveal that TRPV4 interacts with other crucial regulators of endothelial barrier function, like aquaporins (AQP), cytoskeletal structures such as F-actin and microtubules, as well as key signal molecules involved in barrier regulation such as cAMP, PKA and PKC (Sidhaye et al., 2006; Fan et al., 2009; H. Peng et al., 2010; Shin et al., 2012).

TRPV4 is not only known to be mechanosensitive, but also to be a thermo-, osmo- and Ca^{2+} channel that is involved in multiple physiological mechanisms such as nociception (Alessandri-Haber et al., 2003; Y. Chen et al., 2014) and hearing (Tabuchi et al., 2005), skeletal development (Nilius and Voets, 2013), renal function (Berrout et al., 2012; Köttgen et al., 2008), regulation of the blood pressure (Earley, 2011) and the vascular tone (Watanabe et al., 2003; McHugh et al., 2010; Goldenberg et al., 2015b). The activation of the TRPV4 channel ca be induced by various chemical stimuli like chlorine gas and acid (Balakrishna et al., 2014; Yin et al., 2016), hydrogen peroxide (Suresh et al., 2015), phorbol ester 4α-phorbol 12,13-didecanoate (4αPDD) (Alvarez et al., 2006; Wu et al., 2009), anandamide via cytochrome P450 epoxygenase-dependent formation of epoxyeicosatrienoic acids (EETs) (Watanabe et al., 2003), and the highly selective agonist GSK1016790A (Thorneloe et al., 2008). All TRPV4 activating compounds mimicking a physiological dysregulation and represent

experimental tools for investigations of TRPV4-associated disorders like muscle atrophy, neuropathy and skeletal dysplasia (Schindler et al., 1993) and in particular, the emerging role in edema formation and vascular inflammation in both ARDS and congestive heart failure-associated pulmonary edema (Watanabe et al., 2008; Yin et al., 2016; Dalsgaard et al., 2016; Michalick et al., 2017). Currently, several studies are focusing on development, screening and testing of synthetic TRPV4 antagonists in benchside approaches (Thorneloe et al., 2012; Hilfiker et al., 2013; Kanju et al., 2016; Tsuno et al., 2016). The aim of this research is to translate the most promising compounds into bedside application to treat various cardiovascular and pain-related diseases.

2.3.1 REGULATION OF TRPV4 ACTIVATION

TRPV4 is a non-selective Ca^{2+} channel that consists of six transmembrane domains and an N- and a C-terminal cytoplasmic domain. With 50% of the whole protein, the N-terminus is the longest part and contains a phosphoinositide binding site (PIBS) that enables to bind to PIP_2 in the plasma membrane, six ankyrin repeats (ANK), which regulate the channel oligomerization and location (Arniges et al., 2006), an arachidonate-like region and a proline rich domain (PRD) that binds several kinases like protein kinase C (PKC) and, if deleted, renders TRPV4 insensitive to all stimuli (4αPDD) (Garcia-Elias et al., 2008). The C-terminus contains a calmodulin binding domain (CaMBD) (Strotmann et al., 2003), a putative oligomerization site (TRP box) (Montell, 2005; García-Sanz et al., 2007) and a PDZ-like domain (DAPL as last four amino acids) (van de Graaf et al., 2006; Garcia-Elias et al., 2008), as shown in Figure 2.

The localization of TRPV4 is dependent on targeting and expression on the plasma membrane, which includes cellular processes like endocytosis, ubiquitination and lysosomal degradation. By use of different splice variants, Arniges and colleagues have shown that the N-terminus plays a major role in the localization and oligomerization of TRPV4 (Arniges et al., 2006). TRPV4 localization is affected by proteins such as the synaptic trafficking protein kinase PACSIN-3, which connects the N-terminus via $PI(4,5)P_2$ with the plasma membrane (Cuajungco et al., 2006; D'hoedt et al., 2008), endoplasmic lectin OS-9 (Wang et al., 2007), the ubiquitin ligase AIP4 (Wegierski et al., 2006), the angiotensin receptor AT1aR (Shukla et al., 2010), and the endosomal trafficking proteins caveolin-1 (Saliez et al., 2008) and annexin-2A (Huai et al., 2012). Moreover, it has been shown that TRPV4 interacts via its proximal N-tail with the adherent junctional components E-cadherin and β-catenin in keratinocytes and thus regulates skin barrier integrity (Sokabe et al., 2010). Importantly, Matthews et al. (2010) has shown that forces applied to β1-integrins result in ultra-rapid (within 4 msec) activation of calcium influx through TRPV4 channels and that the TRPV4 channels are rather activated by mechanical strain in the cytoskeletal backbone of the focal adhesion than by deformation of the lipid bilayer or

peripheral cortical cytoskeleton alone (Matthews et al., 2010). This is proposed to cause highly compartmentalized calcium signaling at focal adhesions induced by TRPV4 and facilitates an "integrin-to-integrin" signaling by sensing forces on the ECM (Thodeti et al., 2009; Matthews et al., 2010).

In addition to the functional role of the N-terminus, the C-terminal region of TRPV4 seems to play a major role in sensing cytoskeletal changes through its binding to either tubulin or F-actin (Ramadass et al., 2007; Goswami et al., 2010; Shin et al., 2012). The first evidence that TRPV4´s C-tail interacts with the cytoskeleton has been reported by Suzuki and colleagues, who found an interaction of TRPV4 with microtubule-associated protein 7 (MAP7) (Suzuki et al., 2003). In line with this finding, recent publications described in detail an interaction of TRPV4 with the cytoskeleton via F-actin and its binding to the C-terminal region of TRPV4, which is competitive regulated with the binding of tubulin to the same region (Becker et al., 2009; Shin et al., 2012). Moreover, the activation of TRPV4 itself is mediated by several C-terminal posttranslational modifications, such as *S*-nitrosylation of Cys853 by NO (Yoshida et al., 2006; Lee et al., 2011) and phosphorylation of Ser824 by PKA, PKC and importantly SGK1 (Gao et al., 2003; Fan et al., 2009; Peng et al., 2010; Shin et al., 2012). Both, the activation via PKA as well as PKC are dependent on interaction with kinase-binding scaffold protein AKAP79/150 (a kinase-anchoring protein 79/150) (Fan et al., 2009). Recently, Shin and colleagues identified SGK1 as a novel TRPV4 regulating kinase, which amplifies the subsequent TRPV4 response to appropriate stimuli and enables TRPV4 to bind to F-actin (Shin et al., 2012). In this context, the C-terminal phosphorylation site Ser824 became more prominent over the recent years. Strotman and colleagues described the activation of TRPV4 as a result of Ser824 phosphorylation, which enables CaM to bind to the CaMBD (amino acids 812-831) and leads to a conformational change and dissociation of N- and C-terminus followed by channel opening and Ca^{2+} influx (Strotmann et al., 2003; Figure 2). As a result, Ca^{2+} influx via TRPV4 can initiate a positive feedback loop on itself. In 2008, Garcia- Elias and colleagues found that the CaMBD is overlapping with a binding site for the IP_3 receptor 3 (IP_3R3) and that TRPV4 is activated via IP_3 under low-level stimulation (Fernandes et al., 2008; Garcia-Elias et al., 2008), suggesting that multivariable, and potentially competitive regulators are involved in different activation pathways and levels. Interestingly, latter studies could demonstrate an interaction between TRPV4 C-terminus and endoplasmic membrane protein STIM1 (stromal interaction molecule 1) when Ser824 is not phosphorylated (Shin et al., 2015). STIM1 functions as calcium sensor and regulator of store-operated Ca^{2+} release, gets activated via IP_3 receptor signaling, and when activated, clusters with calcium channels (e.g. calcium release-activated calcium channel protein 1, ORAI 1) in the plasma membrane (Williams et al., 2001; Roos et al., 2005; Liou et al., 2005; Zhou et al., 2013).

These intriguing data lead to the assumption that TRPV4 seems to be regulated by many different intracellular protein-protein interactions, which in turn are potentially affected by changes of intracellular calcium concentrations. The majority of these interaction sites are located in different cellular compartments, such as cytoskeletal structures, the endoplasmic reticulum and the plasma membrane. Of particular interest in this context is the phosphorylation of Ser824 and interaction with various structural and regulatory proteins (tubulin, F-actin, STIM1, CaM, IP_3R and SGK1), which are thought to be essential for channel gating and putative components of the mechanosensing machinery.

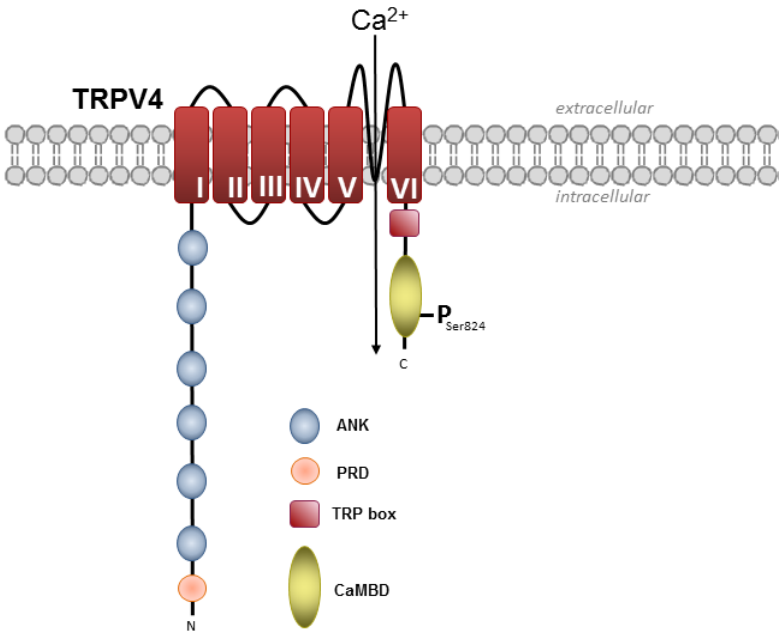

Figure 2: Schematic model of TRPV4. The N-terminus consists of a proline-rich domain (PRD) and six ankyrin repeats (ANK), the C-terminus consists of the TRP box and a calmodulin-binding domain (CaMBD).

2.3.2 SERUM GLUCOCORTICOID-REGULATING KINASE (SGK1): A NOVEL KINASE REGULATING TRPV4

The Serum glucocorticoid-regulated kinase (SGK) 1 is a member of the AGC (protein kinase A; protein kinase G and protein kinase C) subfamily (Lang and Cohen, 2001) and is activated by glucocorticoids, insulin, cytokines and a broad range of other plasma factors (Webster et al., 1993; He et al., 2015). It contains a Gly/Lys-rich nuclear localization signal (NLS), which enables its translocation into the nucleus where it enhances the expression of the potent transcription factor NFκB (Maiyar et al., 2003), resulting in global changes of the inflammatory expression profile in response to cell stress (Firestone et al., 2003; Eylenstein et al., 2012). The activation of SGK1 ensues in two phosphorylation steps. First, SGK1 associates with the rapamycin-mTor2 complex and becomes

phosphorylated in its hydrophobic motif at Ser422, resulting in basal activation. This enables pyruvate dehydrogenase kinase 1 (PDK1) to phosphorylate Thr256 within the activation loop, whereby SGK1 reaches the full activation (Lang and Cohen, 2001; García-Martínez and Alessi, 2008; Lu et al., 2010). Recent studies have shown an enhanced activation of SGK1 through other phosphomotifs by WNK1 (Chen et al., 2009), while SGK1 conversely activates/phosphorylates WNK4 thereby regulating the membrane expression of ROMK (Yue et al., 2009). The ROMK channel activity is inhibited by WNK1 and WNK4, but it is not clear whether this is a direct or indirect effect (Ring et al., 2007; Cheng and Huang, 2011; Na et al., 2013). In addition to these findings, the surface expression of TRPV4 with deleted N-terminus (Δ2-157) is downregulated by coexpression with WNK4, which indicates an indirect effect mediated by SGK1 (Fu et al., 2006). Interestingly, SGK1 gets also activated by increased intracellular Ca^{2+}, which gives the impression that there is a bidirectional activation cascade between TRPV4 and SGK1 (Imai et al., 2003; Na et al., 2013; Brickley et al., 2013). Interestingly, SGK1 facilitates depolymerization of actin (Schmid et al., 2013) and regulates activity of sodium and calcium channels in the plasma membrane such as epithelial Na^+ channel (ENaC), ROMK and TRPV4, and is required for the transcription of ORAI1/STIM1 (Wagner et al., 2001; Debonneville et al., 2001; Smyth et al., 2006; Schmidt et al., 2014). SGK1 is also involved in broad range of cellular stress responses and interestingly, reacts similar to TRPV4 to several stress responses like cell volume regulation (Lang et al., 2011; Wärntges et al., 2002), regulation of cell fluid transport (Sartori and Matthay, 2002), mechanical stress (Baban et al., 2014), inflammation and vascular permeability (Qadri et al., 2014) and, due to its ability to directly and indirectly regulate TRPV4 activity, may present a crucial regulator of TRPV4 function in mechanosensing and mechanotransduction.

2.3.3 Ca^{2+} INFLUX AND DOWNSTREAM ACTIVATION OF Ca^{2+}-ACTIVATED K^+ CHANNELS

The functional role of Ca^{2+}-activated K^+ channels (K_{Ca}) were first described in red blood cells, where K_{Ca} activation leads to membrane hyperpolarization and cell shrinkage (Gardos, 1958). Due to their different conductance K_{Ca} are divided into three subtypes, namely big conductance K_{Ca} (BK), intermediate conductance K_{Ca} (IK) and small conductance K_{Ca} (SK). The subfamily of small/immediate K_{Ca} channels consists of four members termed SK1 ($K_{Ca}2.1$; KCNN1), SK2 ($K_{Ca}2.2$; KCNN2), SK3 ($K_{Ca}2.3$; KCNN3) and IK1 ($K_{Ca}3.1$; KCNN4), which have highly conserved structures across species (Stocker, 2004). Previously, IK channels were considered as members of the SK subfamily (SK4), however, they have recently been reassigned as a novel distinct subfamily of IK channels due to their higher conductance and the fact that their amino acid sequence differs to approximately 50% from SK channels (Ishii et al., 1997; Joiner et al., 1997). Both, SK and IK channels

form tetramers out of four subunits and each subunit contains six alpha helical transmembrane domains and a pore loop between the 5th and 6th transmembrane domain, as well as a cytoplasmic N- and C-terminus (Vergara et al., 1998). SK and IK channels are highly sensitive to intracellular Ca^{2+} concentrations (~300 nMol/L), and activation of the channels is mediated by stereometrical changes following binding of Ca^{2+}-CaM to a C-terminal CaMBD (Hirschberg et al., 1998; Xia et al., 1998). The binding of CaM is inhibited by PKA (Wong and Schlichter, 2014). As such, SK and IK channels function as rapid and high-affinity sensors of intracellular Ca^{2+} levels (within 1 msec for SK, and 5-15 msec for IK channels) that effectively couple intracellular Ca^{2+} to extracellular membrane potential (Xia et al., 1998).

The functional link between TRPV4 and Ca^{2+}-activated K^+ channels was first described in 2012 by Mark Nelson´s lab and Kim Dora´s Lab, who showed that mediated Ca^{2+} influx activates K_{Ca} channels and that these events are localized to specialized microdomains, the myoendothelial junctions. Ultimately, TRPV4 mediated K_{Ca} activation was found to trigger vasodilation in isolated aortic rings by membrane hyperpolarization through simultaneous Ca^{2+} influx and K^+ efflux (Bagher et al., 2012; Sonkusare et al., 2012). More recently, an elegant combination of *in vitro* and *in situ* techniques revealed that the Ca^{2+} entry elicited by activation of TRPV4 channels is amplified by subsequent activation of both IK and SK3 channels (M. T. Lin et al., 2015). Notably, Yue and colleagues (2013) reported recently that SGK1 expression in HEK293 cells is capable to restore WNK4-mediated inhibition of BK channels (Yue et al., 2013), suggesting an inhibitory feedback of WNK4 on K_{Ca} channels that parallels its analogous effects on TRPV4 (Fu et al., 2006).

In summary, Ca^{2+}-activated K^+ channels are putative downstream targets of TRPV4-mediated Ca^{2+} influx and may amplify the latter through a positive feedback loop via membrane hyperpolarization.

2.3.4 HETEROMERIZATION OF TRPV4 WITH OTHER TRP CHANNELS: TRPV1/V4 COMPLEX

In the past decades, the notion has emerged that in addition to their ability to form homotetramers, TRP channels are also capable to interact with each other across the subtypes to form heteromeric channel complexes. The first evidence that TRPV4 forms heteromeric channel complexes with other TRP channels was described by Köttgen and colleagues in 2008, who have postulated an interaction with TRPP2 (polycystic subtype 2) in renal tubular cilium (Köttgen et al., 2008). Subsequent studies identified that TRPV4 may also physically interact with TRPC1, and that the thus formed heteromeric channels contribute to flow-induced Ca^{2+} influx in endothelial cells (Ma et al., 2010a, 2011a). Moreover, it has been shown that all three TRP channels are organized in a multimeric channel complex TRPV4/C1/P2 (Du et al., 2014). Additionally, latter findings of our group demonstrated the evidence that TRPV4 interacts with TRPC6 in pulmonary arterial smooth muscle cells (Goldenberg et al., 2015b)

In the present work, I will describe a novel interaction between TRPV4 and TRPV1. The TRPV1 channel is like TRPV4 a polymodal sensor involved in such diverse responses as nociception (Caterina et al., 2000; Davis et al., 2000), thermoregulation (Gavva et al., 2008), osmosensation (Ciura and Bourque, 2006), and mechanosensation (Birder et al., 2002). TRPV1 is activated by capsaicin, anandamide, and a number of arachidonic acid derivates such as 5-,12-,20-lipoxygenase metabolites (HETEs) or cytochrome P450 epoxygenase-metabolites (EETs) (Wen et al., 2012; Su et al., 2014). In addition, several studies have described that TRPV1 channels are organized in large multiprotein complexes, which likely consist of TRPV1 channels, scaffold proteins like AKAP79/150 and the enzymes PKA and PKC (Bhave et al., 2002, 2003; Distler et al., 2003; Jeske et al., 2008; Schnizler et al., 2008). Thereby, PKA and PKC are important for N- or C-terminal phosphorylation of TRPV1, and thus for $PI(4,5)P_2$ binding via a C-terminal PIBS, which in turn regulates channel sensitivity and membrane insertion (Prescott and Julius, 2003; Nilius et al., 2008; Ufret-Vincenty et al., 2011; Senning et al., 2014). Thereby, the surface expression TRPV1 is dynamically regulated via exocytosis in response to inflammation (Morenilla-Palao et al., 2004) or growth factors, as described for nerve growth factor (NGF) (Zhang et al., 2005). Particular in microvascular endothelial cells it has been shown that stimulation with NGF increased leukocyte adhesion (Raychaudhuri et al., 2001). In addition to the well-documented role of TRPV1 as surface expressed Ca^{2+} channel, it has been shown to induce release of Ca^{2+} from internal stores via ER-localized TRPV1 independent of extracellular Ca^{2+} and that TRPV1-mediated Ca^{2+} signals are localized to specific subcellular ER-microdomains (Marshall et al., 2003; Turner et al., 2003; Wisnoskey et al., 2003). In conformity to these findings, recent data revealed that TRPV1 is capable to form functional Ca^{2+} permeable channels in the endoplasmic reticulum (Gallego-Sandín et al., 2009).

According to the multiple subcellular localization, TRPV1 and also TRPV4 channels show polymodal activation by a broad range of chemical and physical stimuli, such as chemical (Ca^{2+}, capsaicin, EETs, HETEs), mechanical (stretch and shear forces) and physical (temperature, voltage), as excellently reviewed by Zheng (2013). The capability of TRP channels to accumulate in heteromeric channel complexes may present a rapid and highly dynamic adaptation to the strongly fluctuating and fast changing physiological stimuli, as it has been already shown for TRPV4/C1 and TRPV4/P2 (Köttgen et al., 2008; Ma et al., 2010b). In the context of VILI, TRPV1 and TRPV4 are suggested to disrupt endothelial barrier integrity in a synergistic manner.

2.4 MICROPARTICLE FORMATION IN LUNG DISEASE

Microparticles (MPs) are defined as a heterogeneous, bilammellar vesicles of 100 - 1000 nm diameter that are released by evagination of the plasma membrane, and may contain membrane-specific antigens, nucleotides, nucleic acids, lipids, soluble cytoplasmic factors, and even small organelles from with specific characteristics of their respective cell of origin. Almost all cell types are able to form MPs under physiological and pathophysiological conditions, e.g. apoptosis. Recently, MPs have gained considerable interest due to their possible clinical role as biomarkers, and their potential for intercellular or even systemic communication and signal propagation in disease and regeneration processes. Simplistically, this mechanism is described as transfer of MPs from the generating donor cell to downstream acceptor cells. McVey and colleagues (2012) defined four alternative ways through which MPs can act on acceptor cells: (1) via outside-in signaling by binding or cross-linking of surface receptors, or secretion of soluble factors, like cytokines (MacKenzie et al., 2001), (2) through internalization or microparticle clearance (Dasgupta et al., 2012), (3) via complete or selective fusion of MPs with the plasma membrane and transfer of bioactive proteins and lipids (Inal et al., 2013), and (4) through effects on translational expression patterns via the uptake of mRNA or miRNA from MPs (Quesenberry et al., 2010). The generation of MPs is largely regulated by membrane asymmetry: Under resting conditions specific phospholipid transporter enzymes in the plasma membrane such as flippases, floppases and scramblases turn negatively charged phosphatidylserine (PS) to the inner leaflet. When the cellular homeostasis changes due to external or internal signals, the phospholipid transporters are dysregulated, which leads to electrochemical disturbances in the plasma membrane and to exposure of negatively charged PS from the inner leaflet to the outer leaflet. Importantly, the loss of membrane phospholipid asymmetry is at large a Ca^{2+}-dependent process, which is initiated by increased cytoplasmic Ca^{2+} levels. Concomitant with the collapse of the membrane asymmetry, calcium-sensitive enzymes such as calpain and gelsolin are activated, promoting the detachments of membrane proteins to cytoskeletal structures by proteolytic activity and thus enable subsequent blebbing, formation and release of MPs to the extracellular space.

In ARDS patients elevated concentrations of MPs were found in pulmonary edema fluid, and have a higher procoagulant activity than those from patients with cardiogenic pulmonary edema (Bastarache et al., 2006). The elevated procoagulant activity is assumed to be mainly due to the presence of increased concentration of tissue factor in the fluid, which is strongly correlated with microparticle levels (Bastarache et al., 2007). Furthermore, this study showed a trend towards lower MP concentrations in ARDS survivors compared to those who died of the disease. These findings suggest that MPs may play a major role in activation of blood coagulation and fibrin deposition into the alveolar space, which is a characteristic for ARDS progression, and to this end that MPs might represent potential markers of severity of ARDS (Bastarache et al., 2006). Novel findings revealed that

leukocyte-derived MPs (LMPs) are also elevated in plasma and bronchoalveolar lavage fluid in ARDS patients compared (n = 52) to the control group (n = 22) (Guervilly et al., 2011). The study also indicated a strong correlation between the LMP levels and the survival rate in the ARDS group and let suggest that LMPs might be protective in the progression of ARDS compared to other MP subpopulations (Guervilly et al., 2011). In contrast, endothelial-derived MPs (EMPs) have been found to initiate pro-inflammatory signaling cascades by the release of IL-1β and TNF-α and subsequent recruitment and activation of neutrophils as well as edema formation in experimental models of lung injury (Densmore et al., 2006; Buesing et al., 2011).

Therefore, MPs reveal a considerable potential as prognostic biomarkers in the progression VILI and might be associated with mortality or organ dysfunction. Since it has been shown that the central cellular mechanism of MP release is intracellular Ca^{2+} uptake, the mechanosensitive Ca^{2+} channel TRPV4 may present a particular attractive mediator of mechanically induced MP formation during mechanical ventilation.

2.5 AIM OF THIS THESIS

Despite the ongoing research on the mechanisms of ventilator-induced lung injury (VILI), incidence and mortality remained broadly unchanged. This could be explained by the complexity and heterogeneity of pulmonary inflammation, which might be accompanied by the heterogenous distribution of mechanical forces and inspired volumes in response to mechanical ventilation. Therefore, it is an urgent need to identify the molecular mechanisms underlying mechanotransduction in the ventilated lung. The present work focuses on the pathophysiological effects of ventilation with high tidal volumes on the endothelial barrier integrity in the lung. A central actor in regulation of the endothelial barrier is the mechanosensitive Ca^{2+} channel TRPV4. The exact mechanisms of TRPV4-mediated increase of intracellular Ca^{2+} and the thereby induced signaling cascades are still elusive. Therefore, I characterized the effects of endothelial mechanotransduction in pharmacological as well as genetic approaches in a standardized experimental model of VILI, according to the following hypotheses:

1. TRPV4 regulates endothelial barrier integrity in the ventilated lung and its mechanical activation via high tidal volumes results in vascular hyperpermeability and edema formation.
2. TRPV4 activity is enhanced via phosphorylation of Ser824 by the kinase SGK1, and phosphorylation is increased in mechanical-stretched endothelial cells in response to ventilation with high tidal volumes.
3. Mechanosensitive TRPV4-mediated Ca^{2+} influx into pulmonary endothelial cells activates Ca^{2+}-activated K^+ channels downstream and induce a positive feedback on endothelial Ca^{2+} response.
4. TRPV4 interacts with TRPV1, and this interaction drives progression of VILI, presumably by an amplification of the stretch-induced Ca^{2+} response.
5. Stretch-induced Ca^{2+} influx via TRPV1 and TRPV4 promotes formation and release of microparticles from pulmonary microvascular endothelial cells.

3 EXPERIMENTAL METHODS

3.1 *IN VIVO* STUDIES

3.1.1 ANIMALS

Experiments were performed in the form of prospective, randomized, and controlled studies in male C57BL/6J wild type, TRPV4-deficient (*Trpv4*$^{-/-}$) (Liedtke and Friedman, 2003a) and TRPV1-deficient (*Trpv1*$^{-/-}$) (Caterina et al., 2000) mice with body weights (bw) of 25 - 30 g. All procedures were in accordance to institutional and governmental guidelines.

3.1.2 VENTILATION PROCEDURE

Anesthetized male C57BL/6J wild type (wt), *Trpv4*$^{-/-}$ and *Trpv1*$^{-/-}$ mice were anesthetized (ketamine 100 mg/kg, xylazine 20 mg/kg bw) and placed in supine position on a heating pad with a rectal thermal probe to maintain body temperature at 37°C. Following tracheostomy, polyethylene catheters (0.28 mm inner diameter; Smiths Medical, Dublin, OH) were surgically placed into the right carotid artery and left jugular vein. Animals were then randomly assigned to one of two different ventilation modes, in that control mice were ventilated with low tidal volumes (LV_T) of 7 mL/kg bw and a respiratory rate of 150 min^{-1} and mice in the injury groups with high tidal volumes (HV_T) of 20 mL/kg and a respiratory rate of 60 min^{-1} at an inspiratory fraction of oxygen (FiO_2) of 1 for 2 h and a positive end-expiratory pressure (PEEP) of 2 cmH_2O. The respiratory rates were adjusted to keep $PaCO_2$ levels within the physiological range of 35 – 45 mmHg for each group. All experiments were started by a single recruitment maneuver with an inspiratory pressure of 20 mmHg for 5 sec to open up potential atelectatic areas. For inhibitor treatment, the TRPV4 inhibitor HC-067047 (20 nMol/L), the SGK1 inhibitor GSK 650394 (100 nMol/L), the SK1-3 inhibitor apamin (10 nMol/L), the IK1/BK inhibitor charybdotoxin (100 nMol/L), the selective IK1 inhibitor TRAM34 (1 µMol/L), and the TRPV1 inhibitor SB366791 (50 nMol/L) were continuously infused via the right jugular vein at a rate of 400 µL/h for the 2 h duration of mechanical ventilation, while control groups received 400 µL/h 0.9% saline infusion. Human serum albumin (HSA, Baxter, Unterschleißheim, Germany) was given as an intravenous bolus (1 mg) 60 minutes before the end of the experiment for subsequent analysis of pulmonary hyperpermeablitiy to proteins ≥60 kDa (Müller et al., 2010). Unventilated controls were subjected to the same surgical and experimental procedure without connection to the ventilator. The whole ventilation procedure of the *in vivo* ventilation experiments is schematically shown in Figure 3.

After 2 h with or without mechanical ventilation, animals were sacrificed and lungs were excised. Lung edema was estimated as wet-to-dry lung weight ratio from the apical lobe of the right lung. The middle lobe of the right lung was fixed in 4% formaldehyde and paraffin embedded for histological

sectioning; slides were stained by hematoxylin-eosin and lung injury was assessed by use of a semi-quantitative histologic score (Matute-Bello et al., 2011). The lower lobe and accessory lobe of the right lung were frozen in liquid nitrogen, stored at –80°C and utilized for post-hoc immunoprecipitation analyses. The left lung was lavaged with ice-cold PBS (4x 150 µL) and protein concentration in the bronchoalveolar lavage fluid (BALF) was quantified by Bradford assay (Bio-Rad, Hercules, USA). The concentration of HSA in BALF and plasma was measured by ELISA as described in 3.4.2, and the rate of macromolecular extravasation was calculated as the ratio of HSA concentrations in BALF over plasma x 1000. Concentrations of the following cytokines were quantified in BALF by a multiplex assay as described in 3.4.1.

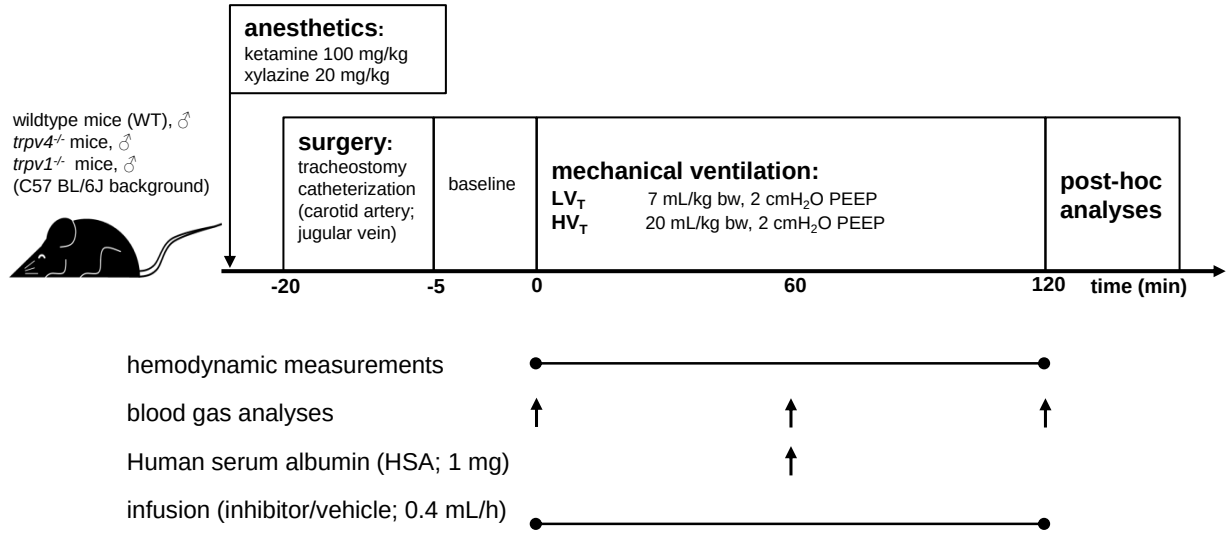

Figure 3: Experimental procedure for *in vivo* ventilation experiments.

3.1.3 BONE MARROW TRANSPLANTATION AND ACID-INDUCED LUNG INJURY

All bone marrow transplantations were done in collaboration with Geraldine Nouailles-Kursar (Department of Internal Medicine/Infectious Diseases and Respiratory Medicine Charité – Universitätsmedizin Berlin). In brief, twenty-four hours before bone marrow transplantation 10-12 weeks old C57BL/6J wild type or *Trpv4*$^{-/-}$ mice were lethally irradiated two times with 5.5 Gy at an interval of 3 h using a Gammacell 40 Extractor (Best Theratronics, Ottawa, Canada) with two ^{137}Cs sources. Age-matched C57BL/6J wild type or *Trpv4*$^{-/-}$ mice were sacrificed and femur and tibia were dissected and flushed for isolation of bone marrow cells (BMCs). Bone marrow cells of four mice of each background were pooled, washed and centrifuged. Finally, BMCs were resuspended in PBS and 5x10^6 cells were injected intravenously into C57BL/6J wild type (WT) or *Trpv4*$^{-/-}$ (KO) recipient mice according to the following the experimental groups.

Experimental groups	**WTxWT**	**WTxKO**	**KOxKO**	**KOxWT**
Genotype of recipient mice (parenchymal cells)	WT	WT	KO	KO
Genotype of BMCs (hematopoetic cells)	WT	KO	KO	WT

Table 1: Experimental groups for bone marrow chimeras.

All BMC transplanted mice were treated with antibiotics (0.05% Enrofloxacin, Baytril, BAYER, Leverkusen, Germany) in drinking water available *ad libitum* for 4 weeks after irradiation. Bone marrow reconstitution was verified by PCR from whole blood 10-12 weeks after irradiation. For PCR verification, specific primers were used against exon 12 (excised and absent in *Trpv4*$^{-/-}$; present in wild type) and exon 15 as control (present in both) (Liedtke and Friedman, 2003b). Representative pictures of PCR products for each experimental group are shown in Figure 4.

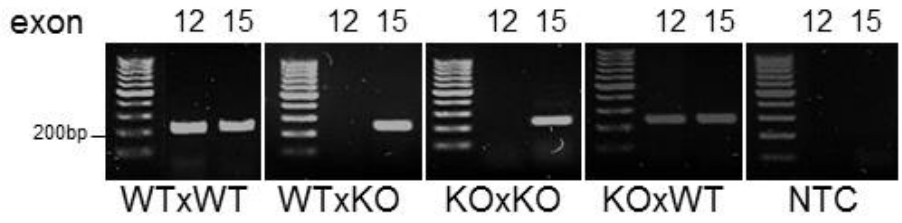

Figure 4: Representative PCR products for successful bone marrow transfer.

Mice were subjected to the same surgical and experimental procedure as described in 3.1.2 with ventilation of 10 ml/kg bw and a respiration rate of 110 min^{-1} and a positive end-expiratory pressure (PEEP) of 2 cmH_2O. ALI was induced by intratracheal instillation of hydrochloric acid (HCl pH 1.5, 2 µL/g bw) while control animals received saline (2 µL/g bw).

3.2 *EX VIVO* STUDIES

3.2.1 ISOLATED AND PERFUSED MOUSE LUNGS

Lungs from C57BL/6J wild type (wt), *Trpv4*$^{-/-}$ and *Trpv1*$^{-/-}$ mice were isolated, ventilated, and continuously perfused with Hanks' balanced salt solution containing 20% fetal bovine serum at a rate of 1 mL/min as previously described (Wang et al., 2012). For imaging of endothelial $[Ca^{2+}]_i$, Fura-2AM (5 µMol/L; Promokine), which de-esterifies intracellularly following its uptake by endothelial cells to the Ca^{2+}-sensitive dye Fura-2, was infused for 20 min as previously described (Samapati et al., 2012). Lungs were positioned under an upright fluorescence microscope on a custom-built stage and superfused with normal saline at 37°C. Fura-2 fluorescence in endothelial cells of subpleural lung microvessels was excited at 340, 360 and 380 nm by monochromatic illumination (Polychrome IV; T.I.L.L. Photonics, Martinsried, Germany), collected through an approchromat objective (UAPO 40x W2/340; Olympus, Hamburg, Germany), dichroic and emission filters (FT 425 and BP 505-530; Zeiss, Jena, Germany) by a CCD camera (Sensicam; PCO, Kehlheim, Germany) and subjected to digital image analysis (TILLvisION 4.01; T.I.L.L. Photonics). Fura-2 loaded endothelial cells in single venular capillaries of 15-30 µm in diameter were imaged during lung inflation with constant positive airway pressure (CPAP) of 5 cmH_2O ($CPAP_{low}$) at baseline and of 15 cmH_2O ($CPAP_{high}$) subsequently over 15 min following an acute increase in CPAP. Changes in endothelial $[Ca^{2+}]_i$ were determined as changes in the 340/380 ratio and are expressed relative to the individual baseline. The loading of Fura-2 dye by insertion of a microcatheter into the vessels and a schematic image of the experimental setup are shown in Figure 5.

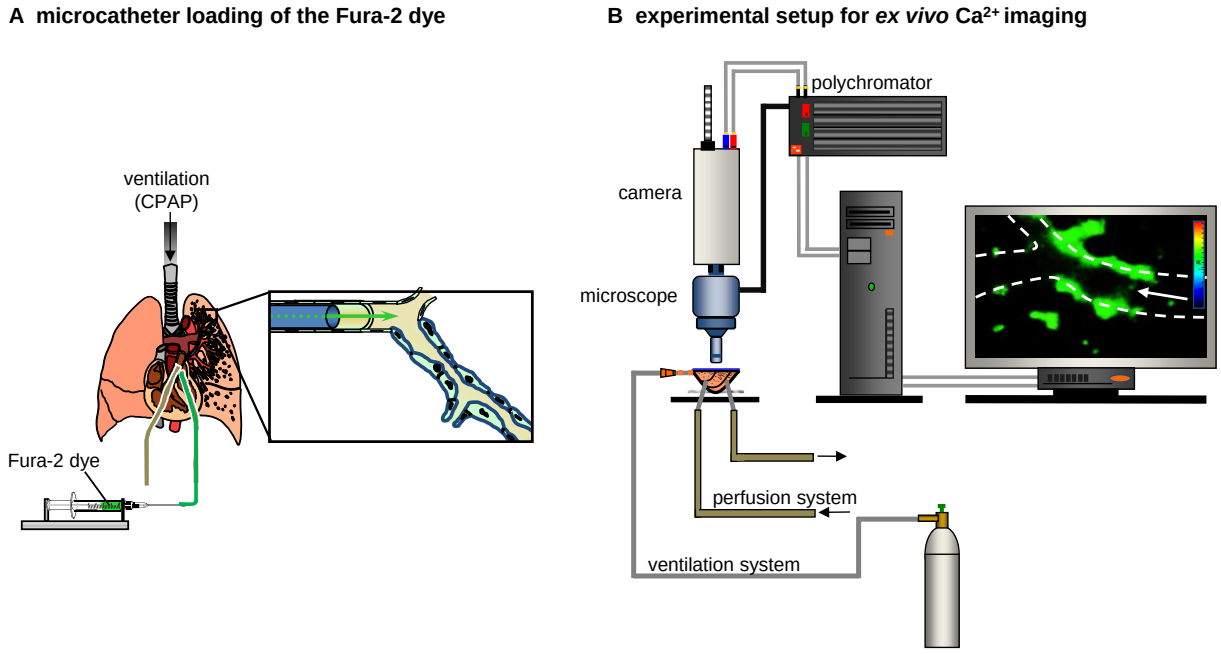

Figure 5: Experimental procedure for *ex vivo* Ca^{2+} imaging in isolated and perfused mouse lungs: (**A**) surgical placement of the intravenous microcatheter and Fura-2 loading; (**B**) microscope setup for Ca^{2+} imaging (modified after Samapati et al., 2012).

3.3 *IN VITRO* STUDIES

3.3.1 CYCLIC STRETCH

All experiments were performed by use of a FX-4000T FLEXCELL® Tension Plus system (Flexcell International, McKeesport, PA) with the 25 mm BioFlex loading station. Primary human pulmonary microvascular endothelial cells (HPMVECs, PromoCell, Heidelberg, Germany) were grown in cell culture media (endothelial growth media, MV, PromoCell, Heidelberg, Germany), which was changed every 48 h. Cells were seeded at standard densities (8 x 10^5 cells/well) onto ProNectin-coated BioFlex plates (Flexcell International, McKeesport, USA). The HPMVEC monolayers were treated (100 nMol/L HC-067047; 100 nMol/L GSK650394; 50 nMol/L SB366791) and mounted onto the FlexCell system and exposed to cyclic stretch of 5% elongation (mimicking low tidal volume ventilation) or 18% elongation (mimicking high tidal volume ventilation) for 2 h. Static controls were placed into the same incubator without stretch application. After 2 h of cyclic stretch the media was removed and used for the enumeration of microparticles and the cells were fixed in 4% formaldehyde for immunofluorescence analyses and Duolink assays, respectively.

3.3.2 CALCIUM IMAGING

HPMVECs were seeded at a density of 5x10^5 cells in a flow chamber (µ-Slide I 0.8 Luer ibiTreat, Ibidi, Martinsried, Germany) and were grown to confluency. For imaging of endothelial $[Ca^{2+}]_i$, HPMVECs were incubated with Fura-2AM (5 µMol/L; Promokine) for 20 min at 37°C. The flow chamber was connected to a custom-made perfusion system with a flow rate of 0.5 mL/min 30 min prior to the start of the experiment to adapt the cells to the flow and establish a stable baseline. The baseline was recorded for 3 min with continuous HBSS perfusion followed by switching to a second buffer reservoir containing HBSS and activators and/or inhibitors (10 µMol/L TRPV1 agonist capsaicin, Alomone, Jerusalem, Israel; 100 nMol/L TRPV4 agonist GSK1016790A, Sigma-Aldrich, Munich, Germany). The resulting $[Ca^{2+}]_i$ response was recorded over a total of 15 min as described in 3.2.1.

3.3.3 ENUMERATION OF MICROPARTICLES

The enumeration of microparticles in cell culture supernatants was performed by my colleague Mazharul Maishan (Department of Physiology, Universtiy of Toronto) as previously described (McVey et al., 2016). To this end, supernatants were analyzed by flow cytometry on a BD FACS ARIA III SORP with a 130 mW 488 nm laser (BD Biosciences, San Jose, USA), 100 µm nozzle, sheath pressurized at 20 PSI, no neutral density filters, fournier optical transformation unit and a small particle detection module allowing for MP enumeration. Supernatant sample data were collected at its slowest settings (>120 sec) to maximize sensitivity and to reduce the "dead space" error in consumption after running 100 nm-filtered sheath fluid (BD Biosciences, San Jose, USA) for 30 to

60 min to minimize instrument background noise. Lipid bilayer microspheres (LBM) are small inert spheroid constructs mimicking lipid bilayer and dual leaflet of cell membranes, and were used for channel gating. The concentration of microparticles in supernatants was calculated as:

$$\mathrm{MP}/\mu\mathrm{L} = \frac{(\#\mathrm{MP\ LBM\ gate})}{((\mathrm{inital} - \mathrm{final\ mass}(\Delta\mathrm{g}) \times 1000\mu\mathrm{g}/\mu\mathrm{L} \times \mathrm{specific\ gravity}\ (1{,}006\mathrm{g}/\mathrm{mL})}$$

3.4 PROCEDURES OF BIOCHEMISTRY AND MOLECULAR BIOLOGY

3.4.1 MULTIPLEX ELISA ASSAY

The concentrations of inflammatory cytokines and chemokines IL-1β, IL-10, MIP-2 (macrophage inflammatory protein 2; CXCL2), KC (keratinocyte-derived chemokine; CXCL1), RANTES (regulated on activation, normal T cell expressed and secreted; CCL5) and MCP-1 (monocyte chemotactic protein; CCL2) in BALF were quantified by a multiplex assay (BioRad, Hercules, California, USA).

3.4.2 MEASUREMENT OF PULMONARY HYPERPERMEABILITY.

Extravasation of HSA into the alveolar space was assessed by quantification of BALF and plasma HSA by ELISA (Bethyl, Montgomery, USA) according to the manufacturer's instructions. Pulmonary hyperpermeability to albumin was calculated as ratio: $[cHSA_{BALF}/cHSA_{Plasma}] \times 1000$, as previously described by Müller and colleagues, 2010.

3.4.3 MEASUREMENT OF MYELOPEROXIDASE ACTIVITY

Myeloperoxidase (MPO) activity was determined in homogenized lung tissue as described by (Kuebler et al., 1996), and analyses were performed by my colleague Lasti Erfinanda (Institute of Physiology, Charité – Universitätsmedizin Berlin). In brief, lung tissues were homogenized using 0.02 Mol/L potassium phosphate buffer, pH 7.4, followed by centrifugation at 30,000 g and 4°C for 15 min. The pellets of the homogenized lung tissue were collected and incubated for 2 hours at 60°C. MPO was extracted from the lung tissue pellet by resuspending the pellet with 0.5% hexadecyl-trimethylammonium bromide (HTAB) in 0.05 Mol/L potassium phosphate buffer, pH 6.0, following sonication in an ice bath for 1 h. The suspensions were freeze-thawed three times after which sonication was repeated. Suspensions were centrifuged at 12,000 g and 4°C for 30 min and the supernatants were collected. For spectrophotometrically measurement of MPO activity, the supernatants were mixed with 1.6 Mol/L tetramethylbenzidine and 0.6 Mol/L hydrogen peroxide dissolved in 0.08 Mol/L sodium phosphate buffer, pH 5.4. The reaction was stopped after 5 min with 2 Mol/L hydrogen sulphate and the absorption was measured at 450 nm to estimate MPO activity and were calculated as enzymatic activity per g tissue.

3.4.4 IMMUNOPRECIPITATION

For co-immunoprecipitation analyses lungs tissue was homogenized in lysis buffer (see 3.5.1), centrifuged (12,000 g, 15 min), and protein concentrations of the supernatant was determined by Bradford assay (Bio-Rad, Hercules, USA) (Bradford, 1976). 500 µg total protein was precleared with 20 µL magnetic beads (Cell Signaling, Danvers, Massachusetts, USA). After preclearing lysate was incubated with TRPV4 antibody (Cuajungco et al., 2006) and captured with 30 µL magnetic beads over night at 4°C. Captured proteins were denaturated in 3x Laemmli buffer for 10 min at 95°C.

3.4.5 BIOTINYLATION OF SURFACE PROTEINS

HPMVECs were washed with cold rinsing solution (1x PBS pH 7.5 containing 0.1 mMol/L $CaCl_2$ and 1 mMol/L $MgCl_2$) to remove the residual amines. Surface proteins were labeled with rinsing solution containing 1 mg/mL EZ-Link Sulfo-NHS-SS-Biotin (Pierce, Rockford, USA) and gentle agitation for 30 min at 4°C. Unbound biotin was quenched with rinsing solution containing 100 mMol/L glycine for 30 min at 4°C followed by washing in rinsing solution. Cells were lysed with RIPA buffer (see 3.5.1) containing 1x protease inhibitor cocktail (Roche, Germany) and 1x Phosphatase inhibitor (Pierce Rockford, USA). For precipitation, the lysate was incubated with 30 µl monomeric avidin agarose beads (NeutrAvidin Agarose Resin; Thermo scientific, Rockford, USA). The bound proteins were analyzed as surface fraction and the supernatant as intracellular fraction.

3.4.6 WESTERN BLOTTING

Proteins from human pulmonary microvascular endothelial cells were lysed in lysis buffer (see 3.5.1), centrifuged (12,000 g, 15 min), and protein concentrations of the supernatant were again determined by Bradford assay. Immunoprepicitates or lysates were separated by sodium dodecyl sulfate polyacrylamide gel electrophoresis (SDS-PAGE) in a 10% separation gel using a Mini-PROTEAN electrophoresis system (Bio-Rad, Hercules, USA) (Laemmli, 1970). Proteins were transferred onto a nitrocellulose membrane (Whatman, Dassel, Germany) over 90 min at 90 V, 4°C using tank blot procedure (Towbin et al., 1979). Membranes were blocked with 5% BSA in TBS-T (TBS containing 0.1% Tween 20) for at least 30 min, followed by incubation of the first antibody dissolved in 3% BSA TBS-T over night at 4°C. After three washes in TBS-T, membranes were incubated with the appropriate peroxidase-conjugated secondary antibody at room temperature for at least 1h, followed by three additional washing steps. Captured proteins of interest were visualized by a chemiluminescent substrate (Amersham, Freiburg, Germany). Chemiluminescence was captured with Celvin® Chemiluminescence Imaging System and quantified using *LI-COR* Image Studio™ Software.

3.4.7 PROXIMITY LIGATION ASSAY USING DUOLINK®

Stretched HPMVECs from ProNectin-coated BioFlex plates (Flexcell International, McKeesport, USA) were fixed and permeabilized. Formaldehyde crosslinking was quenched, and protein interactions were fluorescent visualized by proximity ligation assay using Duolink® (Sigma-Aldrich, Munich, Germany) according to the manufacturer's instructions. Protein-protein interactions were visualized as red puncta by confocal microscopy (Nikon A1Rsi+, Düsseldorf, Germany) and evaluated by FIJI software (ImageJ) with the measurement of particles option (particles were counted in a range of 5-100 pixel).

3.4.8 GENOTYPING

For genotyping of *Trpv1*$^{-/-}$ or *Trpv4*$^{-/-}$ mice DNA was extracted from tail biopsies or ear punches and the tissue was digested by 500 µL SNET buffer containing 10 mg/mL proteinase K over night at 37°C. For precipitation of nucleic acids 275 µL of 5 Mol/L ammonium acetate were added to the digested tissue and incubated over 5 min at 65°C, followed by 10 min on ice. After gently inversion of the tubes and 500 µL chloroform was added, followed by vortexing and centrifugation at 13,000 g for 2 min. The nucleic acids in the supernatant were precipitated with 1 mL isopropyl alcohol, inverted and incubated for 5 min at room temperature, and centrifuged at 13,000 g for 5min and wash 2x with 70% ethanol. After discarding the ethanol DNA pellet was died and dissolved in 100 µL ultra-pure water. All PCR reactions were prepared in a final volume of 12 µL containing 1x Dream Taq buffer, 2.5 mMol/L $MgCl_2$, 0.2 mMol/L dNTPs, 0.5 µMol/L forward primer, 0.5 µMol/L reverse primer, 0.05 µMol/L Dream Taq DNA polymerase and 2 µL template DNA.

For TRPV4 the following PCR program was applied:

Initial denaturation	:	95°C	10 min	
Denaturation	:	95 °C	30 sec	35 cycles
Annealing	:	65 °C	1 min	
Elongation	:	72 °C	30 sec	
Final elongation	:	72 °C	5 min	

For TRPV1 the following PCR progam was applied:

Initial denaturation	:	95°C	5 min	
Denaturation	:	95 °C	30 sec	35 cycles
Annealing	:	68 °C	30 sec	
Elongation	:	72 °C	30 sec	
Final elongation	:	72 °C	7 min	

3.4.9 IMMUNOFLUORESCENCE

For immunofluorescent staining, HPMVECs were grown to confluency on 2% gelatine-coated coverslips and fixed with 4% formaldehyde for 30 min at 4°C. The fixed cells were washed with PBS and permeabilized for 5 min with 0.1% Triton-X 100 in PBS and formaldehyde crosslinking was quenched with 20 mMol/L glycine in PBS. Coverslips were blocked with 1% BSA 5% FBS in TBS for 1 h at room temperature, and were incubated afterwards with the first antibodies in blocking buffer over night at 4 °C. Cells were washed 3x with TBS and incubated with an appropriate secondary Alexa Fluor® dye-conjugated antibodies for 1 h at room temperature. The coverslips were washed again three times with TBS and were mounted (Duolink® *In Situ* Mounting Medium with DAPI, Sigma Aldrich, Munich, Germany) on glass slides. Immunofluorescent stainings were visualized by confocal microscopy (Nikon A1Rsi+, Düsseldorf, Germany).

3.4.10 LIGHT SHEET FLUORESCENCE MICROSCOPY

Lungs from C57BL/6J wild type mice were isolated, ventilated as described by Wang and colleagues (2012), and perfused with 1 mL PBS to remove blood cells, followed by intratracheal instillation of 1% low melting point agarose in PBS. Lungs were dissected, fixed and cooled down over night at 4°C. Lungs were cut into slices (< 0.5 mm) and washed in a hybridization oven at 37°C for 2h to get rid of the agarose. Lung slices were then permeabilized for 20 min with 0.1% Triton-X 100 in PBS and formaldehyde crosslinking was quenched with 20 mMol/L glycine in PBS for 10min. After blocking of the lung slices in 1% BSA 5% FBS PBS for 1h at room temperature, they were incubated with the first antibody in blocking solution over night at 4°C. Lung slices were washed three times in PBS and incubated with the appropriate secondary Alexa Fluor® dye-conjugated antibody for at least 1h at room temperature, followed by additional washing steps and embedding into 1% low melting point agarose in a cut 1 mL syringe, which could be placed into the sample holder of the light sheet fluorescence microscope (Lightsheet Z.1, Zeiss, Jena, Germany). Protein signals were visualized and processed with Zeiss ZEN imaging software.

3.5 MATERIAL AND SUBSTANCES

3.5.1 SUBSTANCES AND BUFFERS

Lysis buffer:
137 mMol/L NaCl
20 mMol/L Tris
2 mMol/L EDTA
1 mMol/L PMSF
10% Glycerol
1% Nonidet P-40
1x protease and phosphatase inhibitor cocktail
pH adjusted with HCl to pH 7.4

1x PBS:
137 mMol/L NaCl
2.7 mMol/L KCl
10 mMol/L Na_2HPO_4
1.8 mMol/L KH_2PO_4
pH adjusted with HCl to pH 7.4

RIPA buffer:
50 mMol/L Tris
150 mMol/L NaCl
1% Nonidet P-40
0.1% SDS
0.5% deoxycholate
1x protease and phosphatase inhibitor cocktail
pH adjusted with HCl to pH 7.4

SNET buffer:
10 mMol/L Tris pH 8.0
0.1 Mol/L EDTA
0.5 % SDS

1x TBS: 150 mMol/L NaCl

50 mMol/L Tris

pH adjusted with HCl to pH 7.6

3.5.2 ANTIBODIES

Primary Antibodies	**Cat.No**	**Company**
Anti-BK	APC-151	Alomone, Jerusalem, Israel
Anti-GAPDH	ab9485	Abcam, Cambridge, UK
Anti-IK1	APC-064	Alomone, Jerusalem, Israel
Anti-SGK	sc-28338	Santa Cruz, Dallas, USA
Anti-SK1	APC-039	Alomone, Jerusalem, Israel
Anti-SK2	ab85401	Abcam, Cambridge, UK
Anti-SK3	APC-025	Alomone, Jerusalem, Israel
Anti-TRPV1	ACC-030	Alomone, Jerusalem, Israel
Anti-TRPV4	-	(Cuajungco et al., 2006)
Anti-TRPV4	sc-16485	Santa Cruz, Dallas, USA
Phalloidin-FITC	P5282	Sigma-Aldrich, St. Louis, USA
pSer824 (RXRXXS*/T*)	#9611; #10001	Cell Signaling, Leiden, Netherlands
Secondary Antibodies	**Cat.No**	**Company**
Alexa Fluor®594	A11012	Life Technologies, Carlsbad, USA
Anti-mouse IgG-HRP	NA931VS	GE Healthcare, Freiburg, Germany
Anti-rabbit IgG-HRP	sc-2004	Santa Cruz, Dallas, USA
Anti-rabbit IgG-HRP	sc-2030	Santa Cruz, Dallas, USA

Table 2: List of antibodies used for immunoblotting, immunofluorescence and proximity ligation assay (PLA).

3.5.3 PRIMER

Primer	**Sequence (5' → 3')**	**Company**
TRPV4exon12for	GGACAACTTGTACGAATAGCGGGA	Eurofins Genomics
TRPV4exon12rev	TGCACCAACATGAAGGTCTGTGACG	Eurofins Genomics
TRPV4exon15for	CCTGTCCTTCGTCATTAGCTGGAT	Eurofins Genomics
TRPV4exon15rev	CTGATTCATTTAACCAGGTGAGGCC	Eurofins Genomics
TRPV1WTfor	TGG CTC ATA TTT GCC TTC AG	Eurofins Genomics
TRPV1KOfor	TAA AGC GCA TGC TCC AGA CT	Eurofins Genomics
TRPV1rev	CAG CCC TAG GAG TTG ATG GA	Eurofins Genomics

Table 3: Primer sequences used for genotyping.

3.5.4 SUBSTANCES

Substance	**Function**	**Company**
Apamin	non-specific antagonist of SK channels (affinity: SK3 > SK2 > SK1)	Sigma-Aldrich
Charybdotoxin	non-specific antagonist of IK1 and BK channels	Sigma-Aldrich
Capsaicin	specific TRPV1 agonist	Alomone
GSK650394	specific SGK1 antagonist	Tocris bioscience
GSK1016790A	specific TRPV4 agonist	Sigma-Aldrich
HC-067047	specific TRPV4 antagonist	Sigma-Aldrich
SB366791	specific TRPV1 antagonist	Cayman Chemicals
TRAM34	specific IK1 antagonist	Alomone

Table 4: Activators and inhibitors used in the experiments.

3.6 *IN SILICO* ANALYSES

PSORT II program (*psort.hgc.jp/form2.html*) was used to predict the protein localizations. Therefore, the amino acid sequences of TRPV1 (ID: Q8NER1) and TRPV4 (ID: Q9HBA0) were processed by the software and calculated as percental localization prediction.

3.7 STATISTICAL ANALYSES

Experiments were performed as a prospective, randomized and controlled study. Post-hoc analyses, including biochemical assays and histological assessment were performed in a blinded fashion. The sample sizes were based on previous experience (Yin et al., 2016). Statistical analysis was performed by use of GraphPad Prism software (GraphPad Prism 6.0; GraphPad Software Inc., La Jolla, CA). All data are presented as means ± SEMs. Different treatment groups were compared by Mann-Whitney U-test or one-way analysis of variance (ANOVA) for repeated measures followed by Dunnett's post-hoc test, or two-way ANOVA followed by Šidák´s post-hoc test as appropriate. Correlation was tested by calculation of the Pearson product-moment coefficient, and linear regression analysis was performed. The inhibitor correlation was computed by the Pearson product-moment correlation coefficient from all measured means of GSK650394 and HC-067047. Statistical significance was assumed at $*P < 0.05$; $**P < 0.01$; $***P < 0.001$.

4 RESULTS

4.1 TRPV4 DEFICIENCY OR INHIBITION PREVENTS EXPERIMENTAL ACUTE LUNG INJURY *IN VIVO*.

Transient receptor potential vanilloid 4 (TRPV4) cation channel has previously been implicated in stretch-induced capillary barrier failure in isolated lungs and therefore, represents an interesting candidate for mechanotransduction in VILI (Balakrishna et al., 2014; Hamanaka et al., 2007; Yin et al., 2008). As putative mechanosensor, TRPV4 is widely expressed over different cell types in the lung. This ubiquitous distribution of TRPV4 in the lung is shown in Figure 6, as a 3D image captured by light sheet fluorescence microscopy from murine lung slices from the distal tip of the right lower lobe. The representative image reveals a pronounced expression of TRPV4 (red) in the pulmonary macrovasculature (e.g. endothelial cells and smooth muscle cells), in the microvasculature (mainly endothelial cells) and in the alveoli (epithelial cells).

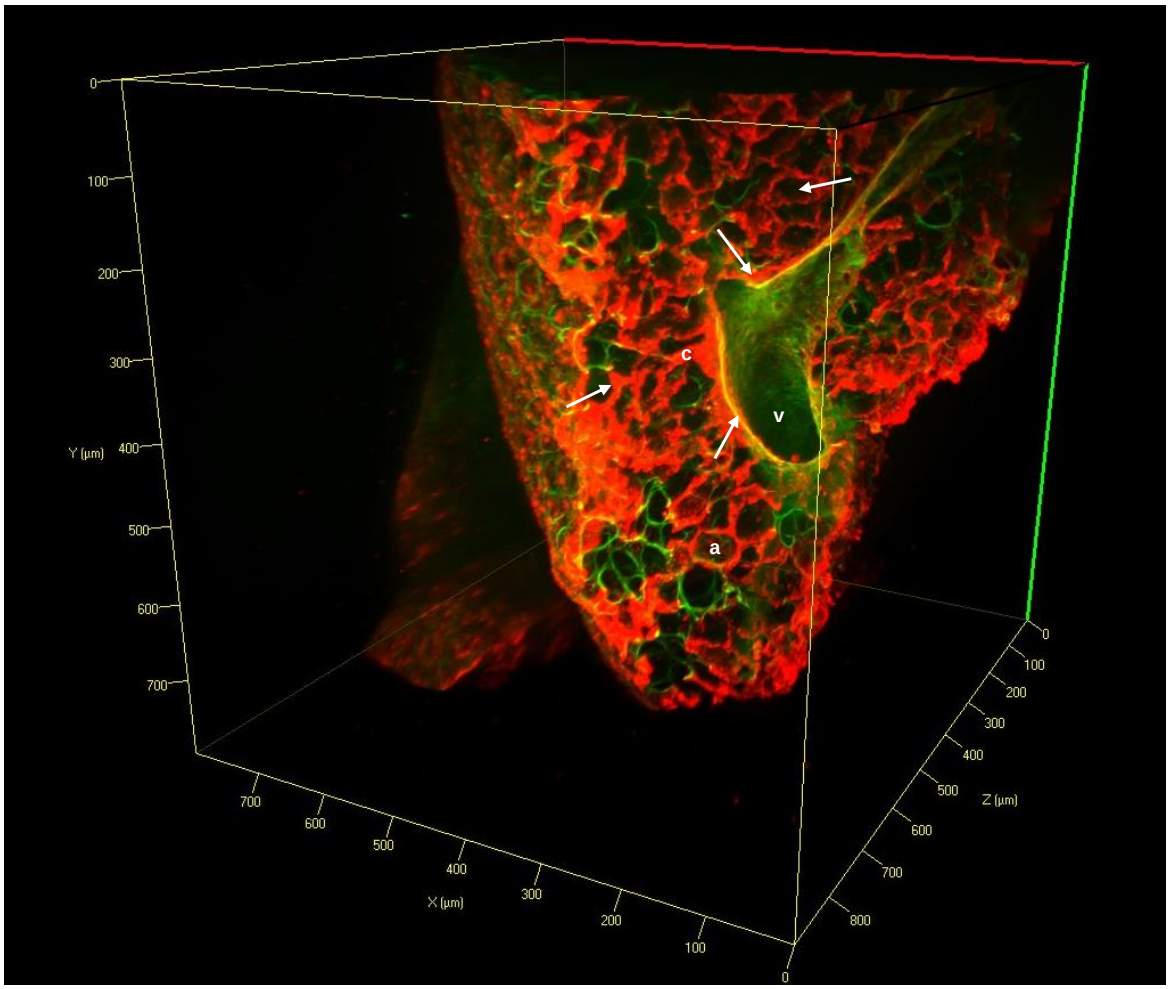

Figure 6: Ubiquitous distribution of TRPV4 in the murine lung. Representative 3D image of TRPV4 expression in the distal tip of the right lower lobe assessed by light sheet fluorescence microscopy. TRPV4 expression is shown in red and pulmonary structures (collagen scaffold) by green autofluorescence. White arrows indicate the expression of TRPV4 along alveoli (a), capillaries (c) and larger blood vessels (v). Scale bars are shown along x-, y- and z-axes in a maximal range of 800-900 µm.

To assess the functional role of TRPV4 in an *in vivo* scenario of ventilator-induced lung injury, the effects of genomic TRPV4 deficiency or pharmacological inhibition were quantified in mice during mechanical ventilation with pathological high tidal volumes of 20 mL/kg body weight as described in section 3.1.2. Mechanical ventilation with high tidal volumes caused an increase in lung wet-to-dry weight ratio (Figure 7 A), indicating the formation of lung edema, compared to animals ventilated with low tidal volumes or unventilated controls. High tidal volume ventilation also reduces barrier function, indicated by increased protein concentration in BALF and HSA extravasation into the alveolar space (Figure 7 B-C). These measures of lung hyperpermeability were significantly attenuated by HC-067047 (20 nMol/L), showing that TRPV4 inhibition has attenuated the detrimental effects of HV_T on barrier function and edema formation. A similar protective effect against overventilation induced vascular barrier failure was evident in TRPV4-deficient mice (Figure 7 A-C).

Histological examination and evaluation of lung injury score in HE-stained lung sections revealed lung parenchymal damage, thickening of alveolar septa and severe infiltration of neutrophils in HV_T lungs (Figure 7 E), which was accordingly reflected in a marked increase in the histological lung injury score (Figure 7 D) as compared to LV_T lungs or unventilated controls. In line with the protective effects on vascular hyperpermeability, HC-067047-treated and TRPV4-deficient HV_T groups showed less lung injury in representative histological images and had lower lung injury scores.

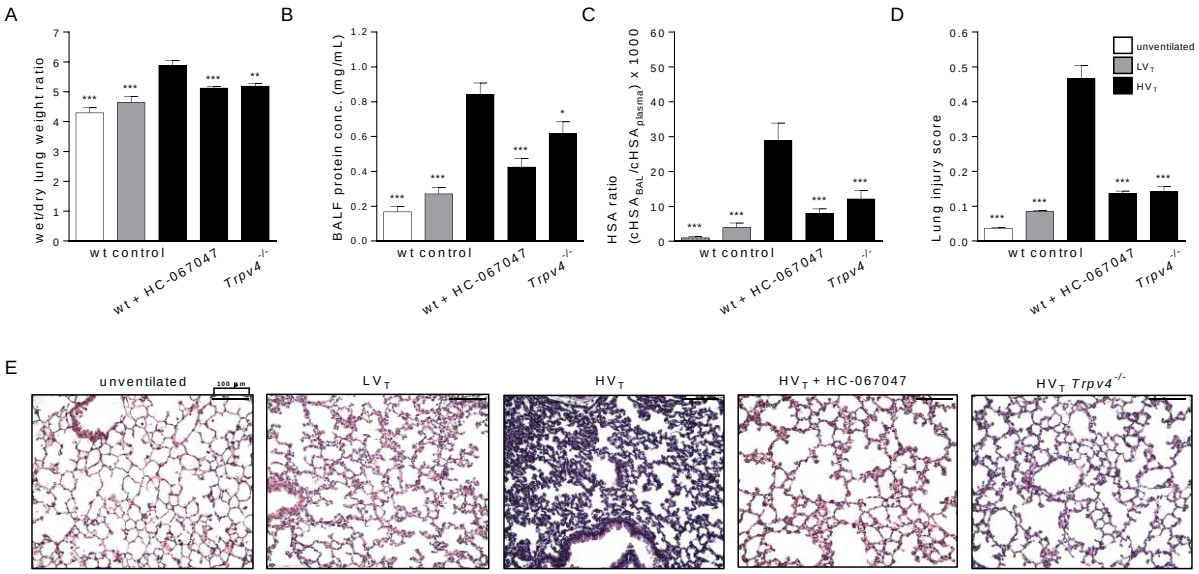

Figure 7: Pharmacological TRPV4 inhibition or genetic deficiency attenuate formation of lung edema, protein extravasation and histological characteristics of lung injury in a 2 h murine VILI model: (**A**) Wet/dry lung weight ratio; (**B**) protein concentration in BALF, (**C**) HSA BALF/plasma concentration ratio as measure of protein hyperpermeability and (**D**) semi-quantitative analysis of histological signs of lung injury are given for unventilated mice, or mice ventilated with either low V_T (LV_T) of 7 mL/kg bw or high V_T (HV_T) of 20 mL/kg without (wt control) or with treatment with the TRPV4 antagonist HC-067047 (20 nMol/L), or in *Trpv4*$^{-/-}$ mice. (**E**) Representative histological images show HE-stained lung sections, scale

bar is 100 µm; n = 5 - 8 for unventilated and LV_T, n = 8 - 12 for HV_T groups; *$P < 0.05$; **$P < 0.01$; ***$P < 0.001$ versus HV_T wt control (modified after Michalick et al., 2017).

Inflammation at the alveolo-capillary barrier is a critical hallmark of VILI and contributes to barrier failure. Therefore, the involvement of TRPV4 in the release of inflammatory cytokines was quantified by determination of regulatory and pro-inflammatory cytokine concentrations of IL-1β and IL-10 as well as the chemokines MCP-1, RANTES, MIP-2 and KC, in the BALF. These cytokines are crucial mediators of leukocyte recruitment (Figure 8 A-F). For all tested cytokines, except MCP-1, a significantly increased in HV_T could be determined as compared to LV_T lungs or lungs from unventilated mice. The HV_T-associated inflammation was strongly attenuated by TRPV4 inhibition or deficiency, indicating a stabilizing effect on alveolar-capillary barrier and a reduction of inflammation at this site. In summary, these data demonstrate the critical role of TRPV4 as a central mediator of the characteristic hallmarks of VILI, such as pulmonary vascular hyperpermeability, edema formation, infiltration of immune cells and the release of inflammatory cytokines.

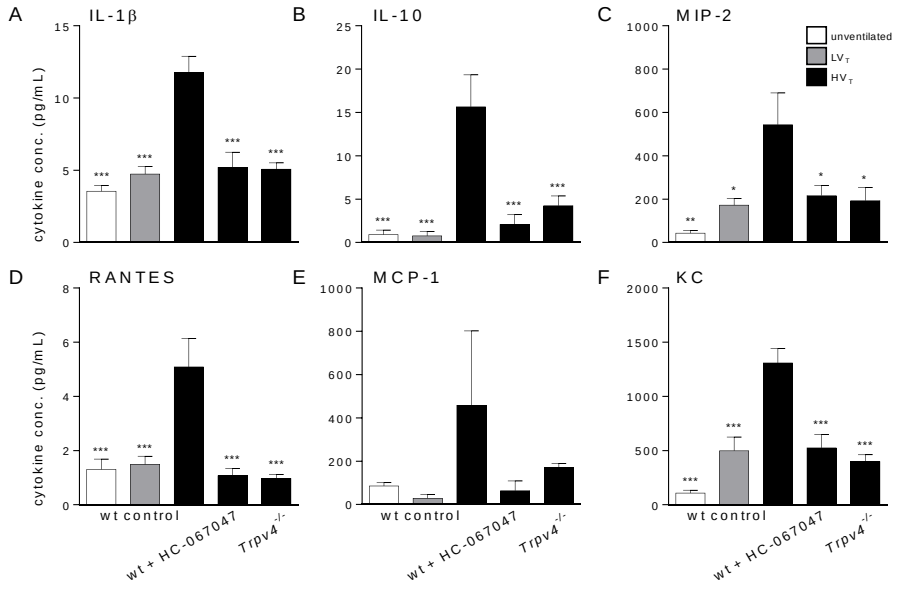

Figure 8: Pharmacological TRPV4 inhibition or genetic deficiency attenuate increased cytokine concentrations in bronchoalveolar lavage fluid in a 2 h murine VILI model: (**A**) IL-1β, (**B**) IL-10, (**C**) MIP-2; (**D**) RANTES, (**E**) MCP-1 and (**F**) KC were determined in BALF of unventilated, LV_T or HV_T ventilated mice without (wt control) or with treatment with HC-067047 (20 nMol/L), or in *Trpv4*$^{-/-}$ mice; n = 4 - 5 for unventilated and LV_T, n = 5 - 7 for HV_T groups; *$P < 0.05$; **$P < 0.01$; ***$P < 0.001$ versus HV_T wt control (modified after Michalick et al., 2017).

In the past decades, TRPV4 has gained more and more recognition as a critical mediator in a broad range of lung diseases including pulmonary hypertension (Song et al., 2014), lung fibrosis (Rahaman

et al., 2014), and allergic asthma (Cenac et al., 2010). Recently, our group could show that TRPV4 is not only an important mediator of pulmonary endothelial barrier integrity (Yin et al., 2008), but contributes critically to acute lung injury in a variety of different animal models including acid-induced lung injury (Yin et al., 2016). The rationale for these studies was the well-established major role that neutrophils play in the development and pathogenesis of lung injury and lung vascular barrier failure. As previous studies had suggested high expression levels of TRPV4 in human leukocytes (Spinsanti et al., 2008), we speculated that TRPV4 might critically regulate neutrophil function and that this effect may contribute relevantly to the development of TRPV4-dependent lung injury. To probe for the relative contribution of TRPV4 in pulmonary endothelial cells or other parenchymal cells versus TRPV4 on circulating blood cells including neutrophils, we generated TRPV4 chimeric mice by bone marrow transfer from *Trpv4*$^{+/+}$ or *Trpv4*$^{-/-}$ donor mice into previously lethally irradiated *Trpv4*$^{+/+}$ or *Trpv4*$^{-/-}$ recipient mice. Lung vascular permeability as well as protein extravasation into the alveolar space in response to acid instillation, measured as wet-to-dry lung weight ratio and protein concentration in bronchoalveolar lavage fluid, was largely reduced by genetic deficiency of TRPV4 in parenchymal cells, but not by TRPV4 deficiency in circulating blood cells (Figure 9 A, B). In line with these findings, lung injury scores and HE-stained lung sections revealed no protective effect of TRPV4 deficiency in circulating blood cells, whereas parenchymal loss of TRPV4 shows a similar effect on protection of lung structures as initially detected in *Trpv4*$^{-/-}$ (Figure 9 D, E). In contrast, myeloperoxidase activity as a measure for neutrophil infiltration into the extravascular space was significantly reduced by genetically encoded TRPV4 deficiency in circulating blood cells as well as in parenchymal cells (Figure 9 C). The parenchymal TRPV4 deficiency was also capable to protect from inflammation determined by BALF cytokine concentration given for IL-6, RANTES and MCP-1. These data show a clear trend against the expectation that inflammatory cytokines to be blocked by strategies targeting immune cells rather than parenchymal cells, although the differences in cytokine levels are not statistically significant, due to the small sample size. Moreover, it also seems that myeloid TRPV4 deficiency also blocks the secretion of MCP-1 and even more RANTES (Figure 9 F-H).

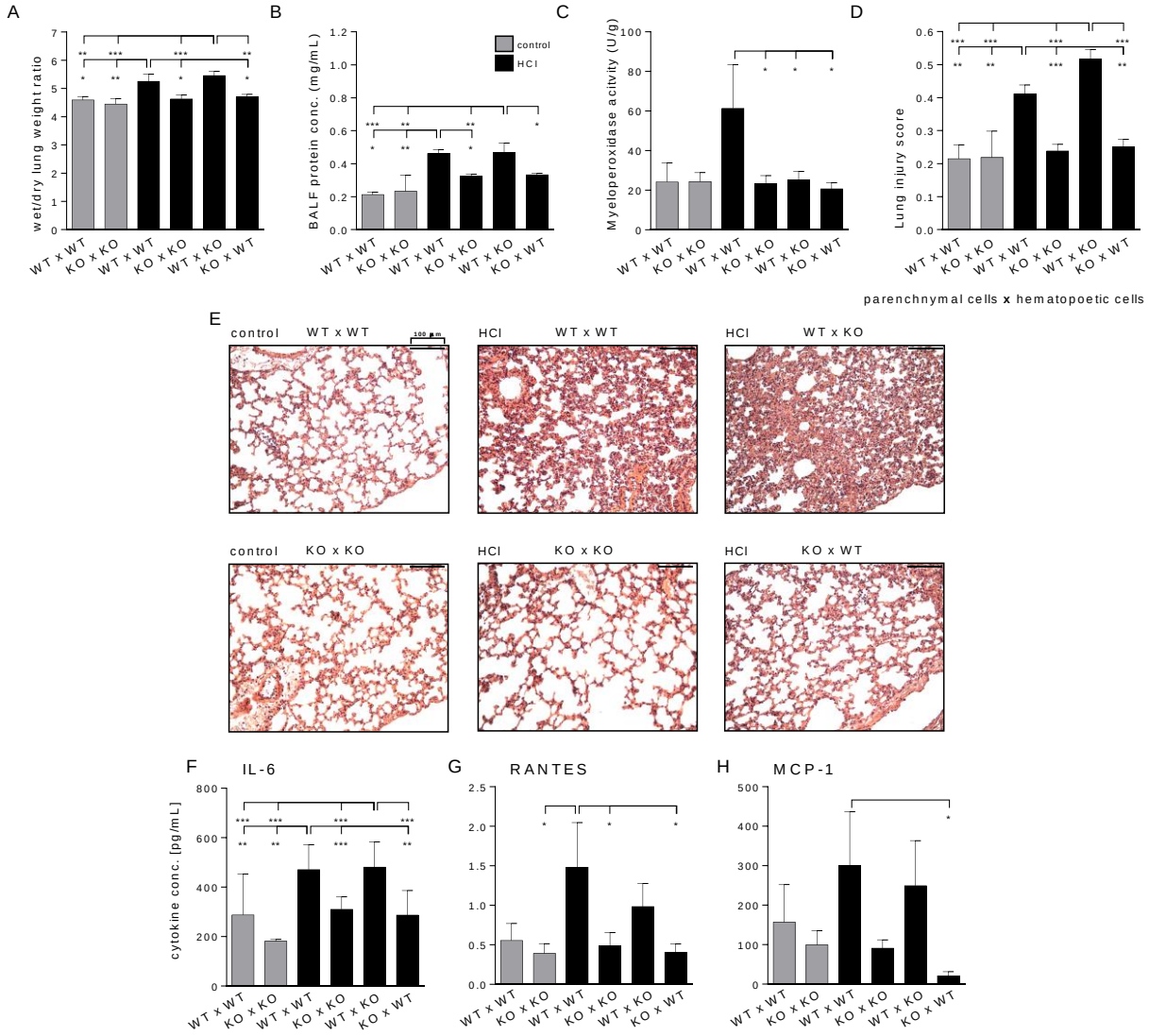

Figure 9: Role of TRPV4 in acid-induced acute lung injury relates primarily to TRPV4 expression on lung parenchymal rather than circulating blood cells: Group data show the effects of parenchymal (recipient) or myeloid (bone marrow) TRPV4 deficiency (*Trpv4*$^{-/-}$, KO vs wild type, WT) in bone marrow-transplanted chimeric mice following induction of acute lung injury by intratracheal instillation of HCl (black bars) or in control animals (grey bars). (**A**) Wet/dry lung weight ratio; (**B**) protein concentration in BALF, (**C**) lung myeloperoxidase (MPO) activity as a measure of neutrophil invasion and (**D**) semi-quantitative analysis of histological signs of lung injury are given for ventilated mice with intratracheal instillation of saline (control) or hydrochloric acid (HCl). (**E**) Representative histological images show HE-stained lung sections, 200x, scale bar is 100 µm. Cytokine concentrations in bronchoalveolar lavage fluid: (**F**) IL-6; (**G**) RANTES, (**H**) MCP-1; n = 3 for controls, n = 5 - 6 for HCl groups; **P* < 0.05; ***P* < 0.01; ****P* < 0.001 versus WTxWT (HCl) or WTxKO (HCl) groups (modified after Yin et al, 2016).

These results indicate that TRPV4 inhibition or deficiency has protective effects on pulmonary endothelial barrier function, alveolar inflammation and parenchymal microstructure.

4.2 SGK1 INHIBITION PREVENTS EXPERIMENTAL VILI *IN VIVO*.

Recently, Shin and colleagues identified SGK1 as novel regulator of TRPV4 (Shin et al., 2012). Similar to TRPV4, SGK1 is involved in osmoregulation and cell volume homeostasis (Wärntges et al., 2002; Lang et al., 2011; He et al., 2015), both of which are essentially mechanosensing and –transduction processes as they are largely regulated via membrane stretch. For that reason, we supposed that SGK1 is also involved in VILI-associated endothelial mechanotransduction and tested the effects of the pharmacological SGK1 antagonist GSK650394 in our model of experimental VILI. Analogous to TRPV4 antagonization, the inhibition of SGK1 was able to attenuate lung edema formation and pulmonary hyperpermeability in HV_T lungs by reducing the wet-to-dry lung weight ratio (Firgure 10 A), the protein accumulation in bronchoalveolar lavage fluid (Firgure 10 B), and the extravasation of HSA (Firgure 10 C) as compared to untreated HV_T mice. Similarly, SGK1 inhibition attenuated histological signs of lung injury in representative H&E sections (Firgure 10 E) and a semi-quantitative histological score (Firgure 10 D).

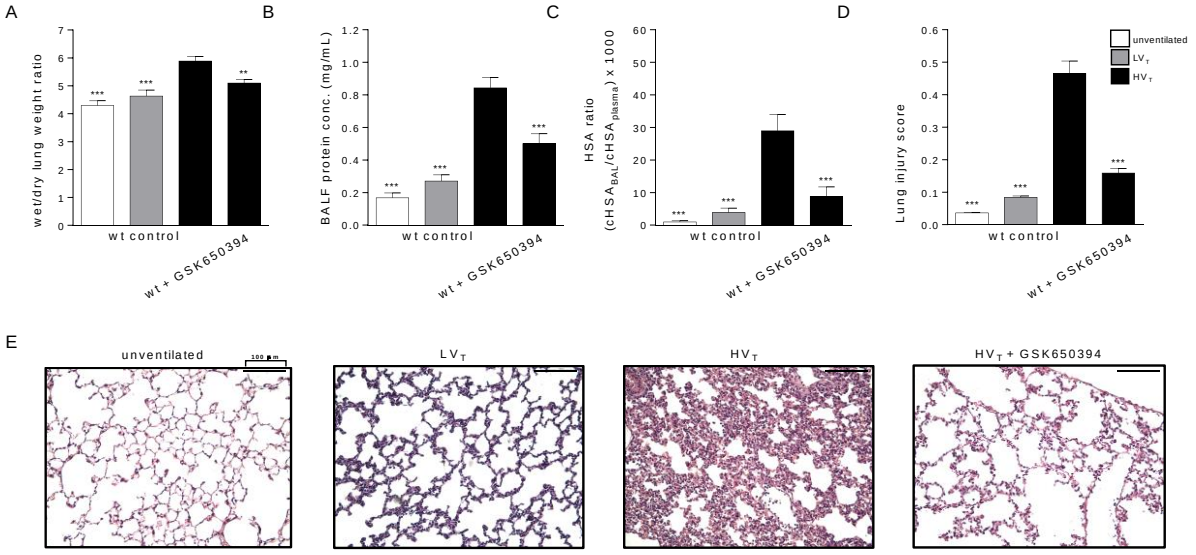

Figure 10: Pharmacological SGK1 inhibition attenuates formation of lung edema, protein extravasation and histological characteristics of lung injury in a 2 h murine VILI model: (**A**) Wet/dry lung weight ratio; (**B**) protein concentration in BALF; (**C**) HSA BALF/plasma concentration ratio as measure of protein hyperpermeability*;* and (**D**) semi-quantitative analysis of histological signs of lung injury are given for unventilated mice or mice ventilated with either low V_T (LV_T) of 7 mL/kg bw or high V_T (HV_T) of 20 mL/kg without (wt control) or with treatment with the SGK1 inhibitor GSK650394 (100 nMol/L). (**E**) Representative histological images show HE-stained lung sections, scale bar is 100 µm; n = 5 - 8 for unventilated and LV_T, n = 8 - 12 for HV_T groups; **P* < 0.05; ***P* < 0.01; ****P* < 0.001 versus HV_T wt control (modified after Michalick et al., 2017).

Inhibition of SGK1 could also attenuate the VILI-associated release of inflammatory, modulatory and chemotactic cytokines in the alveolar space except for MPC-1 due to considerable data variability in the HV_T group (Figure 11 A-F).

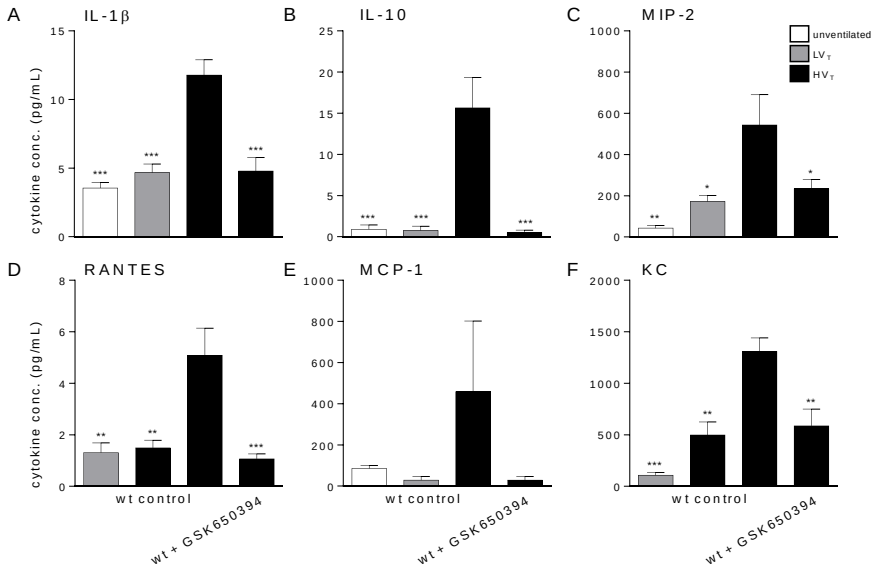

Figure 11: Pharmacological SGK1 inhibition attenuates the increase of cytokine concentrations in bronchoalveolar lavage fluid in a 2 h murine VILI model: (**A**) IL-1β, (**B**) IL-10, (**C**) MIP-2; (**D**) RANTES, (**E**) MCP-1 and (**F**) KC were determined in BALF of unventilated, LV_T or HV_T ventilated mice without (wt control) or with treatment with GSK650394 (100 nMol/L); n = 4 - 5 for unventilated and LV_T, n = 5 - 7 for HV_T groups; * $P < 0.05$; ** $P < 0.01$; *** $P < 0.001$ versus HV_T wt control (modified after Michalick et al., 2017).

Taken together, the inhibition of SGK1 was able to replicate the effects of TRPV4 antagonization in a murine VILI model, indicating a potential functional coupling of both molecules in lung mechanotransduction. In line with the view that SGK1 and TRPV4 participate in the same mechanotransduction pathway, the relative mitigating effects of both TRPV4 and SGK1 inhibition on the various read-out parameters of lung injury in overventilated mice showed a strong linear correlation (Figure 12).

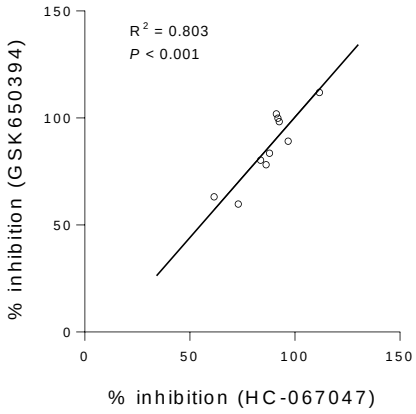

Figure 12: Correlation between the mitigating effects of TRPV4 versus SGK1 inhibition on characteristics of ventilator-induced lung injury. Scatter plot, followed by linear regression analysis show the relative inhibition induced by the TRPV4 inhibitor HC-067047 versus the relative inhibition of the same parameter by the SGK1 inhibitor GSK650394. Relative inhibition was calculated as (HV_T inhibitor – HV_T control)/(LV_T control – HV_T control) [in %] for mean values of the wet-to-dry lung weight ratio, protein concentration in BALF, HSA BALF/plasma concentration ratio, histological lung injury score, and BALF concentrations of IL-1β, IL-10, MIP-2, RANTES, MCP-1 and KC. Each individual parameter is represented by one single data point. $R^2 = 0.803$; $P < 0.001$ (modified after Michalick et al., 2017).

4.3 TRPV4 AND SGK1 MEDIATE THE ENDOTHELIAL $[Ca^{2+}]_i$ RESPONSE TO VENTILATION-INDUCED MECHANICAL STRETCH.

In previous work by us and others, Ca^{2+} influx via TRPV4 was identified as a key regulator of lung endothelial permeability and inflammatory cell signaling (Hamanaka et al., 2007; Jian et al., 2008; Yin et al., 2008, 2016). According to this, SGK1 is assumed to be involved in this scenario in which SGK1 phosphorylates TRPV4 and enhances channel gating in response to overventilation and results in increased endothelial $[Ca^{2+}]_i$ signaling, specifically in lung microvascular endothelial cells. To quantify the endothelial $[Ca^{2+}]_i$ response in the isolated, buffer-perfused mouse lung, the lung was continuously inflated with a baseline pressure of 5 cmH_2O ($CPAP_{low}$) following elevation to 15 cmH_2O ($CPAP_{high}$), whereby the applied pressures corresponded to the peak airway pressures, which were recorded in the ventilation experiments *in vivo* for LV_T (5.275 ± 0.11 cmH_2O) and HV_T (15.35 ± 0.45 cmH_2O), respectively. The rapid increase of the inflated pressure to 15 cmH_2O caused a correlating enhancement of endothelial $[Ca^{2+}]_i$, in untreated lungs from wild type mice (wt control), which was quantified as an elevated 340/380 Fura-2 fluorescence ratio. Notably, the elevated endothelial $[Ca^{2+}]_i$ sustained for more than 15 min after CPAP elevation (Figure 13 B,D). In lungs from mice lacking functional TRPV4 or pretreated with TRPV4 inhibitor, the endothelial $[Ca^{2+}]_i$ response to CPAP elevation was attenuated. In line with the proposed role of SGK1 as regulator of TRPV4 activity, the inhibition by GSK650394 was able to mitigate the effects of acute increase of inflation pressure on endothelial $[Ca^{2+}]_i$ (Figure 13 C,D). In summary, these data identified TRPV4 and its upstream regulating kinase SGK1 as key regulators of the mechanosensitive $[Ca^{2+}]_i$ response in the pulmonary microvascular endothelium.

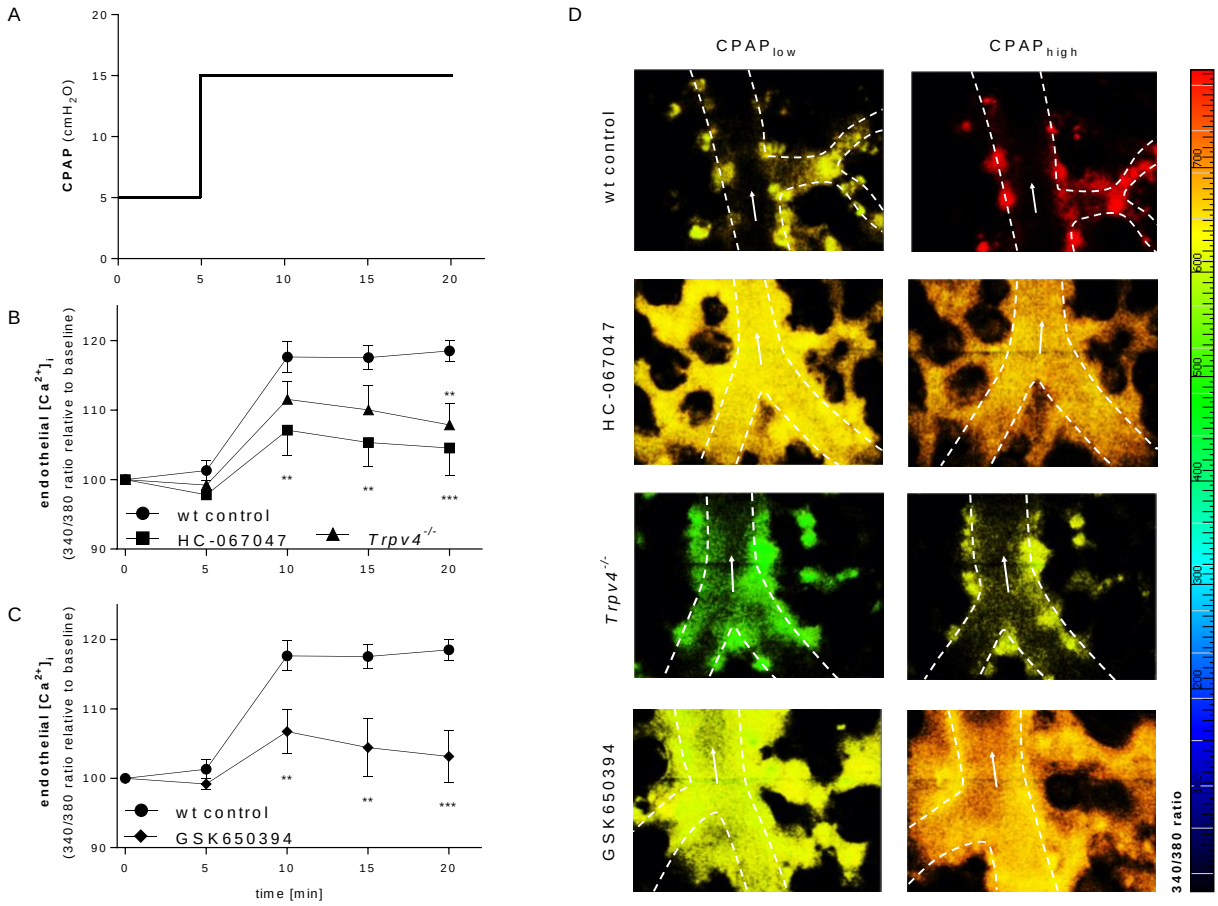

Figure 13: TRPV4 and SGK1 mediate endothelial Ca^{2+} influx in response to ventilation-induced mechanical stretch in isolated perfused mouse lungs: (**A**) Experimental protocol. Line and scatter plots show endothelial $[Ca^{2+}]_i$ (as 340/380 ratio relative to the individual baseline) at low (5 cmH_2O) and high (15 cmH_2O) continuous positive airway pressure (CPAP) in the absence (wt control) or presence of (**B**) the TRPV4 inhibitor HC-067047 (20 nMol/L), or in *Trpv4*$^{-/-}$, or (**C**) in the presence of the SGK1 inhibitor GSK650394 (100 nMol/L); (**D**) representative images of endothelial $[Ca^{2+}]_i$ (color-coded for 340/380 ratio) in microvessels of the isolated perfused mouse lung; white arrows indicate the direction of blood flow, dotted lines the vessel margins; n = 7-9 each; $*P < 0.05$; $**P < 0.01$; $***P < 0.001$ versus wt control at the identical timepoints (modified after Michalick et al., 2017).

4.4 SGK1 BINDS TO TRPV4 AND PHOSPHORYLATES AT SER824 *IN VITRO.*

The study by Shin and colleagues (2012) revealed also that SGK1 acts as a novel regulator of TRPV4 by phosphorylation of its Ser824 and thereby enhancing channel activity and TRPV4-mediated Ca^{2+} influx (Shin et al., 2012). To follow up these interesting findings, I assume that SGK1 phosphorylates TRPV4 in a ventilation volume-dependent manner in our experimental model of VILI. By co-immunoprecipitation analyses, TRPV4-immunoprecipitates were immunoblotted against SGK1 and observed an interaction of TRPV4 with SGK1, which was increased in the HV_T lungs as compared to lungs ventilated with low volume (Figure 14 A). In a next step, TRPV4-immunoprecipitates from lung lysates were immunoblotted against the phosphorylation of the Ser824 phosphosite (Figure 14 B), and determined in post-hoc densitometry the band intensities of pSer824 over total TRPV4 (Figure 14 C). These data could detect an enhanced phosphorylation of TRPV4 at Ser824 in the HV_T group as compared to unventilated or LV_T lungs. The treatment with the SGK1 inhibitor was capable to attenuate TRPV4 phosphorylation at this phosphosite about approximately 50% as compared to the HV_T lungs, which not received the inhibitor.

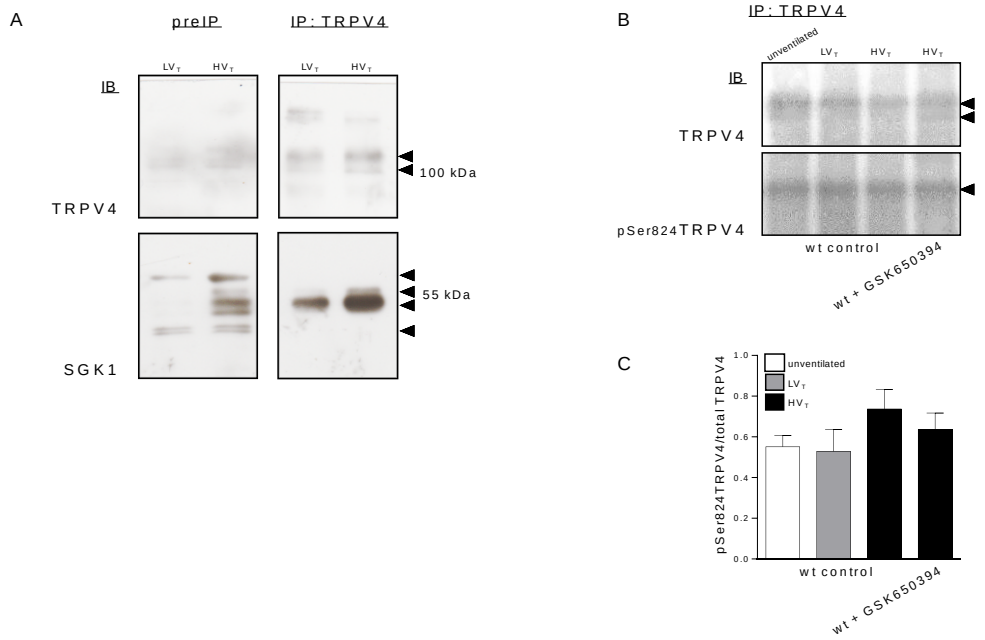

Figure 14: SGK1 interacts with TRPV4 and phosphorylates Ser824 in overventilated lungs: (**A**) Wild-type mice were subjected to either low tidal volume (LV_T) of 7 mL/kg bw or high tidal volume (HV_T) of 20 mL/kg for 2 h, and whole-lung lysates were collected. Immunoprecipitation was performed using an anti-TRPV4 antibody. Captured proteins were electrophoresed and subsequently immunoblotted for TRPV4 or SGK1 with 500 µg total protein for IP, or 30 µg for PreIP, respectively. Replicated in n = 3 each. (**B**) Wild-type mice were left unventilated, or subjected to either LV_T or HV_T in the absence or presence of the SGK1 inhibitor GSK650394 (100 nMol/L). Whole-lung lysates were collected, immunoprecipitated for TRPV4 and immunoblotted for total TRPV4 and the phospho-motif pSer824. (**C**) Densitometric quantification shows expression of the pSer824 (RXRXXS*/T*) motif relative to total TRPV4 (*LI-COR* Image Studio lite™); n = 3-4 individual experiments each (modified after Michalick et al., 2017).

As it is rather atypical that soluble cytoplasmic enzymes like SGK1 will bind to their substrate for a detectable period of time, I applied the more direct PLA assay on stretched HPMVECs to test whether TRPV4 as a transmembrane protein binds directly to SGK1. To this end, 18 % stretch (mimicking high tidal volume ventilation) was applied to adherent cells and compared to 5 % stretch (mimicking low tidal volume ventilation) or a static control. Indeed, PLA analysis revealed a significant increase of direct interaction (i.e. a proximity between interaction partners of 30 nm or less) between SGK1 and TRPV4 (Figure 15). As such, I was able to verify in two independent approaches that SGK1 interacts directly or indirectly with TRPV4 in stretched endothelial cells or lungs, respectively. A possible explanation for the assumed longevity of this interaction, which is supposed to underlie its detectability by co-immunoprecipitation and PLA assays, respectively. This finding could be the result of a direct interaction of both proteins or an indirect interaction facilitated by scaffold proteins, like AKAP79/150.

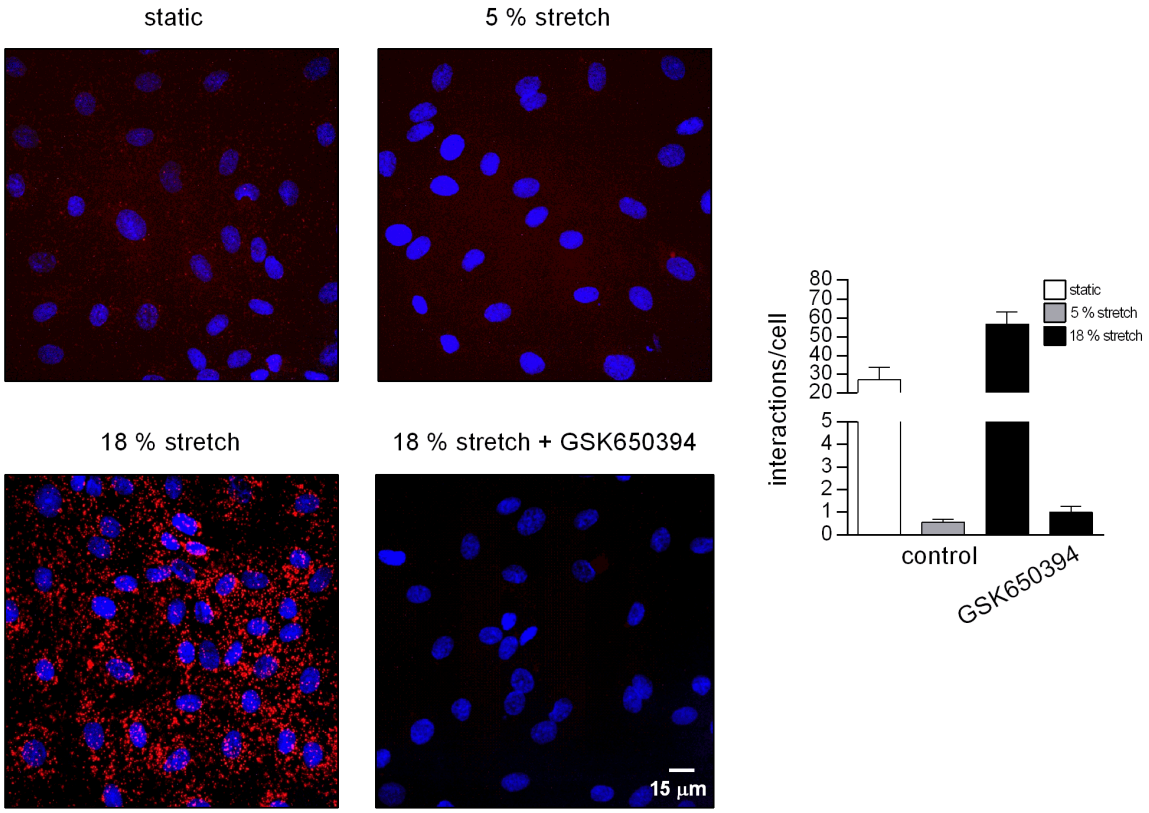

Figure 15: Stretch-induced interaction between TRPV4 and SGK1. Confocal microscopy in combination with proximity ligation assay was applied to assess the interaction between TRPV4 and SGK1. Human pulmonary microvascular endothelial cells were exposed to static conditions or cyclic stretch of either 5% or 18% elongation in the absence or presence of the SGK1 inhibitor GSK650394 (100 nMol/L) for 2 h. The interactions of TRPV4 with SGK1 are represented by red puncta, DNA was counterstained with DAPI (blue). Scale bar represents 15 µm. Representative images and quantitative bar graph show enhanced interaction between TRPV4 and SGK1 at 18% stretch that is prevented by SGK1 inhibition. Data from n = 2 independent replicates with 5 image sections averaged per slide.

To circumvent the putative dilutive effect of precipitated TRPV4 from different, and perhaps not stretch-responsive cell types in the whole lung, PLAs were used to quantify the Ser824 phosphorylation of TRPV4 in cultured HPMVECs after cyclic stretch. The PLA assay, which was applied here to assess phosphorylation of a specific protein residue rather than protein-protein interaction, revealed a significant increase in Ser824 phosphorylation after stretching the cells with 18% biaxial stretch as compared to 5% stretch or static controls, yet pharmacological inhibition of SGK1 by GSK650394 attenuated Ser824 phosphorylation in cells 18%-stretched cells (Figure 16). These findings underline the co-imunopreciptiation data and show that SGK1 mediates TRPV4 phosphorylation at Ser824 induced by stretch of cultured HPMVECs or overventilated lungs *in vivo*.

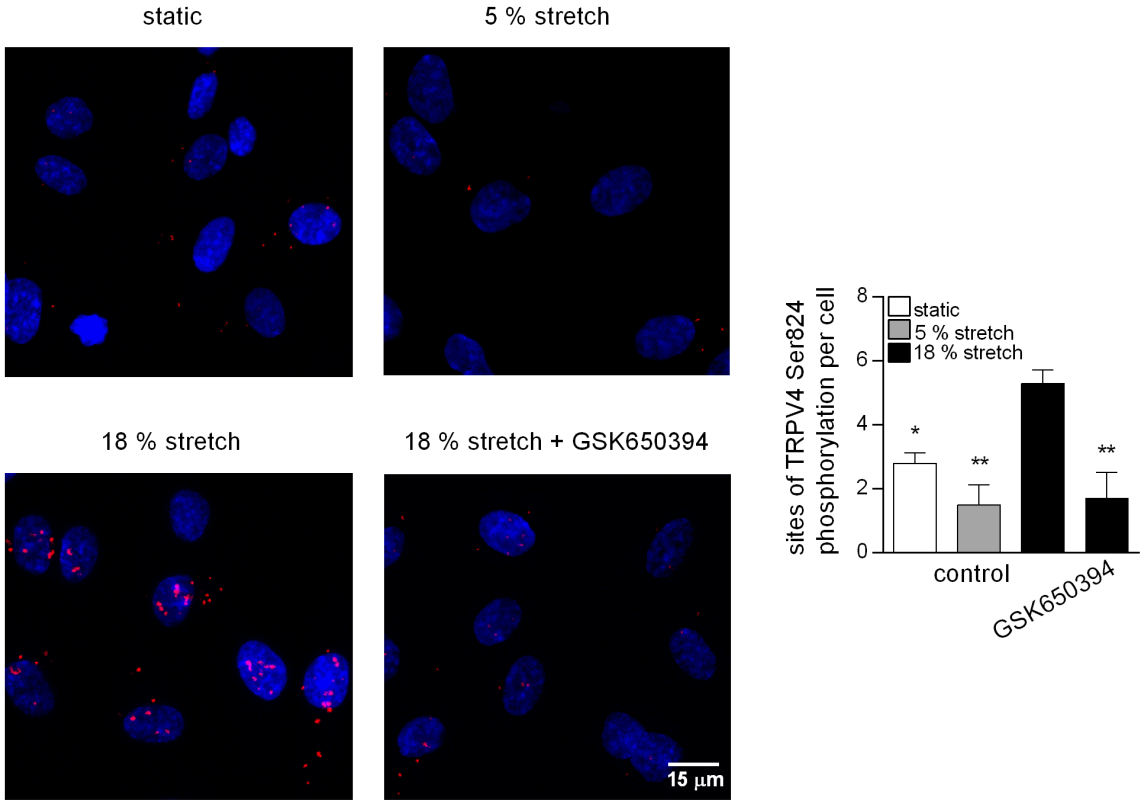

Figure 16: Stretch-induced phosphorylation of TRPV4 at Ser824 is mediated by SGK1. Confocal microscopy in combination with proximity ligation assay was applied to assess phosphorylation of TRPV4 at Ser824. Human pulmonary microvascular endothelial cells were exposed to static conditions or cyclic stretch of either 5% or 18% elongation in the absence or presence of the SGK1 inhibitor GSK650394 (100 nMol/L) for 2 h. Sites of TRPV4 phosphorylation are represented by red puncta, DNA was counterstained with DAPI (blue). Scale bar represents 15 µm. Representative images and quantitative bar and scatter graph show enhanced Ser824 phosphorylation of TRPV4 at 18% stretch that is prevented by SGK1 inhibition. Data from n = 3 independent replicates with 5 image sections averaged per slide; $*P < 0.05$; $**P < 0.01$ versus 18 % stretch control (modified after Michalick et al., 2017).

Interestingly, in all PLA experiments static cultured HPMVECs showed higher levels of SGK1-TRPV4 interaction or TRPV4 phosphorylation as compared to cultures, which were stretched with 5% elongation. As cyclic elongation by approximately 5% reflects the physiological situation in the living organism, these results suggest that not only higher level of endothelial stretch, but likewise complete absence of stretch in a static cell culture of endothelial cells induces mechanical stress signaling.

Taken together, the present results demonstrate a critical role for TRPV4 channel activity in ventilation-induced mechanotransduction and the subsequent endothelial $[Ca^{2+}]_i$ response, vascular barrier failure, and pro-inflammatory signaling in the pulmonary microvasculature *in vivo*, *ex vivo* and *in situ*. Additionally, SGK1 could be identified as activity-regulating kinase of the TRPV4 Ca^{2+} channel in the context of endothelial barrier disruption in response to mechanical stress.

4.5 Ca^{2+}-ACTIVATED K^+ CHANNELS PLAY A CRITICAL ROLE IN VILI

Ca^{2+}-activated K^+ channels are classic responders to increased intracellular Ca^{2+} levels. Activation by binding of Ca^{2+}-CaM to the C-terminal CaMBD of these channels leads to channel opening and K^+ efflux, which in turn causes hyperpolarization of the plasma membrane. Here, I hypothesized that i) TRPV4-mediated Ca^{2+} signaling in VILI will activate K_{Ca} channels, ii) that the resulting hyperpolarization may act as a positive feedback on TRPV4 activity, and iii) that pharmacological inhibition of Ca^{2+}-activated K^+ channels may thus prevent or attenuate the characteristic signs of VILI. To address these hypotheses, the endothelial expression of all putatively involved Ca^{2+}-activated K^+ channels in HPMVECs was assessed by SDS-PAGE followed by western blotting in three independent approaches (Figure 17).

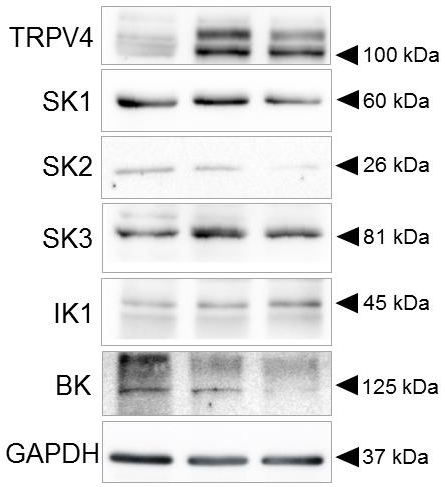

Figure 17: Expression of TRPV4 and Ca^{2+}-activated K^+ channels in HPMVECs. Cell lysates were collected and 10 µg were separated in a 10% SDS-PAGE. For immunoblotting, the PVDF-Membrane was incubated with primary antibodies raised against TRPV4 (1:5000, Stefan Heller, Stanford University), SK1 (1:400), SK2 (1:1000); SK3 (1:400), IK1 (1:400), BK (1:400) and GAPDH (1:5000).

Similar to SGK1 inhibition, non-selective blocking of Ca^{2+}-activated K^+ channels as a putative downstream target of TRPV4 activation by 10 nMol/L apamin for SK1-3 or 100 nMol/L charybdotoxin for IK1 and BK channels reduced overventilation-induced lung edema (Figure 18 A,E). Notably, treatment with charybdotoxin also significantly reduced pulmonary hyperpermeability while corresponding effects of apamin failed to reach significance (Figure 18 B, C). In addition, the analysis of histological samples showed less cellular infiltration by neutrophils, alveolar wall thickening and proteinaceous debris in both, apamin and charybdotoxin-treated lungs (Figure 18 D,E). Since it has been shown that TRPV4 activation has little impact on BK currents (M. T. Lin et al., 2015), and since expression levels of BK are low as compared to SK and IK channels in HPMVECs (Figure 17), IK1

channels became more into focus of interest, and the application of the selective IK1 blocker TRAM34 (1 µMol/L) in this *in vivo* model. The data from these experiments showed a similar attenuating effect of TRAM34 on lung injury as seen with charybdotoxin (Figure 18), but bordered the statistical significance level in W/D ratio. This let suggest that SK1-3 as well as IK1 play an important role in the pathogenesis of VILI, presumably by inducing endothelial cell membrane hyperpolarization, and amplification of TRPV4 channel activity.

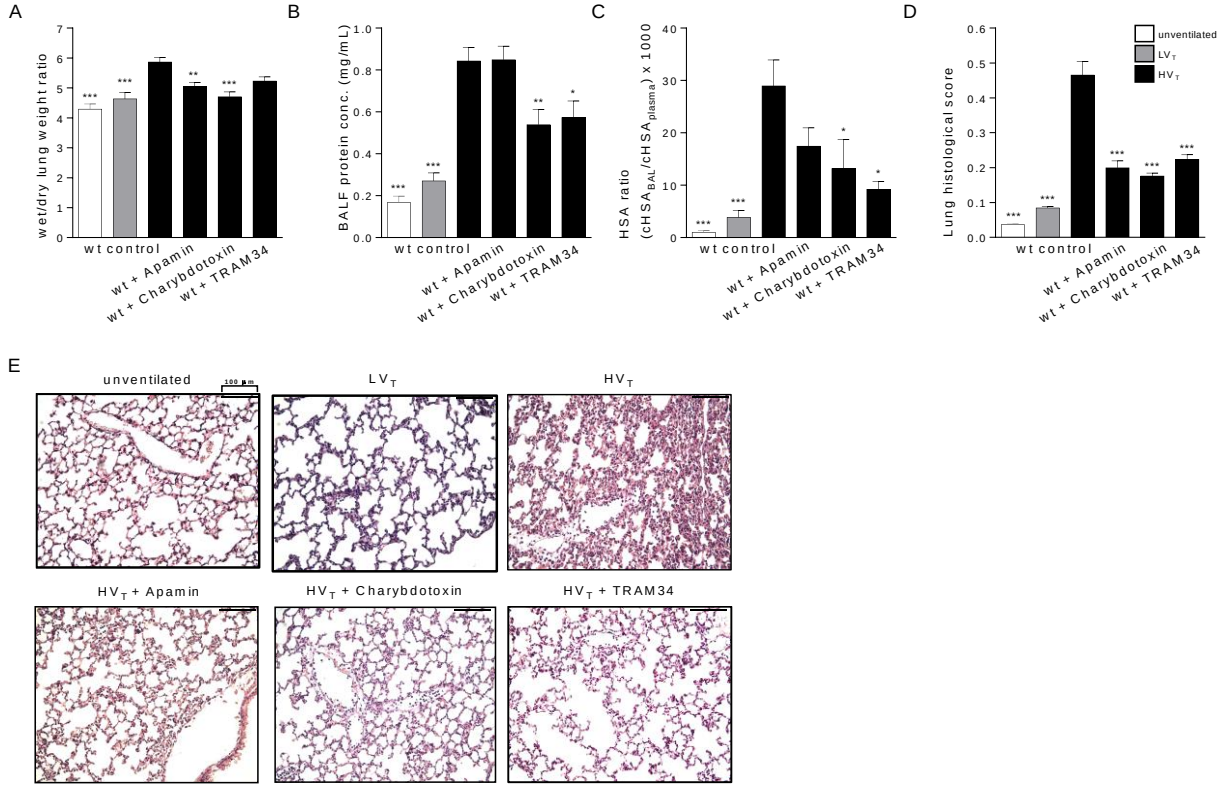

Figure 18: Pharmacological inhibition of Ca^{2+} activated K^+ channels attenuate formation of lung edema, protein extravasation and histological characteristics of lung injury in a 2 h murine VILI model: (**A**) Wet/dry lung weight ratio; (**B**) protein concentration in BALF, (**C**) HSA BALF/plasma concentration ratio as measure of protein hyperpermeability and (**D**) semi-quantitative analysis of histological signs of lung injury are given for unventilated mice, or mice ventilated with either low V_T (LV_T) of 7 mL/kg bw or high V_T (HV_T) of 20 mL/kg without (wt control) or with treatment with 10 nMol/L apamin (SK1-SK3 antagonist), 100 nMol/L charybdotoxin (IK1, BK antagonist), or 1 µMol/L TRAM34 (selective IK1 antagonist); (**E**) representative histological images show HE-stained lung sections, scale bar is 100 µm; n = 5 - 8 for unventilated and LV_T, n = 6-8 for HV_T groups; **P* < 0.05; ***P* < 0.01; ****P* < 0.001 versus HV_T wt control.

Similar to the effects of TRPV4 and SGK1 inhibition, antagonization of Ca^{2+}-activated K^+ channels attenuated VILI-associated airspace inflammation, as measured by the release of inflammatory, modulatory and chemotactic cytokines in the alveolar space. Blocking of SK1-3 channels by apamin showed a moderate tendency to decrease inflammatory cytokine concentrations in bronchoalveolar

fluid, yet without reaching significance, whereas inhibition of IK1 channels by either charybdotoxin or TRAM34 resulted in a strong and significant reduction of cytokine levels (Figure 19 A-F). These findings promote the hypothesis that the IK1 channel is not only a major regulator of endothelial permeability, but plays also a key role in the inflammatory signaling of VILI.

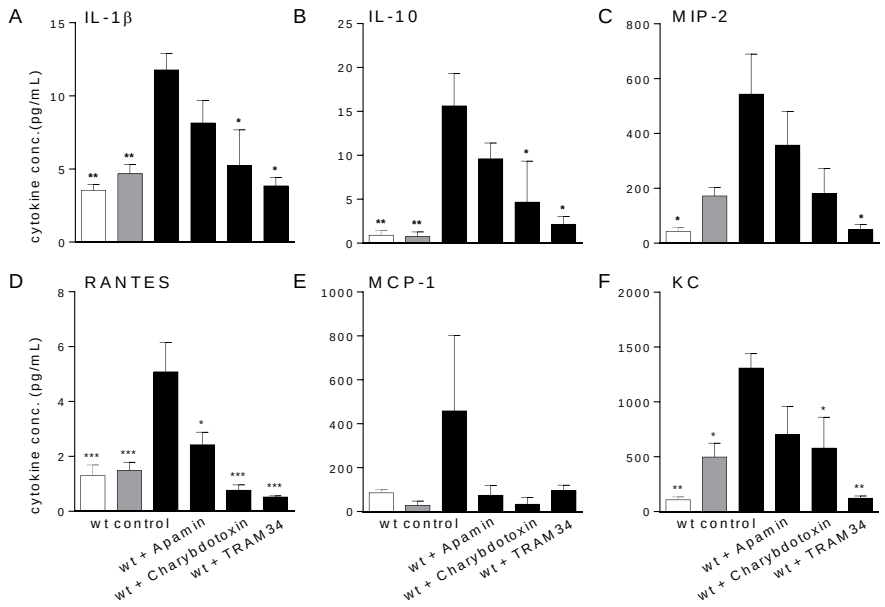

Figure 19: Pharmacological inhibition of Ca^{2+} activated K^+ channels attenuates increased cytokine concentrations in bronchoalveolar lavage fluid in a 2 h murine VILI model: (**A**) IL-1β, (B) IL-10, (**C**) MIP-2; (**D**) RANTES, (**E**) MCP-1, and (**F**) KC were determined in BALF of unventilated, LV_T or HV_T ventilated mice without (wt control) or with treatment with 10 nMol/L apamin (SK1-SK3 antagonist), 100 nMol/L charybdotoxin (IK1, BK antagonist), or 1 µMol/L TRAM34 (selective IK1 antagonist); n = 4 - 5 for unventilated and LV_T, n = 3 - 6 for HV_T groups; *$P < 0.05$; **$P < 0.01$; ***$P < 0.001$ versus HV_T wt control.

Previously in this work, it has been shown that TRPV4 acts as critical mechanosensor in the pulmonary endothelium that mediates the endothelial $[Ca^{2+}]_i$ response to mechanical stretch, and as such, plays a critical role in the pathophysiology of VILI. Based on the rationale that increased cytoplasmic Ca^{2+} levels will activate K_{Ca} channels, resulting in membrane hyperpolarization and – in a positive feedback loop - amplification of TRPV4 activity and ultimately, VILI, the inhibition of K_{Ca} channel activity might attenuate the endothelial $[Ca^{2+}]_i$ response to mechanical stretch in the intact lung. To this end, I quantified the endothelial $[Ca^{2+}]_i$ response in the isolated, buffer-perfused mouse lung to an increased CPAP, as described previously. In the untreated control lungs, a rapid increase in 340/380 Fura-2 fluorescence ratio was detectable upon a step-increase in CPAP (Figure 20 B–D). Administration of the nonselective K_{Ca} inhibitors apamin (10 nMol/L) or charybdotoxin (100 nMol/L) or treatment with the selective IK1 blocker TRAM34 (1 µMol/L) resulted in a less

pronounced increase in the 340/380 ratio as compared to the untreated control (Figure 9 B–D). Interestingly, the initial $[Ca^{2+}]_i$ increase following a step increase in CPAP was almost comparable in inhibitor-treated groups relative to untreated controls, yet the $[Ca^{2+}]_i$ signal decreased faster over time in the groups treated with K_{Ca} inhibitors. This suggests that K_{Ca} channel blockers inhibit the sustained response, but not the initial Ca^{2+} influx. These results are essentially in line with a positive feedback amplification mechanism regulating Ca^{2+} influx, and potentially TRPV4 by K_{Ca} channels, particularly IK1.

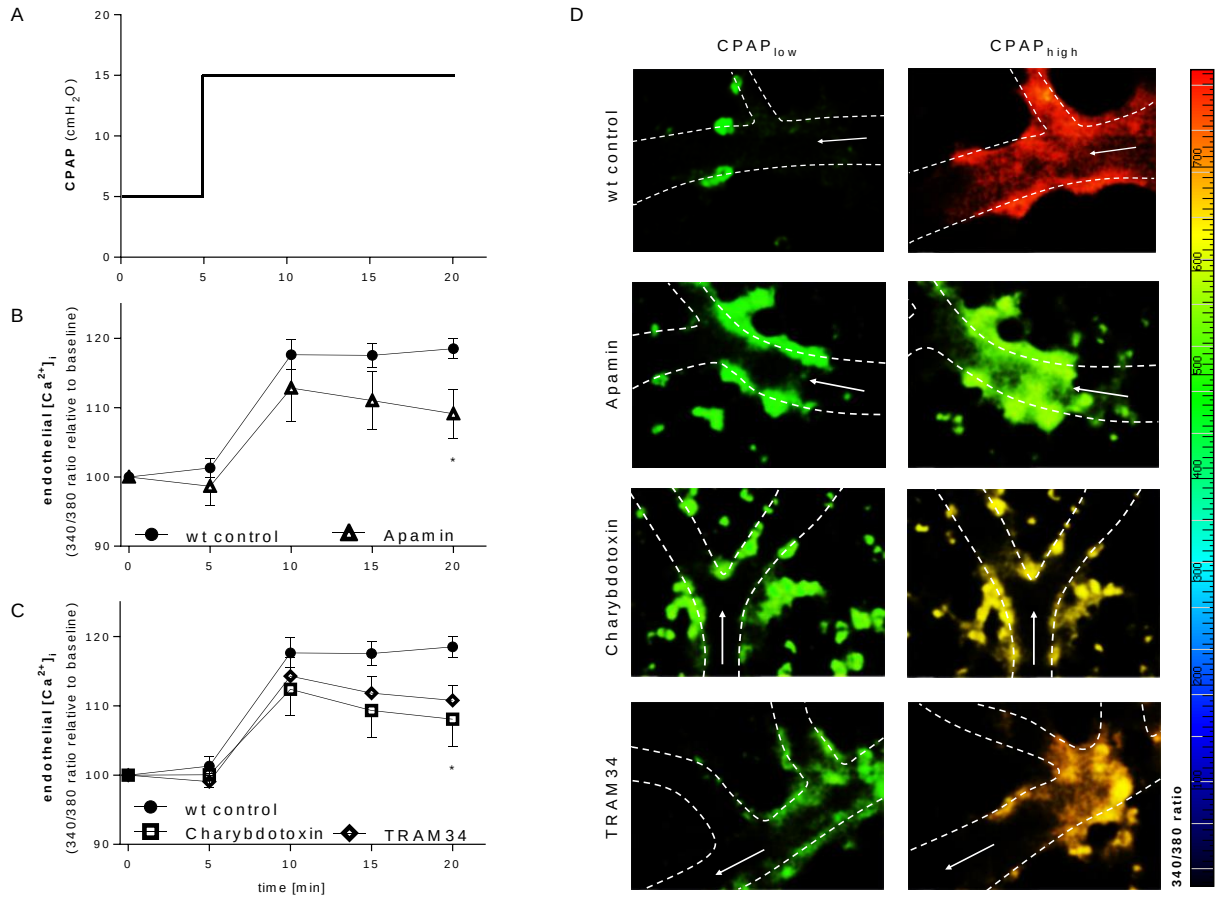

Figure 20: Ca^{2+} activated K^+ channels regulate endothelial Ca^{2+} influx in response to ventilation-induced mechanical stretch in isolated perfused mouse lungs: (**A**) Experimental protocol. Line and scatter plots show endothelial $[Ca^{2+}]_i$ (as 340/380 ratio relative to the individual baseline) at low (5 cmH_2O) and high (15 cmH_2O) continuous positive airway pressure (CPAP) in the absence (wt control) or presence of (**B**) the SK1-3 non-selective inhibitor apamin (10 nMol/L), or (**C**) in the presence of the IK1/BK non-selective inhibitor charybdotoxin (100 nMol/L), or the selective IK1 antagonist TRAM34 (1 µMol/L); (**D**) representative images of endothelial $[Ca^{2+}]_i$ (color-coded for 340/380 ratio) in microvessels of the isolated perfused mouse lung; white arrows indicate the direction of blood flow, dotted lines the vessel margins; n = 5–9 each; *$P < 0.05$; **$P < 0.01$; ***$P < 0.001$ versus wt control at the identical timepoints.

Taken together, the presented findings identify a novel downstream regulatory feedback on TRPV4-mediated Ca^{2+}- influx through Ca^{2+}-activated K^+ channels that amplifies and sustains endothelial Ca^{2+} signaling, vascular barrier failure, and ultimately, contributes to the pathophysiology of VILI.

4.6 TRPV1 REPRESENTS A NOVEL ACTOR IN THE PATHOPHYSIOLOGY OF VILI AND INTERACTS WITH TRPV4 DEPENDENT ON TRPV4 PHOSPHORYLATION OF SERINE RESIDUE 824

Recent work in collaboration with the group of Prof. Dr. Maik Gollasch shows a synergistic, but narrow, specialized role of TRPV1 and a more global role for TRPV4 in the regulation of renal vasodilatation (L. Chen et al., 2014). Based on these findings, I speculated that TRPV1 channel activity might be similarly involved into pulmonary endothelial mechanotransduction and progression of VILI as a result of functional coupling of both channels. Co-IPs from lung lysates obtained from mice subjected to unventilated, LV_T or HV_T revealed an interaction of TRPV4 with TRPV1, and the following densitometric analysis could show that the extent of this interaction is dependent on the ventilation mode in that the most interaction between the two channels could be detected in overventilated lungs. Interestingly, the level of interaction in response to overventilation was decreased in channel pore-deleted *Trpv4*$^{-/-}$ mice or by pharmacological inhibition of TRPV4 by HC-067047 or SGK1 inhibition by GSK650394 (Figure 21 A-B). Notably, the comparison of all densitometric analyses of TRPV4 – pSer824 and TRPV4 – TRPV1 revealed similar profiles over the different ventilation modes and inhibitor treatments (Figure 21), indicating an important regulatory connection between SGK1-mediated phosphorylation Ser824 and the interaction between the two TRPV channels. Taken together, these data show for the first time that TRPV4 interacts with TRPV1, and that this interaction is enhanced by mechanical overventilation, presumably in a manner that is dependent on the Ser824 phosphorylation status of TRPV4.

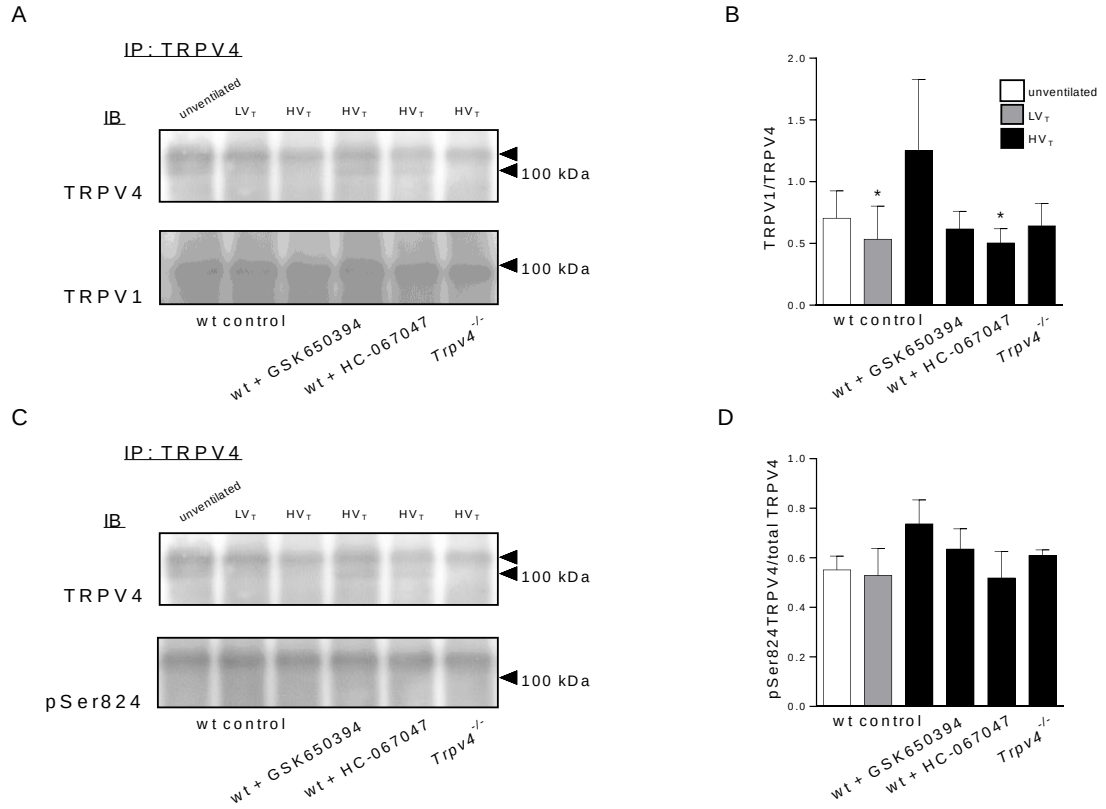

Figure 21: TRPV4 interacts with TRPV1 and the interactions show a similar profile to TRPV4 phosphorylation at Ser824: (**A**) Wild type or *Trpv4*$^{-/-}$ mice were subjected to either low tidal volume (LV_T) of 7 mL/kg bw or high tidal volume (HV_T) of 20 mL/kg for 2 h HV_T in the absence or presence of the SGK1 inhibitor GSK650394 (100 nMol/L), the TRPV4 inhibitor HC-067047 (10 nMol/L), or in *Trpv4*$^{-/-}$ mice, and whole-lung lysates were collected. Immunoprecipitation was performed using an anti-TRPV4 antibody. Captured proteins were electrophoresed and subsequently immunoblotted for total TRPV4 and TRPV1. (**B**) Densitometric quantification shows expression of TRPV1 relative to total TRPV4 (**C**) Immunoprecipitation of whole-lung lysates was performed using an anti-TRPV4 antibody. Captured proteins were electrophoresed and subsequently immunoblotted for total TRPV4 and the phospho-motif pSer824. (**D**) Densitometric quantification shows expression of the pSer824 (RXRXXS*/T*) motif relative to total TRPV4 (*LI-COR* Image Studio lite™); n = 3-4 individual experiments each; $*P < 0.05$ vs HV_T control.

To assess, whether TRPV1 itself is contributing to the progression of VILI, I next tested the highly specific TRPV1 inhibitor SB366791 (50 nMol/L) or used TRPV1-deficient mice in the experimental VILI-model *in vivo*. Both, functional knockout and pharmacological inhibition of the TRPV1 channel significantly reduced pulmonary hyperpermeability, measured as lung wet-to-dry ratio (Figure 22 A), protein content of BALF (Figure 22 B) and HSA extravasation into the alveolar space (Figure 22 C), showing that loss of TRPV1 function has a stabilizing effect on the vascular endothelial barrier in response to mechanical stress due to overventilation.

In line with these findings, histological examinations revealed less parenchymal damage, alveolar septal thickening and neutrophil infiltration after TRPV1 inhibitor treatment or in *Trpv1*$^{-/-}$ mice as demonstrated by representative HE-stained lung sections and the histological lung injury score (Figure **22** D, E).

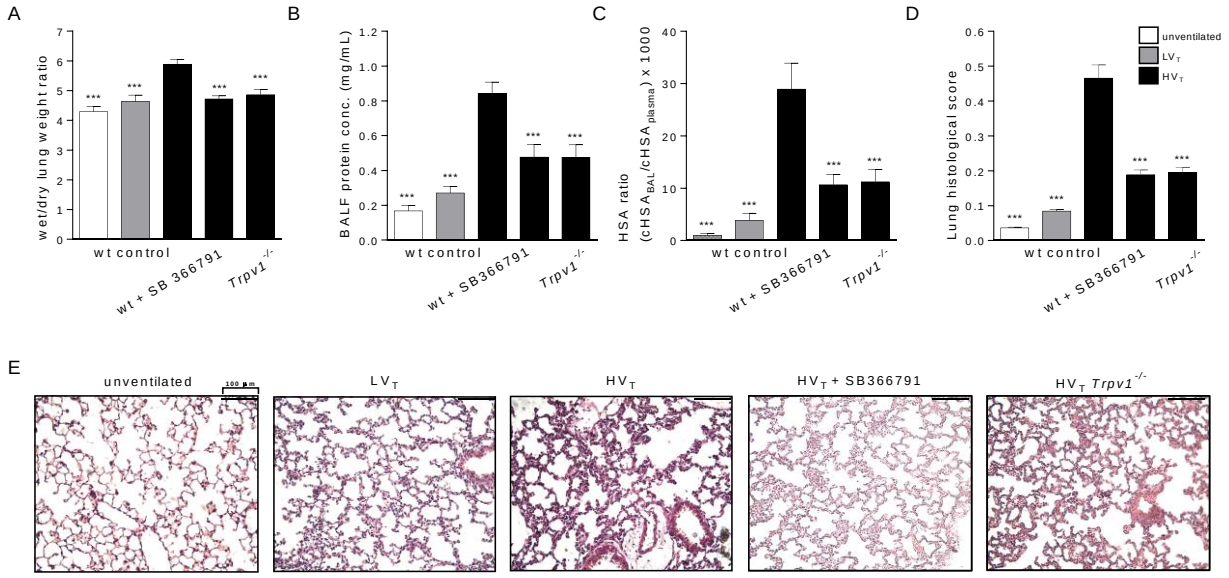

Figure 22: Pharmacological TRPV1 inhibition or genetic deficiency attenuate formation of lung edema, protein extravasation and histological characteristics of lung injury in a 2 h murine VILI model: (**A**) Wet/dry lung weight ratio; (**B**) protein concentration in BALF, (**C**) HSA BALF/plasma concentration ratio as measure of protein hyperpermeability and (**D**) semi-quantitative analysis of histological signs of lung injury are given for unventilated mice, or mice ventilated with either low V_T (LV_T) of 7 mL/kg bw or high V_T (HV_T) of 20 mL/kg without (wt control) or with treatment with the TRPV1 antagonist SB366791 (50 nMol/L), or in *Trpv1*$^{-/-}$ mice. (**E**) Representative histological images show HE-stained lung sections, scale bar is 100 µm; n = 5 - 8 for unventilated and LV_T, n = 8 - 11 for HV_T groups; **P* < 0.05; ***P* < 0.01; ****P* < 0.001 versus HV_T wt control.

After having shown that TRPV1 is required for induction of VILI, presumably by mediating endothelial Ca^{2+} signaling, I next aimed to test whether TRPV1 activation *per se* is sufficient to induce endothelial Ca^{2+} influx and subsequent barrier failure, or whether TRPV1 needs to act in conjunction with activation of other signaling pathways or ion channels such as TRPV4. To this end, real-time imaging in the isolated, buffer-perfused mouse lung was applied to quantify the endothelial $[Ca^{2+}]_i$ response to an increase in CPAP from 5 to 15 cmH_2O (Figure 23 A). In isolated and perfused mouse lungs from *Trpv1*$^{-/-}$ mice compared to wild type controls, the endothelial $[Ca^{2+}]_i$ response to overdistension was significantly reduced. Unexpectedly, treatment with the specific TRPV1-inhibitor SB366791 (50 nMol/L) could only diminish the sustained $[Ca^{2+}]_i$ response, but not the initial Ca^{2+} increase (Figure 23 B-C). While both TRPV1 deficiency and inhibition would block TRPV1-mediated

Ca^{2+} influx, TRPV1 deficiency, yet not TRPV1 inhibition may be expected to disrupt the protein-protein interaction between TRPV4 and TRPV1. Hence, the present data let suggest that the lung protective effect of TRPV1 deficiency *in vivo* and the reduced endothelial $[Ca^{2+}]_i$ responses of TRPV1-deficiency *ex vivo* are rather attributable to a structural interaction of TRPV1 with TRPV4 than on direct Ca^{2+} influx via TRPV1.

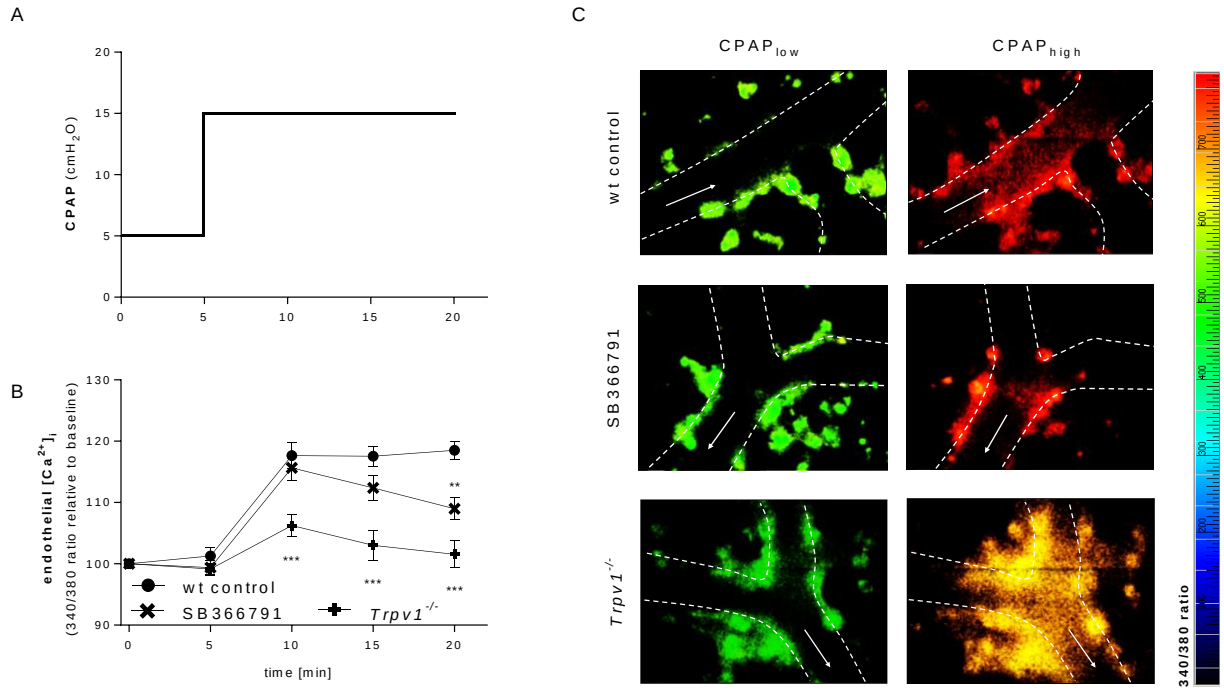

Figure 23: Role of TRPV1 in the endothelial $[Ca^{2+}]_i$ response to ventilation-induced mechanical stretch in isolated perfused mouse lungs: (**A**) Experimental protocol. Line and scatter plots show endothelial $[Ca^{2+}]_i$ (as 340/380 ratio relative to the individual baseline) at low (5 cmH_2O) and high (15 cmH_2O) continuous positive airway pressure (CPAP) in the absence (wt control) or presence of (**B**) the TRPV1 inhibitor SB366791 (50 nMol/L), or in *Trpv1*$^{-/-}$ mice, and (**C**) representative images of endothelial $[Ca^{2+}]_i$ (color-coded for 340/380 ratio) in microvessels of the isolated perfused mouse lung; white arrows indicate the direction of blood flow, dotted lines the vessel margins; n = 7–8 each; **P* < 0.05; ***P* < 0.01; ****P* < 0.001 versus wt control at the identical timepoints.

To validate this notion, the effect of direct TRPV1 and/or TRPV4 activation in HPMVECs was tested *in vitro*. Surprisingly, the selective TRPV1 agonist capsaicin had almost no effect on $[Ca^{2+}]_i$ in HPMVECs, while pharmacological activation of both TRPV1 by capsaicin and TRPV4 by GSK1016790A, however, resulted in a more pronounced and longer sustained $[Ca^{2+}]_i$ response (> 15 min) as compared to the activation of TRPV4 only (Figure 24). These data underline the notion that TRPV1 does not primarily act as an independent Ca^{2+} channel by itself, but rather serves to increase and prolong the activation of TRPV4.

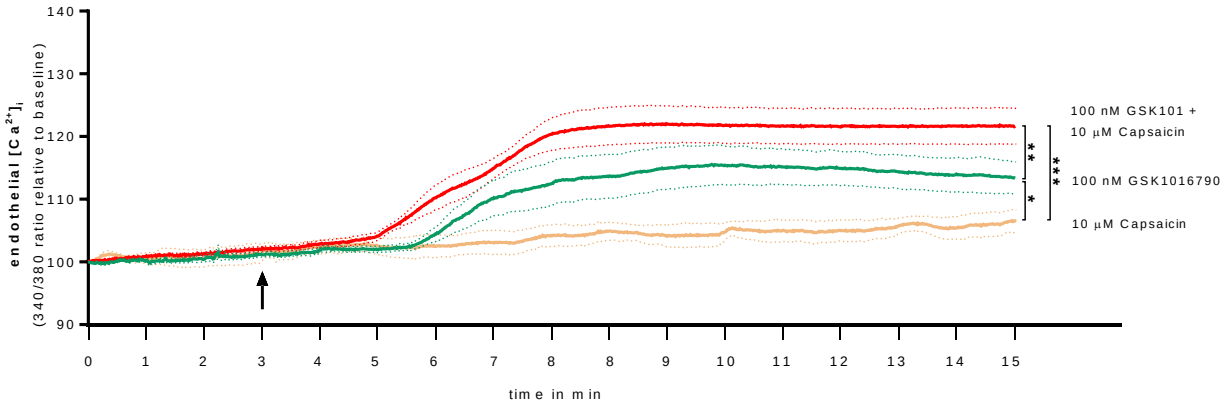

Figure 24: Activation of TRPV4 or TRPV1/TRPV4, but not TRPV1 activation alone induces a $[Ca^{2+}]_i$ response in HPMVECs. Line graphs show endothelial $[Ca^{2+}]_i$ as 340/380 ratio relative to the individual baseline. Baseline was recorded for 3 min followed by perfusion with either the TRPV1 agonist capsaicin (10 µMol/L), the TRPV4 agonist GSK1016790A (100 nMol/L) or both, starting at the time point indicated by the black arrow; dotted lines represent the SEMs color-matched for each line graph; n = 5-6 individual replicates each; $*P < 0.05$; $**P < 0.01$; $***P < 0.001$.

To further consolidate whether TRPV1 or TRPV4 activation has an impact on endothelial permeability or cell morphology *in vitro*, immunofluorescent staining from HPMVECs treated for 2 h with either TRPV1 or TRPV4 activator was performed by tagging TRPV4 (red), F-actin (green), and DAPI (blue). Activation of TRPV4 by GSK1017690A (100 nMol/L) for 2 h led to contraction and a massive gap formation within the monolayer compared to the control but with no visible changes in TRPV4 intracellular localization (Figure 25). In contrast, treatment with the TRPV1 agonist capsaicin (10 mMol/L) induced no gap formation, but a pronounced increase in TRPV4 immunofluorescence, which indicates that TRPV1 may have a stabilizing effect on TRPV4 at the plasma membrane (e.g. by protection against ubiquitination and degradation).

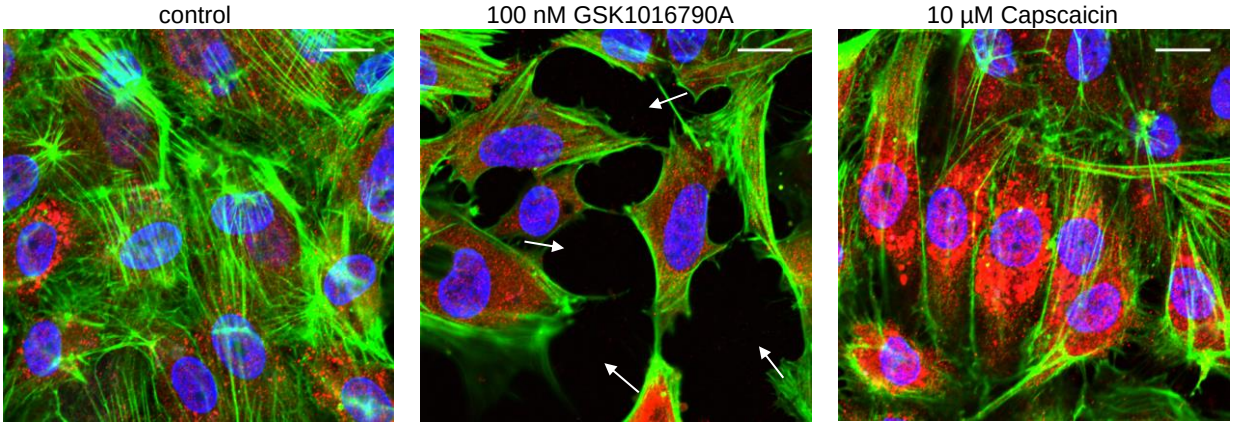

Figure 25: Activation TRPV4 induces contraction and gap formation in HPMVEC monolayers, but not activation of TRPV1. Cells were treated with 100 nMol/L TRPV4 activator GSK1016790A or 10 µMol/L TRPV1 activator for 2 h. The white arrows indicate the gaps in HPMVECs monolayers from static cultures. The bar is 15 µm; n = 2 individual experiments.

In immunofluorescence of HPMVECs, TRPV4 appeared to be localized rather in internal cell compartments than at the cell surface. In line with the immunofluorescence, i*n silico* analyses of TRPV4 by using PSORTII software tool predicted a higher probability of a subcellular location of TRPV4 in the endoplasmic reticulum (43.5%) than in the plasma membrane (39.1%). Similar to TRPV4, TRPV1 is predicated to be located both in the plasma membrane (43.5%) and in intracellular compartments (prediction: endoplasmic reticulum: 26.1%, mitochondria: 13%, nucleus: 8.7%; Table 5).

TRPV1 subcellular localization prediction		
	plasma membrane	43.5 %
	endoplasmic reticulum	26.1 %
	mitochondrial	13.0 %
	nuclear	8.7 %
	vesicles of serectory system	4.3 %
	Golgi	4.3 %
TRPV4 subcellular localization prediction		
	endoplasmic reticulum	43.5 %
	plasma membrane	39.1 %
	vesicles of serectory system	4.3 %
	Golgi	4.3 %
	nuclear	4.3 %
	mitochondrial	4.3 %

Table 5: *In silico* analyses of putative subcellular localization of TRPV1 and TRPV4 using PSORTII subcellular localization prediction software (*psort.hgc.jp/form2.html*).

To further investigate the intracellular distribution of TRPV1 and TRPV4, surface proteins were randomly captured by using surface biotinylation assay and immunoblotted against TRPV4 or TRPV1, respectively. TRPV4 was detectable at the plasma membrane, yet interestingly the majority of TRPV4 protein was found to be located in the intracellular compartment. This finding is in line with *in silico* analyses for subcellular localization of both channels. Notably, in the surface fraction of unstimulated HMPVECs, only the non-glycosylated form of TRPV1 was detectable. In the intracellular fraction both glycosylated and non-glycosylated forms could be observed. *N*-glycosylation at Asn604 of TRPV1 is a major determinant of TRPV1 function and channel permeability (Veldhuis et al., 2012). The finding that resting HPMVECs are not responding to capsaicin may thus be attributable to predominant surface expression of non-glycosylated TRPV1, which was found to not be sensitive to capsaicin (Veldhuis et al., 2012). Notably, this may differ in activated HPMVECs.

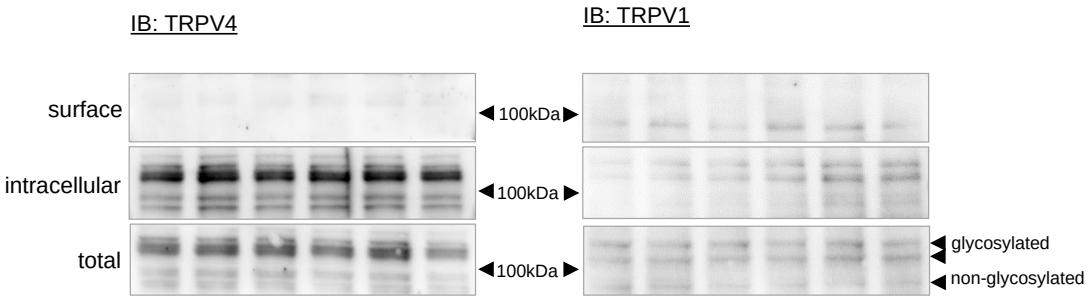

Figure 26: TRPV4 and TRPV1 are expressed both on the cell surface and in the intracellular compartment of HMPVECs. Surface expressed proteins were labeled with EZ-Link Sulfo-NHS-SS-Biotin, precipitated and separated into the distinct fractions. Representative western blots show expression levels of TRPV4 and TRPV1 in the distinct fractions; n = 6 individual replicates.

Taken together, these data suggest that TRPV1 does not act as primary mechanosensor, but as an amplifier of TRPV4-mediated endothelial Ca^{2+} influx. In surface biotinylation experiments, it has been demonstrated that cultured HPMVECs only express the non-glycosylated form of TRPV1 on the cell surface, which has been shown to be insensitive to stimulation by capsaicin (Veldhuis et al., 2012). Thus, it is conceivable that TRPV1 is *N*-glycosylated at Asn604 in a TRPV4-dependent manner, resulting in TRPV1 sensitization and amplification of the TRPV4-induced Ca^{2+} response.

4.7 INHIBITION OF TRPV1, TRPV4 AS WELL AS SGK1 ATTENUATE MICROPARTICLE RELEASE FROM PULMONARY MICROVASCULAR ENDOTHELIAL CELLS

Microparticles (MPs), especially endothelial microparticles (EMPs) are increasingly recognized as critical propagators of acute lung injury (McVey et al., 2012). Ca^{2+} channels are potential initiators of EMP formation, as their activation will increase $[Ca^{2+}]_i$ levels, which in turn may impel dysregulation of membrane transporters, like scamblases, resulting in a local collapse of membrane asymmetry, membrane blebbing and the release of MPs. This mechanism is supposed to disseminate the pulmonary localized inflammation of VILI systemically and contribute to multiorgan failure and increased mortality. In this scenario, stretch-induced Ca^{2+} influx via TRPV4 as well as TRPV1 may present the initial impulse, which ultimately leads to the release of MPs.

In order to investigate this hypothesis, human pulmonary microvascular endothelial cells (HPMVECs) were stretched for 2 h with 5% or 18% elongation, or were kept in the same incubator as static controls. MPs were isolated and enumerated from the supernatant as described in section 3.3.3. Flow-cytometric EMP enumeration using our in-house lipid bilayer microsphere technique (McVey et al., 2016) revealed a strong increase in EMPs as a function of mechanical stretch. Inhibition of TRPV4, either directly by HC-067047 (100 nMol/L) or indirectly via SGK1 inhibition by GSK650394 (100 nMol/L) resulted in a significant reduction of stretch-induced EMP formation. Likewise, treatment with the selective TRPV1 inhibitor SB366791 (50 nMol/L) reduced EMP release to a similar extent as TRPV4 inhibition, suggesting that both, TRPV1 and TRPV4 are critical mediators of EMP formation in response to extensive mechanical stretch mimicking lung overventilation (Figure **27**). While these findings are preliminary at this stage, they give rise to the exciting possibility that stretch-induced, TRPV4/TRPV1-dependent formation of EMPs may drive or promote the progression of lung injury from an organ-specific to a systemic disease that ultimately cumulates in multiorgan injury and death.

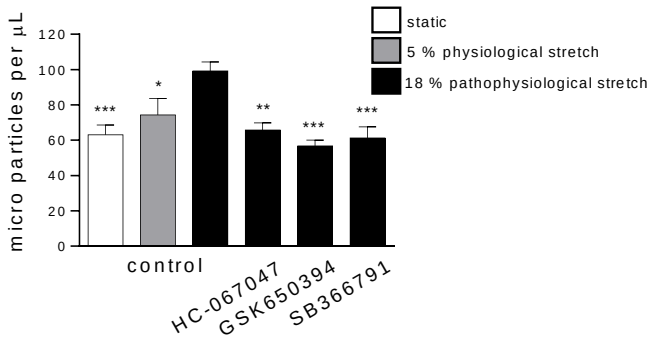

Figure 27: Effects of cyclic stretch on EMP release in HPMVECs. Confluent ECs were subjected to 5% CS or 18% CS for 2 hours or static control. EMPs were analyzed and quantified by flow cytometry using lipid bilayer microsphere gating. **P* < 0.05; ***P* < 0.01; ****P* < 0.001 versus 18% stretch control. n = 4 individual experiments each.

5 DISCUSSION

This work identified a critical role for TRPV4 in experimental VILI *in vivo*, in that pharmacological inhibition or genetic deficiency of TRPV4 blocked or attenuated the injurious effects of high tidal volume ventilation. A similar protective effect was achieved by inhibition of SGK1, a novel upstream regulator of TRPV4, which activates TRPV4 by phosphorylation at Ser824 under stretch. Critical hallmarks of VILI could be also diminished by pharmacological inhibition of downstream effectors of TRPV4 such as SK1-3, IK1, respectively. Moreover, this work has shown a novel functional link between TRPV1 and TRPV4, which might be depend on gain of activity of TRPV1 by *N*-glycosylation membrane-bound TRPV1, presumably at Asn604. Finally, these well-orchestrated signaling pathways lead to the release of endothelial microparticles, which may have critical ramifications for the dissemination and progression of acute lung injury.

5.1 MECHANICAL ACTIVATION OF TRPV4 AND ITS PHOSPHORYLATION VIA SGK1 PROMOTES VENTILATOR-INDUCED LUNG INJURY

TRPV4 is a ubiquitous expressed thermo- and mechanosensitive cation channel with a relatively weak selectivity for divalent cations (Goldenberg et al., 2015a). It is known that TRPV4 plays an important regulatory role in a broad range of different physiological and pathophysiological processes such as nociception (Alessandri-Haber et al., 2003), regulation of vascular tone (Chen et al., 2015; Goldenberg et al., 2015b), or thermo- and osmoregulation (Lee et al., 2005; Liedtke et al., 2000; Strotmann et al., 2000) and, moreover, TRPV4 gene mutations have been found to be associated with skeletal dysplasia (Kang et al., 2012) and motor sensory neuropathies (Nilius and Voets, 2013). TRPV4 is expressed in a broad range of pulmonary cell types, which are supposed to be relevant in the regulation of vascular barrier integrity, vascular tone, inflammatory and immune responses, including in particular microvascular endothelial cells (Yin et al., 2008), alveolar and bronchial epithelial cells (Alvarez et al., 2006; Fernández-Fernández et al., 2008; Lorenzo et al., 2008), vascular smooth muscle cells (Jia et al., 2004; Goldenberg et al., 2015b), alveolar macrophages (Hamanaka et al., 2010), and neutrophils (Yin et al., 2016). The main focus of the present work is the investigation of the role of microvascular expressed TRPV4 and its mechanotransductive response on endothelial barrier integrity in the lung. TRPV4 itself has been associated with vascular hyperpermeability in different experimental models using pharmacological activators by 4αPDD and epoxyeicosatrienoic acids (Alvarez et al., 2006), or chemicals such as hydrogen peroxide (Suresh et al., 2015). Recent findings by us (Yin et al., 2008) and others (Jian et al., 2008; Hilfiker et al., 2013) have shown that hydrostatic stress on the pulmonary microvasculature and occurring high vascular pressures result in a rapid activation of TRPV4, which ultimately results in Ca^{2+}-dependent elevation of endothelial permeability which in turn drives the formation of hydrostatic lung edema. Based on these findings, I expected a comparable role of TRPV4

in mechanically (over-) ventilated lungs, where endothelial cells undergo cyclic stretch (Kuebler, 2009). Indeed, in a previous study in isolated perfused lungs, Hamanaka and Parker demonstrated that the increased vascular hyperpermeability in lungs inflated with high inspiratory pressures is associated with Ca^{2+} entry via TRPV4 (Hamanaka et al., 2007). So far, the function of TRPV4 in the context of VILI and the regulatory mechanisms of mechanotransduction *in vivo* are still unclear. To test the hypothesis whether TRPV4 is a critical regulator of pulmonary vascular permeability and edema formation, I applied pharmacological as well as genetic approaches to minimize putative off-target effects. In experimental VILI, TRPV4 inhibition and deficiency has been shown to attenuate critical hallmarks of lung injury, such as pulmonary vascular hyperpermeability, edema formation, infiltration of immune cells into the interstitial and alveolar space, and release inflammatory cytokines (Michalick et al., 2017). While TRPV4 clearly plays a critical role in ventilation-associated mechanotransduction in lung endothelial cells, a growing controversial discussion has arised about TRPV4 function in other inflammatory or parenchymal cells, in that the notion is supported TRPV4 may not act as a direct mechanosensor, but rather constitutes an essential step upstream in the mechanotransduction pathway (Yin and Kuebler, 2010). Along these lines, previous studies have shown that inhibition of phospholipase A_2 or cytochrome P450 epoxygenase can inhibit the activation of TRPV4 by osmotic cell swelling (Vriens et al., 2004, 2005) or stretch (Jian et al., 2008), indicating an indirect activation of TRPV4 via epoxyeicosatrienoic acids. In contrast, Matthews and colleagues (2010) have shown that applied mechanical forces results into an ultra-rapid (within 4 msec) activation of Ca^{2+} influx through TRPV4 channels, which is rather induced by mechanical strain on the abluminal, cytoskeletal backbone than on deformation of the luminal site of endothelial cells (Matthews et al., 2010), supporting the notion that TRPV4 functions as direct mechanosensor.

Recently, Shin and colleagues identified SGK1 as a novel regulator of TRPV4, facilitating its transition from an inactive into an active form (Shin et al., 2012). In the lung, SGK1 is best known for its ability to regulate the surface expression of the epithelial sodium channel ENaC (Thomas et al., 2011) and as such, mediates the insulin-induced increase in alveolar fluid clearance (Deng et al., 2012; He et al., 2015). In the present study, the treatment with SGK1 inhibitor during ventilation with high tidal volumes was able to replicate the protective effects of TRPV4 inhibition. In fact, both, TRPV4 and SGK1 have been implicated to be involved into mechanotransduction (Wärntges et al., 2002; Sartori and Matthay, 2002; Liedtke and Friedman, 2003a; McHugh et al., 2010). The close link between TRPV4 and SGK1 was confirmed by correlation analyses of the inhibitory effects of all recorded *in vivo* read-out parameters. Additionally, it has been shown by us that the VILI-protective effect of inhibition of TRPV4 and SGK1 is based on endothelial $[Ca^{2+}]_i$ in response in the lung after acute elevation of inflated pressures (Michalick et al., 2017). These data unveil for the first time a functional role of SGK1 in pulmonary microvascular endothelial cells.

Notably, these data reveal also a new double-edged role of SGK1 in lung edema formation, in that SGK1 activation in a murine LPS-induced lung injury has been shown to support ENaC-mediated epithelial fluid clearance in epithelial cells (Deng et al., 2012; He et al., 2015), while concomitantly promoting lung vascular hyperpermeability via its effects on TRPV4 and endothelial $[Ca^{2+}]_i$ signaling. Although, ENaC is expressed in endothelial cells, it has been shown to be inhibited by 11,12 EETs, which in turn are activators of TRPV4 activity (Vriens et al., 2005; Wang et al., 2009). This would implicate that ENaC is indeed expressed in endothelial cells, but its activation threshold is kept low by 11,12 EETs. Hence, the activation of SGK1 and its downstream targets seems to be differential regulated in pulmonary epithelial and endothelial cells.

Previous studies have reported the activation and opening of the TRPV4 channel is regulated by phosphorylation of its C-terminal cytoplasmic domain by various kinases, like PKA and PKC (Baratchi et al., 2015; Fan et al., 2009; Narita et al., 2015; H. Peng et al., 2010; Shin et al., 2015; Zhang et al., 2005). Under resting conditions, the N- and the C-terminus of TRPV4 are closely associated due to their electrical charge, and the channel is closed. During activation of TRPV4, channel phosphorylation enables Ca^{2+}-CaM to bind to the CaMBD, resulting in a change in conformation where the C-terminus dissociates form the N-terminus and the channel opens (Strotmann et al., 2003). According to these findings, Shin and colleagues recently unveiled that SGK1 phosphorylates TRPV4 within the CaMBD at Ser824 and thereby facilitates the subsequent opening and activation of the TRPV4 channel (Shin et al., 2012). Latter findings by us have proven that phosphorylation is increased in lungs from overventilated mice *in vivo* as well as in stretched HPMVECs *in vitro* (Michalick et al., 2017), which was attenuated by inhibition of SGK1. This point out that SGK1-mediated phosphorylation of TRPV4 is a critical step of mechanotransduction.

Interestingly, these data reveal a physical interaction of SGK1 and TRPV4 within a distance of max. 30 nm that is dependent on stretch *in vitro* and *in vivo*. While the phosphorylation of TRPV4 necessarily requires the association and interaction with SGK1, the interaction between the active site of the kinase and its target is commonly considered to be so short-lived and that would exclude the detection by Co-IP. Over recent years, it has become increasingly clear that many kinases utilize so-called docking interactions or modular protein–protein interaction domains to achieve high biological specificity (Reményi et al., 2006). These interactions may be considerably more durable and can be detected by Co-IP. Notably, docking is particularly prevalent in serine/threonine kinases. As such, SGK1 has been shown to directly interact with target proteins like the E3 ubiquitin ligase Nedd4-2 via WW domains (Snyder, 2009; Wiemuth et al., 2010). WW domains represent small modular protein motifs, acting similar to src-homology domains, by recognizing proline-rich or proline-containing motifs of target proteins and mediate protein interactions (Chen and Sudol, 1995). These interactions may occur either directly or, in contrast, occur indirectly via scaffolding or adaptor proteins. In case

of TRPV4, a similar binding of PKC via kinase-anchoring proteins has previously been reported (Mercado et al., 2014; Sonkusare et al., 2014).

This finding is in line with the enhanced interaction between SGK1 and TRPV4 previously detected in overventilated lungs, and furthermore suggests that this association is likely independent of the direction of stretch, which is predominantly longitudinal in the *in vivo* overventilation experiments (Kuebler, 2009), but biaxial in the *in vitro* stretch assay. The enhanced interaction of SGK1 and TRPV4 in response to biaxial stretch was almost abolished by inhibition of SGK1, which indicates that activation of SGK1 correlates with its interaction with TRPV4. Notably, the basal interaction in the static controls were quite high compared to 5% stretch (mimicking LV_T), supporting the hypothesis that endothelial cells differ under static conditions (Müller-Marschhausen et al., 2008).

While TRPV4 has not only been found to be expressed and functionally relevant in endothelial cells, it is conceivable that also in circulating or resident immune cells such as macrophages (Hamanaka et al., 2010) or neutrophils (Sostegni et al., 2015) contributing to the progression of lung injury. Indeed, TPRV4 activation by 4αPDD has previously been shown to stimulate the production of reactive oxygen species and nitric oxide, as well as spreading and lamellipodia formation of alveolar macrophages harvested from *Trpv4*$^{+/+}$, but not in those from *Trpv4*$^{-/-}$ mice (Hamanaka et al., 2010). This study revealed that mechanically induced TRPV4 activation in macrophages contributes to barrier failure in overventilated isolated mouse lungs and unveil a correlation of mechanical activation and spreading of alveolar macrophages (Hamanaka et al., 2010). Experiments in generated bone marrow chimeric mice lacking TRPV4 either in parenchymal or circulating blood cells could identify that TRPV4 expression and function in parenchymal cells correlates with lung hyperpermeability and edema formation in a model of acid-induced lung injury (Yin et al., 2016). It therefore can be concluded that the pro-inflammatory role of TRPV4 is preferentially based on its expression in the lung parenchyma. Nevertheless, we cannot exclude that mechanotransduction via the pulmonary endothelium and epithelium may trigger inflammatory signaling and the release of inflammatory cytokines into the alveolar space.

In conclusion, the present study identifies TRPV4 as a central regulator of cellular mechanotransduction in the pulmonary microvasculature in response to mechanical stretch as it occurs during mechanical ventilation. In this scenario, SGK1 has been shown for the first time to be involved in the regulation of endothelial barrier integrity by phosphorylation and subsequent activation of TRPV4. Therefore, both, TRPV4 and SGK1 represent promising pharmacological targets in the prevention or treatment of VILI.

5.2 Ca^{2+}-ACTIVATED K^+ CHANNELS PROMOTE LUNG INJURY VIA POSITIVE FEEDBACK ON TRPV4

The Ca^{2+}-activated K^+ channels are crucial responders towards increased in $[Ca^{2+}]_i$, as their gating is regulated by one of the most important Ca^{2+}-dependent second messengers, CaM (Xia et al., 1998; Joiner et al., 2001). In other experimental models, it has been shown that mediated formation of Ca^{2+}-CaM complexes is responsible for subsequent activation/ opening of Ca^{2+}-activated K^+ channels by direct binding of Ca^{2+}-CaM to the C-terminal CaMBD of these channels, which in turn causes K^+ efflux and hyperpolarization of the plasma membrane (Fleming et al., 2007; Saliez et al., 2008; Wong and Schlichter, 2014).

Recent studies have indicated subcellular functional coupling between TRPV4, SK3, and IK channels in several systemic vascular beds, while coupling of TRPV4 with BK channels remains a matter of debate (Hannah et al., 2011; Earley, 2011; Bagher et al., 2012; Sonkusare et al., 2012). In the pulmonary vascular endothelium this mechanism has been described to contribute to stretch-induced Ca^{2+} influx and increased pulmonary hyperpermeability (Michalick et al., 2014; M. T. Lin et al., 2015). Reversely, stretch-induced activation of TRPV4 and K_{Ca} channels initiate a bidirectional positive feedback loop. Therefore, Ca^{2+}-induced K^+ efflux via K_{Ca} channels is suggested to permit a sustained Ca^{2+} influx and subsequent elevation of the electrochemical gradient across the plasma membrane and thereby hyperpolarizes the membrane potential, presumably in a TRPV4-dependent manner (Fleming et al., 2007; Yaron et al., 2015). Notably, inconsistent findings reveal either an elevated or prolonged Ca^{2+} response induced by K_{Ca} activation and membrane hyperpolarization (Fleming et al., 2007; Bagher et al., 2012; Michalick et al., 2014; M. T. Lin et al., 2015) or showed no impact on endothelial Ca^{2+} entry (Cohen and Jackson, 2005). Whether K_{Ca} activation is the underlying mechanism of the sustained Ca^{2+} response or the sustained response is independent of changes in the membrane potential has not been finally clarified in detail yet. The present data reveal that activation of K_{Ca} channels in response to mechanical stretch promotes vascular hyperpermeability and in alveolar inflammation, which is a result of sustained endothelial $[Ca^{2+}]_i$ response. This anti-inflammatory effect of K_{Ca} channel blockers may result from the immunosuppressive properties of these inhibitors on immune cells (Toldi et al., 2011; Koshy et al., 2013; Kahlfuß et al., 2014). Therefore, our *in vivo* model cannot preclude an additive effect due to the immunosuppressive nature of the applied inhibitors, but could also show in detail that all three interventions (K_{Ca} blockers) attenuated the subsequent sustained $[Ca^{2+}]_i$ elevation in the pulmonary endothelium and that the protective effect is also an result of stabilization of the endothelial barrier integrity inhibition of K_{Ca} channels.

Although, all K_{Ca} channel subtypes abundant are expressed in HPMVECs, the prolongation of the Ca^{2+} signal is mainly based on the positive feedback of SK and IK channels, since it has been shown by Lin, M.T. et al., 2015 that TRPV4 activation on BK channel currents. This can be explained by the

differential activation of BK channels either in a Ca^{2+}-dependent or voltage-gated manner, whereas SK and IK channels are lacking the voltage-sensitive domain (Bao et al., 2004; Vergara et al., 1998). Intracellular Ca^{2+} increase and subsequent elevated binding of Ca^{2+}-CaM to the CaMBD of SK and IK channels has been also suggested to regulate their trafficking and surface expression (Joiner et al., 2001; Lee et al., 2003) which therefore also contributes to the sustainability of stretch-induced Ca^{2+} influx via TRPV4. Moreover, in endothelial cells it has been shown that TRPV4 as well as SK3 interact with caveolin-1, a major structural component of caveolae, (Absi et al., 2007; Saliez et al., 2008). Contrarily, IK1 channels are exclusively localed to the plasma membrane (Absi et al., 2007). Due to their different subcellular localization, it is conceivable that K_{Ca} channels may assume different tasks in intracellular Ca^{2+} signaling. In line with this view, studies revealed that K_{Ca} channel subtypes have different conductances and sense intracellular Ca^{2+} in distinct ranges. In brief, dose-response curves have shown a half-maximal activation value (EC_{50}) of SK at ≈ 300 –500 nMol/L $[Ca^{2+}]_i$, while IK1 has a higher EC_{50} of approximately 740 nMol/L in cultured mouse aortic endothelial cells (Ishii et al., 1997; Bond et al., 2004; Ahn et al., 2004). The present data indicate a stronger attenuation of hallmarks of VILI in response to overventilation when IK1 channels were blocked by either charybdotoxin or TRAM34, which in turn may indicate a strong endothelial $[Ca^{2+}]_i$ response reaching the sensing threshold of preferentially IK1 than SK channels. The tight regulation of K_{Ca} channels in response to intracellular Ca^{2+} increase and their different conductance ranges may present a dynamic and rapid adaption to different stimuli activating distinct types of Ca^{2+} channels.

5.3 SYNERGISTIC EFFECT OF TRPV1 WITH TRPV4

Originally, it has been suggested that TRP channels preferentially form homomeric tetramers at the plasma membrane (Schaefer, 2005; Hellwig et al., 2005; Cheng et al., 2010). This notion has been revised over recent years in that it has become evident that TRP channels can not only form homomeric, but also heteromeric channels across different TRP channel subfamilies (Schaefer, 2005). The best investigated TRP channel heteromers to date are TRPV1/TRPA1, TRPPV1/TRPV3, TRPP2/TRPC1, TRPP2/TRPV4, TRPC1/TRPV4 and TRPC3/TRPC4. Yet, the molecular determinants facilitating channel multimerization remain largely elusive. It has been reported that a tetrameric assembly domain (TAD) comprising 21 amino acids, which are located on the C-terminal site of the TRP-box (residues 752-772 in the case of mouse TRPV1) may facilitate a direct subunit-subunit interaction between TRPV channels when induced by appropriate stimuli (García-Sanz et al., 2004; Zhang et al., 2011). These TAD is closely located to the N-terminal part of the CaMBD (residues 768-802 of mouse TRPV1), thus modulating Ca^{2+}-CaM binding and channel sensitization (Prescott and Julius, 2003; Lau et al., 2012). A similar regulation could be shown for TRPV4, in that the heteromerization of TRPV4 with TRPC1 alters the kinetics of TRPV4-mediated $[Ca^{2+}]_i$ transients in response to flow by prolongation of the flow-induced Ca^{2+} influx (Ma et al., 2010c). The latter study also reported that HEK cells transfected with both, TRPV4 and TRPC1 channels lead to a stronger Ca^{2+} influx in response to hypotonicity compared to transfection with TRPV4 only (Ma et al., 2011b). Over and above these dual-protein heteromers, Du and colleagues (2014) detected the first heteromeric channel complex consisting of three different TRP channels of different TRP subfamilies (TRPV4/TRPC1/TRPP2). Of particular interest for the present study, they also showed that TRPV4/TRPC1 may assemble with BK channels to a signaling complex, which mediates hyperpolarization and relaxation of vascular smooth muscle cells (Du et al., 2014; Ma et al., 2015).

The present study reveals the evidence for an interaction of TRPV4 and TRPV1, putatively organized as heteromeric TRP complex, in that this interaction between both channels is dependent on mechanical stretch and SGK1-mediated phosphorylation of TRPV4 at Ser824 in co-immunoprecipitations from lung lysates of overventilated mice. Notably, this interaction was diminished by selective inhibition of TRPV1, TRPV4 and SGK1, as well as in *Trpv4*$^{-/-}$ mice and, moreover, was able to reduce the interaction levels to the baseline level of the control groups (unventilated, LV_T). Interestingly, the interaction between TRPV1 and TRPV4 corresponds to the level of Ser824 phosphorylation of TRPV4, indicating a correlation between phosphorylation of TRPV4 and its interaction with TRPV1, which is presumably based on structural changes as consequence of phosphorylation. Whether this heteromeric complexes are formed through direct interactions or are indirectly mediated via scaffold proteins, like AKAP79/150, needs to be clarified (Distler et al., 2003; Jeske et al., 2008; Schnizler et al., 2008; Fan et al., 2009; Sonkusare et al., 2014).

Accordingly, TRPV1 inhibition by SB366791 or genetic deficiency replicated the protective effects of TRPV4 inhibition in experimental VILI as shown by reduced edema formation, protein extravasation and protected the pulmonary microstructure in response to overventilation. In *in vitro* cultured HPMVECs, TRPV4 activation by selective agonist GSK1016790A results in a rapid and sustained endothelial $[Ca^{2+}]_i$ response, whereby simultaneous TRPV1 activation by capsaicin amplified this effect. In contrast, TRPV1 activation *per se* did not cause any increase in endothelial $[Ca^{2+}]_i$. These findings let suggest that the initial Ca^{2+} influx in response to mechanical stretch occurs via activation of TRPV4 and not TRPV1; however, activation of both channels shows synergistic effects on the endothelial $[Ca^{2+}]_i$ increase. This synergistic effect might be a result of i) an enhanced sensitization of TRPV4 by interaction with TRPV1 as it has previously described for TRPC1/V4 heteromeric complexes (Ma et al., 2010c), ii) TRPV4-mediated increase TRPV1 surface expression (Zhang et al., 2005) or iii) activation of TRPV1 by posttranslational modification, and thus amplification of the TRPV4-mediated $[Ca^{2+}]_i$ response (Lu et al., 2008; Veldhuis et al., 2012). In line with these findings, TRPV4 activation induces cell contraction and massive gaps in the monolayers of cultured HPMVECs, but not activation of TRPV1. Interestingly, TRPV1 inhibition by SB366791 could only diminish the endothelial $[Ca^{2+}]_i$ response to high inflated pressures over time, but not the initial $[Ca^{2+}]_i$ increase after raising the CPAP from 5 to 15 cmH_2O compared to wild type controls in isolated-perfused lungs. It is tempting to speculate that this observation may be attributable to the fact that in unstimulated endothelial cells TRPV1 is located in its non-glycosylated form in the plasma membrane. *N*-glycosylation at Asn604 sensitizes TRPV1 and increases its ionic permeability of and therefore, regulates channel function (Veldhuis et al., 2012). It is conceivable that TRPV1 becomes glycosylated at Asn604 and subsequently activated via a TRPV4-mediated mechanism. Interestingly, functional deficiency of TRPV1 attenuated not only the sustained, but also the initial the endothelial $[Ca^{2+}]_i$ response to high inflation pressures in isolated, perfused mouse lungs. The different effects of genetic deficiency or inhibition of TRPV1 could be explained by the putative off-target effects of applied inhibitor SB366791, on the one hand, which have not been shown yet, or by the genetic generation of this mouse strain, on the other hand, in that the exon expressing the channel pore including Asn604 has been deleted (Caterina et al., 2000).

In line with the notion that *N*-glycosylation sensitizes TRPV1, the present data reveal the expression of only non-glycosylated TRPV1 on the cell surface of untreated HPMVECs. Moreover, the surface biotinylation experiments demonstrates that the expression levels of both, TRPV1 as well as TRPV4 are unexpected low at the cell surface in unstimulated endothelial cells. The majority of both proteins seems to be localized in the intracellular fraction, suggesting that they are not exclusively located to the plasma membrane and might play a role in distinct Ca^{2+}-regulated pathways in other subcellular compartments, like the endoplasmic reticulum or mitochondria. Consistent with these findings, *in silico* analyses of both channels predict for TRPV4 a higher subcellular localization in the

endoplasmic reticulum than in the plasma membrane (43.5% vs. 39.1%) and for TRPV1 a higher prevalence in the plasma membrane as compared to the ER and mitochondria (43.5% vs. 26.1% vs. 13%; Table 5). Thereby, a marked amount of TRPV1 and TRPV4 is predicted to be localized in the ER, which could be simply due to *de novo* protein synthesis. More likely, there is an upcoming notion that TRP channels are also located in the ER and contribute to store-operated Ca^{2+} entry (Arniges et al., 2006; Gallego-Sandín et al., 2009; G. Peng et al., 2010). Moreover, the variable subcellular localization of both channels correlates with versatile functions in response to various physiological and pathological stimuli. Thereby, modification by alternative splicing and/or subsequent trafficking to different cellular compartments, which enables a crosstalk over different organelles (Arniges et al., 2006; Zhao and Tsang, 2016).

In summary, these findings identify an interaction and functional coupling of TRPV1 and TRPV4 in response to mechanical stretch during ventilation. In this scenario, TRPV1 activation seems to be a secondary effect of TRPV4 activation and mediates an amplification and prolongation of TRPV4-induced endothelial $[Ca^{2+}]_i$ response. I assume that synergistic Ca^{2+} gating of TRPV1 and TRPV4 is facilitated by a thus far unknown mechanism of TRPV1 activation, presumably by *N*-glycosylation of Asn604. With respect to the different subcellular localization, it is conceivable that both channels could be translocated from ER to the plasma membrane after mechanical stimulation, which needs to be conclusively clarified. TRPV1 and TRPV4 have been shown to act as mediators of overlapping signaling pathways, such as nociception, thermal, osmotic and mechanical sensing, although at times with opposing functions (Caterina et al., 2000; Davis et al., 2000; Birder et al., 2002; Alessandri-Haber et al., 2003; Liedtke and Friedman, 2003b; Rong et al., 2004; Lee et al., 2005; Yin and Kuebler, 2010). Recently, Kim et al., 2016 found evidences for the TRPV1-mediated amplification of TRPV4 activity in a murine itch model. Other publications revealed a critical role of both channels in different lung pathologies, which are accompanied by changes in lung mechanics, such as cigarette smoke-induced chronic obstructive pulmonary disease (COPD) and pulmonary hypertension (Baxter et al., 2014; Parpaite et al., 2016). All these findings, indicate that, both, TRPV4 as well as TRPV1 are critical mediators of cellular mechanotransduction. Therefore, the TRPV4-mediated Ca^{2+} response is amplified and prolonged via activation of TRPV1, which in turn leads to a disruption of the endothelial barrier, pulmonary vascular hyperpermeability and lung edema.

5.4 TRPV4 AND MICROPARTICLE FORMATION IN VILI

The recent recognition of microparticles as biomarkers and intercellular signal transducers in inflammatory diseases raises an unmet need to understand how the different MPs from different donor cell types develop, how their specific composition may change and be regulated, and their role in disease progression and recovery at both the local and systemic level, as well as their clearance. Specifically, MPs are released from endothelial cells in response to changes of flow, stretch or shear forces, or changes of the stiffness of the vascular bed (Andrews et al., 2016; Vion et al., 2013; Tual-Chalot et al., 2010) and have been shown to contribute to vascular dysfunction, such as hypertension, thrombosis and atherosclerosis (Chironi et al., 2009; Boulanger, 2010; Baron et al., 2012; Lacroix et al., 2013). In line with the clinical results reported by Cabrera-Benítez and colleagues (2015), we detected an increased release of EMP from HMPVECs exposed to pathological stretch of 18% elongation. Importantly, this effect was abolished by inhibition of TRPV1, TRPV4 or SGK1, in line with the notion that Ca^{2+} influx and increased $[Ca^{2+}]_i$ are critical triggers for MP formation in endothelial cells (Dachary-Prigent et al., 1995; Pasquet et al., 1996). At present, the cellular mechanisms by which Ca^{2+} signaling promotes membrane asymmetry and subsequent MP formation remain largely unclear. One potential mechanistic link in this scenario is the transmembrane protein 16F (TMEM16F), which represents a Ca^{2+}-activated lipid scramblase (Suzuki et al., 2013).

The TMEM16 protein family or anoctamins consists of 10 members (A-K), which were originally described to act as Ca^{2+}-activated Cl^- channels (Hartzell et al., 2009). This notion has since been revised as it has been shown that TMEM16F functions as Ca^{2+}-activated lipid scramblase, which upon activation exposes phosphatidylserine (PS) and phosphatidylethanolamine (PE) to the outer leaflet and internalizes phosphatidylcholine (PC) and sphingomyelin (Suzuki et al., 2010). Among the 10 TMEM16 members two are Ca^{2+}-activated Cl^- channels (16A and 16B) and five have Ca^{2+}-activated lipid scramblase function (16C, 16D, 16F, 16G, and 16J) with different preference to lipid substrates (Caputo et al., 2008; Stöhr et al., 2009; Suzuki et al., 2013). Real-time PCR analysis for TMEM16 family member mRNA in murine lung tissue revealed the highest expression levels for TMEM16A and TMEM16F (Suzuki et al., 2013). Consistent with an important role for TMEM16A in MP formation, it has recently been shown that deletion of TMEM16F reduces PS exposure and formation of platelet-derived microparticles after platelet activation (Fujii et al., 2015).

The activation of scramblases via intracellular Ca^{2+} increase in response to pro-apoptotic signals results in changes in the membrane asymmetry of the outer leaflet, where PS exposure leads to microparticle release and ultimately culminates in phagocytosis of these cells. Moreover, the activation of scramblases also modifies the composition of phospholipids in the inner leaflet, which in turn leads to $PI(4,5)P_2$ hydrolysis, PKC activation, and the dissociation of arachidonic acids (Perret et al., 1979; Plantavid et al., 1982; Berridge, 2009; Nakamura and Yamamura, 2010). In particular, TRPV1

activity is regulated by lipid second messengers (Senning et al., 2014). Potentially, all of these metabolic modifications at the inner leaflet may provide a direct feedback on TRPV1 or TRPV4 expression on the plasma membrane (Qin, 2007). Both channels are also known to be regulated via arachidonic acid derivates (epoxyeicosatrienoic acids; EETs) and play an important role in endothelial NO production (Vriens et al., 2005; Su et al., 2014). Concomitant, both are sensitized via PKC (Bhave et al., 2002; H. Peng et al., 2010). Furthermore, TRPV4 activity is increased by hydrolysis of $PI(4,5)P_2$ and a direct interaction of ankyrin domains with $PI(4,5)P_2$ (Takahashi et al., 2014). A similar binding of $PI(4,5)P_2$ could be demonstrated for TRPV1 (Lukacs et al., 2013). Notably, also opening probabilities of Ca^{2+}-activated K^+ channels have been shown to be modulated by $PI(4,5)P_2$ (Tian et al., 2015). Thus, it can be speculated that $PI(4,5)P_2$ has regulatory effects on TRPV1, TRPV4 and presumably Ca^{2+}-activated K^+ channels in the plasma membrane and that a putative TRPV4-mediated activation of phospholipid scramblases triggers a positive feedback loop in the highly dynamic processes of mechanotransduction. Further investigations will be necessary to clarify this hypothesis in detail.

In conclusion, the findings of the present study provide novel insights into the function, regulation, and interaction partners of TRPV4 and identifies a novel signaling cascades of endothelial mechanotransduction, in that i) TRPV4 is a major regulator of VILI, which is positively regulated by SGK1-dependent phosphorylation of Ser824, ii) TRPV4-mediated Ca^{2+} influx sensitizes downstream Ca^{2+}-activated K^+ channels, which generates a positive feedback on TRPV4-mediated Ca^{2+} influx, presumably via hyperpolarization of the cell membrane, iii) TRPV4 interacts with TRPV1, which in turn amplifies endothelial Ca^{2+} influx, iv) TRPV1 and TRPV4 are not exclusively localized in the plasma membrane, but also in other subcellular compartments, and v) TRPV1 and TRPV4 activation results in microparticle release under excessive mechanical stress. In further investigations it needs to be clarified a) whether K_{Ca} channels give a positive feedback on TRPV4 via hyperpolarization of the plasma membrane, b) whether the interaction between TRPV1 and TRPV4 within the heteromeric complex is directly or mediated via scaffold proteins, c) where TRPV1 and TRPV4 are exactly located in the cell and whether changes in the localization correlates with different functions (e.g. store-operated Ca^{2+} entry), d) which Ca^{2+}-activated phospholipid scramblases are activated by TRPV1/4-mediated Ca^{2+} influx (presumably TMEM16F) and e) how dynamic modulations of membrane asymmetry may lead to regulatory feedback on TRPV1/TRPV4, presumably via $PI(4,5)P_2$, which might have a stabilizing effect of these complexes in the plasma membrane (Figure 28).

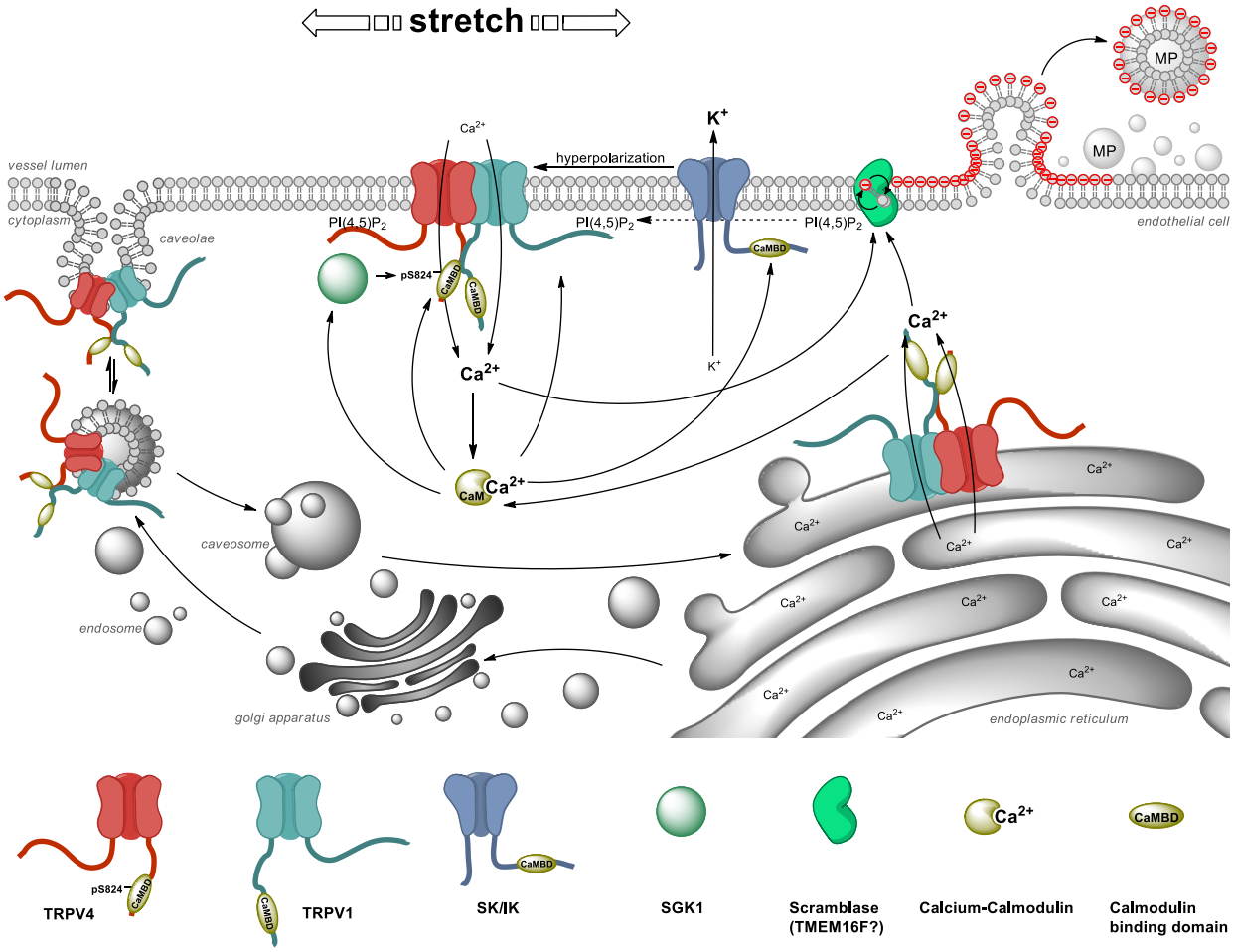

Figure 28: Proposed signaling pathways in TRPV4-mediated mechanotransduction in the pulmonary microvasculature. TRPV4 is a major regulator of VILI and is activated by SGK1-dependent phosphorylation of Ser824. TRPV4-mediated Ca^{2+} influx sensitizes downstream SK/IK channels and the resulting K^+ efflux creates a positive feedback on TRPV4-mediated Ca^{2+} influx. TRPV4 interacts with TRPV1 and this interaction depends on mechanosensitive TRPV4 activity. Both TRPV1 and TRPV4 are not exclusively located in the plasma membrane, but also in the vesicular compartment as well as in the ER and therefore presumably translocated via vesicular/caveolar trafficking or might be involved in store-operated Ca^{2+} entry. TRPV1 or TRPV4-mediated increase of $[Ca^{2+}]_i$ induces $[Ca^{2+}]_i$ microparticle (MP) release, which is suggested to exacerbate the progression VILI. MP formation is a result of changes in membrane asymmetry and exposure of negatively charged phosphatidylserine (-) on the outer leaflet. This process is regulated by scramblases. The Ca^{2+}-activated scramblases TMEM16F represent a particular important link between increased $[Ca^{2+}]_i$ concentrations and MP formation. Moreover, it is conceivable that changes in the membrane asymmetry and the resulting lipid second messengers may provide an additional positive feedback on TRPV1 and/or TRPV4.

5.5 EXPERIMENTAL MODEL DISCUSSION

The findings of the present work are in line with other studies that detected the characteristic features of acute lung injury including lung vascular barrier failure, histological signs of lung injury, and increased release of pro-inflammatory cytokines after 2 h of HV_T with 20 mL/kg in overventilated control mice. Outcome parameter of different laboratories vary due to different experimental settings and different investigators. The reasons for this great variability of the obtained data are mostly cause by indispensable circumstances, such as differences in animal handling and procedures to differences between animal providers (Jiang et al., 2015), in varying microbiomes (Souza et al., 2004), circadian changes of the immune system (Scheiermann et al., 2013), or even in olfactory stress depending on the sex of the investigator (Sorge et al., 2014). These differences of outcome measures underpin once again the importance of appropriate controls.

In the data sets of this study, the data sets of HV_T groups with or without treatments or obtained from genetically modified mice were presented in comparison to the LV_T control and the unventilated control group. All inhibitors as well as the knockout groups were also tested in LV_T. All data revealed no difference compared to the given controls and are not presented to keep the attention on the key data.

For the enumeration of MPs, we used serum-free media for all experiments, as sera of animal origin has been found to contain high amounts of MPs and generate false-positive results. For every experimental approach, all counted MP numbers were normalized to the amount in the used serum-free media as correction of false-positive counts.

Furthermore, the applied cyclic stretch of 18% elongation is based on the occurring mechanical strain experienced by alveolar epithelium during ventilation, so-called cyclic deformations. Thereby, cyclic stretch leads to massive increase in cell surface area 37-50% and a linear distension 17-22%, which is suggested to be sufficient to mimic the mechanical forces during ventilation (Tschumperlin et al., 2000). The occurring mechanical forces at the distal part of are predicted to be nearly identical in alveolar epithelia cells and its neighboring microvascular endothelial cells.

Here, I used a murine model of 2 h overventilation at a HV_T of 20 mL/kg and a PEEP of 2 cmH_2O to induce VILI. Studies have queried the sufficiency of this inspired volume to induce lung injury and recommend instead volumes of 40 mL/kg to mimic features of clinical relevance in experimental VILI, but also accompany a high mortality of the laboratory animals subjected to ventilation with these excessive volumes (Wilson et al., 2012). In contrast, several studies reported characteristic signs of overventilation-induced lung injury in mice following ventilation with high tidal volumes in the range of 12-20 mL/kg for several hours, including impaired oxygenation, alveolar protein leak and infiltration of inflammatory cells, histological signs of lung injury, and release of inflammatory

cytokines into the alveolar space and the systemic circulation (Akram et al., 2010; Müller et al., 2010; Puntorieri et al., 2013). Other studies have evaluated and compared features of across experimental lung injury, such as the semi-quantitative histological lung injury score used in the present study (Matute-Bello et al., 2011). The chosen volume of 20 mL/kg was therefore defined by clinical features of ARDS patients. The ventilated volume of these patients is compared to non-ARDS patients functionally small, as described by Gattinoni and Pesenti (2005) in the concept of "baby lung". Beitler and colleagues (2016) confirmed this notion by measuring the inspiratory capacity in lungs of ARDS patients. The measured inspiratory capacity in lungs of ARDS patients is reduced to almost one third of the predicted inspiratory capacity, indicating that two thirds of the total lung volume are not participate in mechanical ventilation (Beitler et al., 2016). Hence, the experimental model applied in the present study with a LV_T of 7 mL/kg compared to a HV_T of 20 mL/kg mimics the delivered tidal volume to aerated lung regions in the clinical situation of ventilated ARDS patients. Therefore, the applied experimental model mimics perfectly the clinical features and occurring mechanical forces of VILI.

5.6 CLINICAL IMPLICATIONS

To date, mechanical ventilation is the only life-saving intervention in patients with respiratory failure caused by ARDS. In contrast, mechanical ventilation as sole treatment in ARDS has also emerged to trigger critical adverse effects by the occurring excessive mechanical stress during long-term ventilation, which ultimately leads to the loss of endothelial cell barrier integrity, edema formation and lung injury up to systemic inflammation, a symptomatic called VILI. Many approaches have focused on the reduction the biomechanical stress during mechanical ventilation, like lowering tidal volumes from 12 to 6 mL/kg , applying high positive end-expiratory pressures and recruitment maneuvers, prone positioning of the patients, high-frequency oscillatory ventilation, administration of neuromuscular blocking agents or Neurally Adjusted Ventilatory Assist (NAVA®) (ARDS Definition Task Force et al., 2012; Slutsky and Ranieri, 2013; Terragni et al., 2015; Doorduin et al., 2015). Despite all approaches to minimize the biomechanical stress on lung tissue, just the lowering of tidal volumes have shown to effectively reduce mortality about 22% (ARDSNet, 2000). Additionally, numerous of promising preclinical, pharmacological interventions of VILI have failed to show benefits in multicenter clinical trials (Calfee and Matthay, 2007; Levitt and Matthay, 2012). The poor outcome of all these studies, underlines the importance of ongoing translational studies focusing on the molecular mechanisms underlying cellular mechanotransduction and inflammatory processes to develop an effective pharmacological therapy. Therefore, the emerging role of TRPV4 as a mechanosensitive Ca^{2+} channel and regulator of vascular barrier integrity represents a critical new drug target in the preventive treatment of VILI and one TRPV4 blocker is tested in the first clinical trials to reduce interstitial lung edema (NCT02497937). Nevertheless, the importance of understanding the whole process of mechanotransduction at the alveolar-capillary barrier is essential to develop therapeutic strategies.

This work identified TRPV4 as central mechanosensor in response to mechanical stretch during ventilation and shed light on the regulation of TRPV4 activity by phosphorylation via SGK1 or on downstream mediators of TRPV4, like K_{Ca} channels and TRPV1. I could show that all interventions and pharmacological approaches resulted in a reduction of features of inflammation and vascular hyperpermeability in an experimental VILI model. In addition, my data have shown that endothelial cells release MPs in a stretch-dependent manner and this is mediated by TRPV1 and TRPV4 activity. All these findings support the clinical relevance of the applied model and potential translational impact on future studies to shed light on the molecular mechanisms underlying mechanotransduction. Taken together, the present work provides a detailed insight into cellular responses to mechanical forces, identified novel regulators with respect to ventilation-induced pulmonary barrier failure and represented several options of promising new drug targets to prevent and treat VILI.

6 REFERENCES

Absi, M., Burnham, M.P., Weston, A.H., Harno, E., Rogers, M., Edwards, G., 2007. Effects of methyl beta-cyclodextrin on EDHF responses in pig and rat arteries; association between SK(Ca) channels and caveolin-rich domains. Br. J. Pharmacol. 151, 332–340. doi:10.1038/sj.bjp.0707222

Ahn, S.C., Seol, G.H., Kim, J.A., Suh, S.H., 2004. Characteristics and a functional implication of Ca(2+)-activated K(+) current in mouse aortic endothelial cells. Pflüg. Arch. Eur. J. Physiol. 447, 426–435. doi:10.1007/s00424-003-1201-1

Akram, A., Han, B., Masoom, H., Peng, C., Lam, E., Litvack, M.L., Bai, X., Shan, Y., Hai, T., Batt, J., Slutsky, A.S., Zhang, H., Kuebler, W.M., Haitsma, J.J., Liu, M., dos Santos, C.C., 2010. Activating transcription factor 3 confers protection against ventilator-induced lung injury. Am. J. Respir. Crit. Care Med. 182, 489–500. doi:10.1164/rccm.200906-0925OC

Albelda, S.M., Daise, M., Levine, E.M., Buck, C.A., 1989. Identification and characterization of cell-substratum adhesion receptors on cultured human endothelial cells. J. Clin. Invest. 83, 1992–2002. doi:10.1172/JCI114109

Alessandri-Haber, N., Yeh, J.J., Boyd, A.E., Parada, C.A., Chen, X., Reichling, D.B., Levine, J.D., 2003. Hypotonicity induces TRPV4-mediated nociception in rat. Neuron 39, 497–511.

Alvarez, D.F., King, J.A., Weber, D., Addison, E., Liedtke, W., Townsley, M.I., 2006. Transient receptor potential vanilloid 4-mediated disruption of the alveolar septal barrier: a novel mechanism of acute lung injury. Circ. Res. 99, 988–995. doi:10.1161/01.RES.0000247065.11756.19

Andrews, A.M., Lutton, E.M., Merkel, S.F., Razmpour, R., Ramirez, S.H., 2016. Mechanical Injury Induces Brain Endothelial-Derived Microvesicle Release: Implications for Cerebral Vascular Injury during Traumatic Brain Injury. Front. Cell. Neurosci. 10, 43. doi:10.3389/fncel.2016.00043

ARDS Definition Task Force, Ranieri, V.M., Rubenfeld, G.D., Thompson, B.T., Ferguson, N.D., Caldwell, E., Fan, E., Camporota, L., Slutsky, A.S., 2012. Acute respiratory distress syndrome: the Berlin Definition. JAMA 307, 2526–2533. doi:10.1001/jama.2012.5669

Arniges, M., Fernández-Fernández, J.M., Albrecht, N., Schaefer, M., Valverde, M.A., 2006. Human TRPV4 channel splice variants revealed a key role of ankyrin domains in multimerization and trafficking. J. Biol. Chem. 281, 1580–1586. doi:10.1074/jbc.M511456200

Ashbaugh, D.G., Bigelow, D.B., Petty, T.L., Levine, B.E., 1967. Acute respiratory distress in adults. Lancet Lond. Engl. 2, 319–323.

Baban, B., Liu, J.Y., Mozaffari, M.S., 2014. SGK-1 regulates inflammation and cell death in the ischemic-reperfused heart: pressure-related effects. Am. J. Hypertens. 27, 846–856. doi:10.1093/ajh/hpt269

Bagher, P., Beleznai, T., Kansui, Y., Mitchell, R., Garland, C.J., Dora, K.A., 2012. Low intravascular pressure activates endothelial cell TRPV4 channels, local Ca2+ events, and IKCa channels, reducing arteriolar tone. Proc. Natl. Acad. Sci. U. S. A. 109, 18174–18179. doi:10.1073/pnas.1211946109

Balakrishna, S., Song, W., Achanta, S., Doran, S.F., Liu, B., Kaelberer, M.M., Yu, Z., Sui, A., Cheung, M., Leishman, E., Eidam, H.S., Ye, G., Willette, R.N., Thorneloe, K.S., Bradshaw, H.B., Matalon, S., Jordt, S.-E., 2014. TRPV4 inhibition counteracts edema and inflammation and improves pulmonary function and oxygen saturation in chemically induced acute lung injury. Am. J. Physiol. Lung Cell. Mol. Physiol. 307, L158-172. doi:10.1152/ajplung.00065.2014

Bao, L., Kaldany, C., Holmstrand, E.C., Cox, D.H., 2004. Mapping the BKCa channel's "Ca2+ bowl": side-chains essential for Ca2+ sensing. J. Gen. Physiol. 123, 475–489. doi:10.1085/jgp.200409052

Baratchi, S., Almazi, J.G., Darby, W., Tovar-Lopez, F.J., Mitchell, A., McIntyre, P., 2015. Shear stress mediates exocytosis of functional TRPV4 channels in endothelial cells. Cell. Mol. Life Sci. CMLS. doi:10.1007/s00018-015-2018-8

Baron, M., Boulanger, C.M., Staels, B., Tailleux, A., 2012. Cell-derived microparticles in atherosclerosis: biomarkers and targets for pharmacological modulation? J. Cell. Mol. Med. 16, 1365–1376. doi:10.1111/j.1582-4934.2011.01486.x

Bastarache, J.A., Wang, L., Geiser, T., Wang, Z., Albertine, K.H., Matthay, M.A., Ware, L.B., 2007. The alveolar epithelium can initiate the extrinsic coagulation cascade through expression of tissue factor. Thorax 62, 608–616. doi:10.1136/thx.2006.063305

Bastarache, J.A., Ware, L.B., Bernard, G.R., 2006. The role of the coagulation cascade in the continuum of sepsis and acute lung injury and acute respiratory distress syndrome. Semin. Respir. Crit. Care Med. 27, 365–376. doi:10.1055/s-2006-948290

Baxter, M., Eltom, S., Dekkak, B., Yew-Booth, L., Dubuis, E.D., Maher, S.A., Belvisi, M.G., Birrell, M.A., 2014. Role of transient receptor potential and pannexin channels in cigarette smoke-triggered ATP release in the lung. Thorax 69, 1080–1089. doi:10.1136/thoraxjnl-2014-205467

Becker, D., Bereiter-Hahn, J., Jendrach, M., 2009. Functional interaction of the cation channel transient receptor potential vanilloid 4 (TRPV4) and actin in volume regulation. Eur. J. Cell Biol. 88, 141–152. doi:10.1016/j.ejcb.2008.10.002

Beitler, J.R., Majumdar, R., Hubmayr, R.D., Malhotra, A., Thompson, B.T., Owens, R.L., Loring, S.H., Talmor, D., 2016. Volume Delivered During Recruitment Maneuver Predicts Lung Stress in Acute Respiratory Distress Syndrome. Crit. Care Med. 44, 91–99. doi:10.1097/CCM.0000000000001355

Bellani, G., Laffey, J.G., Pham, T., Fan, E., Brochard, L., Esteban, A., Gattinoni, L., van Haren, F., Larsson, A., McAuley, D.F., Ranieri, M., Rubenfeld, G., Thompson, B.T., Wrigge, H., Slutsky, A.S., Pesenti, A., LUNG SAFE Investigators, ESICM Trials Group, 2016. Epidemiology, Patterns of Care, and Mortality for Patients With Acute Respiratory Distress Syndrome in Intensive Care Units in 50 Countries. JAMA 315, 788–800. doi:10.1001/jama.2016.0291

Benn, A., Bredow, C., Casanova, I., Vukičević, S., Knaus, P., 2016. VE-cadherin facilitates BMP-induced endothelial cell permeability and signaling. J. Cell Sci. 129, 206–218. doi:10.1242/jcs.179960

Berridge, M.J., 2009. Inositol trisphosphate and calcium signalling mechanisms. Biochim. Biophys. Acta 1793, 933–940. doi:10.1016/j.bbamcr.2008.10.005

Berrout, J., Jin, M., Mamenko, M., Zaika, O., Pochynyuk, O., O'Neil, R.G., 2012. Function of transient receptor potential cation channel subfamily V member 4 (TRPV4) as a mechanical transducer in flow-sensitive segments of renal collecting duct system. J. Biol. Chem. 287, 8782–8791. doi:10.1074/jbc.M111.308411

Bhave, G., Hu, H.-J., Glauner, K.S., Zhu, W., Wang, H., Brasier, D.J., Oxford, G.S., Gereau, R.W., 2003. Protein kinase C phosphorylation sensitizes but does not activate the capsaicin receptor transient receptor potential vanilloid 1 (TRPV1). Proc. Natl. Acad. Sci. U. S. A. 100, 12480–12485. doi:10.1073/pnas.2032100100

Bhave, G., Zhu, W., Wang, H., Brasier, D.J., Oxford, G.S., Gereau, R.W., 2002. cAMP-dependent protein kinase regulates desensitization of the capsaicin receptor (VR1) by direct phosphorylation. Neuron 35, 721–731.

Birder, L.A., Nakamura, Y., Kiss, S., Nealen, M.L., Barrick, S., Kanai, A.J., Wang, E., Ruiz, G., De Groat, W.C., Apodaca, G., Watkins, S., Caterina, M.J., 2002. Altered urinary bladder function in mice lacking the vanilloid receptor TRPV1. Nat. Neurosci. 5, 856–860. doi:10.1038/nn902

Birukov, K.G., 2009. Small GTPases in mechanosensitive regulation of endothelial barrier. Microvasc. Res. 77, 46–52. doi:10.1016/j.mvr.2008.09.006

Birukova, A.A., Liu, F., Garcia, J.G.N., Verin, A.D., 2004a. Protein kinase A attenuates endothelial cell barrier dysfunction induced by microtubule disassembly. Am. J. Physiol. Lung Cell. Mol. Physiol. 287, L86-93. doi:10.1152/ajplung.00441.2003

Birukova, A.A., Smurova, K., Birukov, K.G., Usatyuk, P., Liu, F., Kaibuchi, K., Ricks-Cord, A., Natarajan, V., Alieva, I., Garcia, J.G.N., Verin, A.D., 2004b. Microtubule disassembly induces cytoskeletal remodeling and lung vascular barrier dysfunction: role of Rho-dependent mechanisms. J. Cell. Physiol. 201, 55–70. doi:10.1002/jcp.20055

Bond, C.T., Herson, P.S., Strassmaier, T., Hammond, R., Stackman, R., Maylie, J., Adelman, J.P., 2004. Small conductance Ca2+-activated K+ channel knock-out mice reveal the identity of calcium-dependent afterhyperpolarization currents. J. Neurosci. Off. J. Soc. Neurosci. 24, 5301–5306. doi:10.1523/JNEUROSCI.0182-04.2004

Bone, R.C., 1993. The ARDS lung. New insights from computed tomography. JAMA 269, 2134–2135.

Boulanger, C.M., 2010. Microparticles, vascular function and hypertension. Curr. Opin. Nephrol. Hypertens. 19, 177–180. doi:10.1097/MNH.0b013e32833640fd

Bradford, M.M., 1976. A rapid and sensitive method for the quantitation of microgram quantities of protein utilizing the principle of protein-dye binding. Anal. Biochem. 72, 248–254.

Brickley, D.R., Agyeman, A.S., Kopp, R.F., Hall, B.A., Harbeck, M.C., Belova, L., Volden, P.A., Wu, W., Roe, M.W., Conzen, S.D., 2013. Serum- and glucocorticoid-induced protein kinase 1 (SGK1) is regulated by store-operated Ca2+ entry and mediates cytoprotection against necrotic cell death. J. Biol. Chem. 288, 32708–32719. doi:10.1074/jbc.M113.507210

Broccard, A., Shapiro, R.S., Schmitz, L.L., Adams, A.B., Nahum, A., Marini, J.J., 2000. Prone positioning attenuates and redistributes ventilator-induced lung injury in dogs. Crit. Care Med. 28, 295–303.

Buesing, K.L., Densmore, J.C., Kaul, S., Pritchard, K.A., Jarzembowski, J.A., Gourlay, D.M., Oldham, K.T., 2011. Endothelial microparticles induce inflammation in acute lung injury. J. Surg. Res. 166, 32–39. doi:10.1016/j.jss.2010.05.036

Cabrera-Benítez, N.E., Valladares, F., García-Hernández, S., Ramos-Nuez, Á., Martín-Barrasa, J.L., Martínez-Saavedra, M.-T., Rodríguez-Gallego, C., Muros, M., Flores, C., Liu, M., Slutsky, A.S., Villar, J., 2015. Altered Profile of Circulating Endothelial-Derived Microparticles in

Ventilator-Induced Lung Injury. Crit. Care Med. 43, e551-559. doi:10.1097/CCM.0000000000001280

Calfee, C.S., Matthay, M.A., 2007. Nonventilatory treatments for acute lung injury and ARDS. Chest 131, 913–920. doi:10.1378/chest.06-1743

Caputo, A., Caci, E., Ferrera, L., Pedemonte, N., Barsanti, C., Sondo, E., Pfeffer, U., Ravazzolo, R., Zegarra-Moran, O., Galietta, L.J.V., 2008. TMEM16A, a membrane protein associated with calcium-dependent chloride channel activity. Science 322, 590–594. doi:10.1126/science.1163518

Caterina, M.J., Leffler, A., Malmberg, A.B., Martin, W.J., Trafton, J., Petersen-Zeitz, K.R., Koltzenburg, M., Basbaum, A.I., Julius, D., 2000. Impaired nociception and pain sensation in mice lacking the capsaicin receptor. Science 288, 306–313.

Cenac, N., Altier, C., Motta, J.-P., d'Aldebert, E., Galeano, S., Zamponi, G.W., Vergnolle, N., 2010. Potentiation of TRPV4 signalling by histamine and serotonin: an important mechanism for visceral hypersensitivity. Gut 59, 481–488. doi:10.1136/gut.2009.192567

Chen, H.I., Sudol, M., 1995. The WW domain of Yes-associated protein binds a proline-rich ligand that differs from the consensus established for Src homology 3-binding modules. Proc. Natl. Acad. Sci. U. S. A. 92, 7819–7823.

Chen, L., Kaßmann, M., Sendeski, M., Tsvetkov, D., Marko, L., Michalick, L., Riehle, M., Liedtke, W.B., Kuebler, W.M., Harteneck, C., Tepel, M., Patzak, A., Gollasch, M., 2015. Functional transient receptor potential vanilloid 1 and transient receptor potential vanilloid 4 channels along different segments of the renal vasculature. Acta Physiol. Oxf. Engl. 213, 481–491. doi:10.1111/apha.12355

Chen, L., Kaßmann, M., Sendeski, M., Tsvetkov, D., Marko, L., Michalick, L., Riehle, M., Wolfgang, L.B., Wolfgang, K.M., Harteneck, C., Tepel, M., Patzak, A., Gollasch, M., 2014. Functional TRPV1 and TRPV4 channels along different segments of the renal vasculature. Acta Physiol. Oxf. Engl. doi:10.1111/apha.12355

Chen, W., Chen, Y., Xu, B., Juang, Y.-C., Stippec, S., Zhao, Y., Cobb, M.H., 2009. Regulation of a third conserved phosphorylation site in SGK1. J. Biol. Chem. 284, 3453–3460. doi:10.1074/jbc.M807502200

Chen, Y., Kanju, P., Fang, Q., Lee, S.H., Parekh, P.K., Lee, W., Moore, C., Brenner, D., Gereau, R.W., Wang, F., Liedtke, W., 2014. TRPV4 is necessary for trigeminal irritant pain and functions as a cellular formalin receptor. Pain 155, 2662–2672. doi:10.1016/j.pain.2014.09.033

Cheng, C.-J., Huang, C.-L., 2011. Activation of PI3-kinase stimulates endocytosis of ROMK via Akt1/SGK1-dependent phosphorylation of WNK1. J. Am. Soc. Nephrol. JASN 22, 460–471. doi:10.1681/ASN.2010060681

Cheng, W., Sun, C., Zheng, J., 2010. Heteromerization of TRP channel subunits. Protein Cell 1, 802–810. doi:10.1007/s13238-010-0108-9

Chien, S., Li, S., Shiu, Y.-T., Li, Y.-S., 2005. Molecular basis of mechanical modulation of endothelial cell migration. Front. Biosci. J. Virtual Libr. 10, 1985–2000.

Chironi, G.N., Boulanger, C.M., Simon, A., Dignat-George, F., Freyssinet, J.-M., Tedgui, A., 2009. Endothelial microparticles in diseases. Cell Tissue Res. 335, 143–151. doi:10.1007/s00441-008-0710-9

Ciura, S., Bourque, C.W., 2006. Transient receptor potential vanilloid 1 is required for intrinsic osmoreception in organum vasculosum lamina terminalis neurons and for normal thirst responses to systemic hyperosmolality. J. Neurosci. Off. J. Soc. Neurosci. 26, 9069–9075. doi:10.1523/JNEUROSCI.0877-06.2006

Cohen, K.D., Jackson, W.F., 2005. Membrane hyperpolarization is not required for sustained muscarinic agonist-induced increases in intracellular Ca2+ in arteriolar endothelial cells. Microcirc. N. Y. N 1994 12, 169–182. doi:10.1080/10739680590904973

Cuajungco, M.P., Grimm, C., Oshima, K., D'hoedt, D., Nilius, B., Mensenkamp, A.R., Bindels, R.J.M., Plomann, M., Heller, S., 2006. PACSINs bind to the TRPV4 cation channel. PACSIN 3 modulates the subcellular localization of TRPV4. J. Biol. Chem. 281, 18753–18762. doi:10.1074/jbc.M602452200

Curry, F.-R.E., 2005. Microvascular solute and water transport. Microcirc. N. Y. N 1994 12, 17–31. doi:10.1080/10739680590894993

Dachary-Prigent, J., Pasquet, J.M., Freyssinet, J.M., Nurden, A.T., 1995. Calcium involvement in aminophospholipid exposure and microparticle formation during platelet activation: a study using Ca2+-ATPase inhibitors. Biochemistry (Mosc.) 34, 11625–11634.

Dalsgaard, T., Sonkusare, S.K., Teuscher, C., Poynter, M.E., Nelson, M.T., 2016. Pharmacological inhibitors of TRPV4 channels reduce cytokine production, restore endothelial function and increase survival in septic mice. Sci. Rep. 6, 33841. doi:10.1038/srep33841

Dasgupta, S.K., Le, A., Chavakis, T., Rumbaut, R.E., Thiagarajan, P., 2012. Developmental endothelial locus-1 (Del-1) mediates clearance of platelet microparticles by the endothelium. Circulation 125, 1664–1672. doi:10.1161/CIRCULATIONAHA.111.068833

Davis, J.B., Gray, J., Gunthorpe, M.J., Hatcher, J.P., Davey, P.T., Overend, P., Harries, M.H., Latcham, J., Clapham, C., Atkinson, K., Hughes, S.A., Rance, K., Grau, E., Harper, A.J., Pugh, P.L., Rogers, D.C., Bingham, S., Randall, A., Sheardown, S.A., 2000. Vanilloid receptor-1 is essential for inflammatory thermal hyperalgesia. Nature 405, 183–187. doi:10.1038/35012076

Debonneville, C., Flores, S.Y., Kamynina, E., Plant, P.J., Tauxe, C., Thomas, M.A., Münster, C., Chraïbi, A., Pratt, J.H., Horisberger, J.D., Pearce, D., Loffing, J., Staub, O., 2001. Phosphorylation of Nedd4-2 by Sgk1 regulates epithelial Na(+) channel cell surface expression. EMBO J. 20, 7052–7059. doi:10.1093/emboj/20.24.7052

del Zoppo, G.J., Milner, R., 2006. Integrin-matrix interactions in the cerebral microvasculature. Arterioscler. Thromb. Vasc. Biol. 26, 1966–1975. doi:10.1161/01.ATV.0000232525.65682.a2

Deng, W., Li, C.-Y., Tong, J., Zhang, W., Wang, D.-X., 2012. Regulation of ENaC-mediated alveolar fluid clearance by insulin via PI3K/Akt pathway in LPS-induced acute lung injury. Respir. Res. 13, 29. doi:10.1186/1465-9921-13-29

Densmore, J.C., Signorino, P.R., Ou, J., Hatoum, O.A., Rowe, J.J., Shi, Y., Kaul, S., Jones, D.W., Sabina, R.E., Pritchard, K.A., Guice, K.S., Oldham, K.T., 2006. Endothelium-derived microparticles induce endothelial dysfunction and acute lung injury. Shock Augusta Ga 26, 464–471. doi:10.1097/01.shk.0000228791.10550.36

Destaing, O., Block, M.R., Planus, E., Albiges-Rizo, C., 2011. Invadosome regulation by adhesion signaling. Curr. Opin. Cell Biol. 23, 597–606. doi:10.1016/j.ceb.2011.04.002

D'hoedt, D., Owsianik, G., Prenen, J., Cuajungco, M.P., Grimm, C., Heller, S., Voets, T., Nilius, B., 2008. Stimulus-specific modulation of the cation channel TRPV4 by PACSIN 3. J. Biol. Chem. 283, 6272–6280. doi:10.1074/jbc.M706386200

Distler, C., Rathee, P.K., Lips, K.S., Obreja, O., Neuhuber, W., Kress, M., 2003. Fast Ca2+-induced potentiation of heat-activated ionic currents requires cAMP/PKA signaling and functional AKAP anchoring. J. Neurophysiol. 89, 2499–2505. doi:10.1152/jn.00713.2002

Doorduin, J., Sinderby, C.A., Beck, J., van der Hoeven, J.G., Heunks, L.M.A., 2015. Assisted Ventilation in Patients with Acute Respiratory Distress Syndrome: Lung-distending Pressure and Patient-Ventilator Interaction. Anesthesiology 123, 181–190. doi:10.1097/ALN.0000000000000694

Dreyfuss, D., Saumon, G., 1998. Ventilator-induced lung injury: lessons from experimental studies. Am. J. Respir. Crit. Care Med. 157, 294–323. doi:10.1164/ajrccm.157.1.9604014

Du, J., Ma, X., Shen, B., Huang, Y., Birnbaumer, L., Yao, X., 2014. TRPV4, TRPC1, and TRPP2 assemble to form a flow-sensitive heteromeric channel. FASEB J. Off. Publ. Fed. Am. Soc. Exp. Biol. 28, 4677–4685. doi:10.1096/fj.14-251652

Dvorak, A.M., Kohn, S., Morgan, E.S., Fox, P., Nagy, J.A., Dvorak, H.F., 1996. The vesiculo-vacuolar organelle (VVO): a distinct endothelial cell structure that provides a transcellular pathway for macromolecular extravasation. J. Leukoc. Biol. 59, 100–115.

Earley, S., 2011. Endothelium-dependent cerebral artery dilation mediated by transient receptor potential and Ca2+-activated K+ channels. J. Cardiovasc. Pharmacol. 57, 148–153. doi:10.1097/FJC.0b013e3181f580d9

Effros, R.M., Darin, C., Jacobs, E.R., Rogers, R.A., Krenz, G., Schneeberger, E.E., 1997. Water transport and the distribution of aquaporin-1 in pulmonary air spaces. J. Appl. Physiol. Bethesda Md 1985 83, 1002–1016.

Eylenstein, A., Schmidt, S., Gu, S., Yang, W., Schmid, E., Schmidt, E.-M., Alesutan, I., Szteyn, K., Regel, I., Shumilina, E., Lang, F., 2012. Transcription factor NF-κB regulates expression of pore-forming Ca2+ channel unit, Orai1, and its activator, STIM1, to control Ca2+ entry and affect cellular functions. J. Biol. Chem. 287, 2719–2730. doi:10.1074/jbc.M111.275925

Fan, H.-C., Zhang, X., McNaughton, P.A., 2009. Activation of the TRPV4 ion channel is enhanced by phosphorylation. J. Biol. Chem. 284, 27884–27891. doi:10.1074/jbc.M109.028803

Fernandes, J., Lorenzo, I.M., Andrade, Y.N., Garcia-Elias, A., Serra, S.A., Fernández-Fernández, J.M., Valverde, M.A., 2008. IP3 sensitizes TRPV4 channel to the mechano- and osmotransducing messenger 5'-6'-epoxyeicosatrienoic acid. J. Gen. Physiol. 131, i2. doi:10.1085/JGP1315OIA2

Fernández-Fernández, J.M., Andrade, Y.N., Arniges, M., Fernandes, J., Plata, C., Rubio-Moscardo, F., Vázquez, E., Valverde, M.A., 2008. Functional coupling of TRPV4 cationic channel and large conductance, calcium-dependent potassium channel in human bronchial epithelial cell lines. Pflugers Arch. 457, 149–159. doi:10.1007/s00424-008-0516-3

Firestone, G.L., Giampaolo, J.R., O'Keeffe, B.A., 2003. Stimulus-dependent regulation of serum and glucocorticoid inducible protein kinase (SGK) transcription, subcellular localization and enzymatic activity. Cell. Physiol. Biochem. Int. J. Exp. Cell. Physiol. Biochem. Pharmacol. 13, 1–12. doi:70244

Fleming, I., Rueben, A., Popp, R., Fisslthaler, B., Schrodt, S., Sander, A., Haendeler, J., Falck, J.R., Morisseau, C., Hammock, B.D., Busse, R., 2007. Epoxyeicosatrienoic acids regulate Trp channel dependent Ca2+ signaling and hyperpolarization in endothelial cells. Arterioscler. Thromb. Vasc. Biol. 27, 2612–2618. doi:10.1161/ATVBAHA.107.152074

Fu, Y., Subramanya, A., Rozansky, D., Cohen, D.M., 2006. WNK kinases influence TRPV4 channel function and localization. Am. J. Physiol. Renal Physiol. 290, F1305-1314. doi:10.1152/ajprenal.00391.2005

Fujii, T., Sakata, A., Nishimura, S., Eto, K., Nagata, S., 2015. TMEM16F is required for phosphatidylserine exposure and microparticle release in activated mouse platelets. Proc. Natl. Acad. Sci. U. S. A. 112, 12800–12805. doi:10.1073/pnas.1516594112

Gallego-Sandín, S., Rodríguez-García, A., Alonso, M.T., García-Sancho, J., 2009. The endoplasmic reticulum of dorsal root ganglion neurons contains functional TRPV1 channels. J. Biol. Chem. 284, 32591–32601. doi:10.1074/jbc.M109.019687

Gao, X., Wu, L., O'Neil, R.G., 2003. Temperature-modulated diversity of TRPV4 channel gating: activation by physical stresses and phorbol ester derivatives through protein kinase C-dependent and -independent pathways. J. Biol. Chem. 278, 27129–27137. doi:10.1074/jbc.M302517200

Garcia, J.G., Davis, H.W., Patterson, C.E., 1995. Regulation of endothelial cell gap formation and barrier dysfunction: role of myosin light chain phosphorylation. J. Cell. Physiol. 163, 510–522. doi:10.1002/jcp.1041630311

Garcia-Elias, A., Lorenzo, I.M., Vicente, R., Valverde, M.A., 2008. IP3 receptor binds to and sensitizes TRPV4 channel to osmotic stimuli via a calmodulin-binding site. J. Biol. Chem. 283, 31284–31288. doi:10.1074/jbc.C800184200

García-Martínez, J.M., Alessi, D.R., 2008. mTOR complex 2 (mTORC2) controls hydrophobic motif phosphorylation and activation of serum- and glucocorticoid-induced protein kinase 1 (SGK1). Biochem. J. 416, 375–385. doi:10.1042/BJ20081668

García-Sanz, N., Fernández-Carvajal, A., Morenilla-Palao, C., Planells-Cases, R., Fajardo-Sánchez, E., Fernández-Ballester, G., Ferrer-Montiel, A., 2004. Identification of a tetramerization domain in the C terminus of the vanilloid receptor. J. Neurosci. Off. J. Soc. Neurosci. 24, 5307–5314. doi:10.1523/JNEUROSCI.0202-04.2004

García-Sanz, N., Valente, P., Gomis, A., Fernández-Carvajal, A., Fernández-Ballester, G., Viana, F., Belmonte, C., Ferrer-Montiel, A., 2007. A role of the transient receptor potential domain of vanilloid receptor I in channel gating. J. Neurosci. Off. J. Soc. Neurosci. 27, 11641–11650. doi:10.1523/JNEUROSCI.2457-07.2007

Gardos, G., 1958. The function of calcium in the potassium permeability of human erythrocytes. Biochim. Biophys. Acta 30, 653–654.

Gattinoni, L., Pesenti, A., 2005. The concept of "baby lung." Intensive Care Med. 31, 776–784. doi:10.1007/s00134-005-2627-z

Gavard, J., Gutkind, J.S., 2006. VEGF controls endothelial-cell permeability by promoting the beta-arrestin-dependent endocytosis of VE-cadherin. Nat. Cell Biol. 8, 1223–1234. doi:10.1038/ncb1486

Gavva, N.R., Treanor, J.J.S., Garami, A., Fang, L., Surapaneni, S., Akrami, A., Alvarez, F., Bak, A., Darling, M., Gore, A., Jang, G.R., Kesslak, J.P., Ni, L., Norman, M.H., Palluconi, G., Rose, M.J., Salfi, M., Tan, E., Romanovsky, A.A., Banfield, C., Davar, G., 2008. Pharmacological blockade of the vanilloid receptor TRPV1 elicits marked hyperthermia in humans. Pain 136, 202–210. doi:10.1016/j.pain.2008.01.024

Goeckeler, Z.M., Wysolmerski, R.B., 1995. Myosin light chain kinase-regulated endothelial cell contraction: the relationship between isometric tension, actin polymerization, and myosin phosphorylation. J. Cell Biol. 130, 613–627.

Goldenberg, N.M., Ravindran, K., Kuebler, W.M., 2015a. TRPV4: physiological role and therapeutic potential in respiratory diseases. Naunyn. Schmiedebergs Arch. Pharmacol. 388, 421–436. doi:10.1007/s00210-014-1058-1

Goldenberg, N.M., Wang, L., Ranke, H., Liedtke, W., Tabuchi, A., Kuebler, W.M., 2015b. TRPV4 Is Required for Hypoxic Pulmonary Vasoconstriction. Anesthesiology 122, 1338–1348. doi:10.1097/ALN.0000000000000647

Goswami, C., Kuhn, J., Heppenstall, P.A., Hucho, T., 2010. Importance of non-selective cation channel TRPV4 interaction with cytoskeleton and their reciprocal regulations in cultured cells. PloS One 5, e11654. doi:10.1371/journal.pone.0011654

Groot-Kormelink, P.J., Fawcett, L., Wright, P.D., Gosling, M., Kent, T.C., 2012. Quantitative GPCR and ion channel transcriptomics in primary alveolar macrophages and macrophage surrogates. BMC Immunol. 13, 57. doi:10.1186/1471-2172-13-57

Guérin, C., Reignier, J., Richard, J.-C., Beuret, P., Gacouin, A., Boulain, T., Mercier, E., Badet, M., Mercat, A., Baudin, O., Clavel, M., Chatellier, D., Jaber, S., Rosselli, S., Mancebo, J., Sirodot, M., Hilbert, G., Bengler, C., Richecoeur, J., Gainnier, M., Bayle, F., Bourdin, G., Leray, V., Girard, R., Baboi, L., Ayzac, L., PROSEVA Study Group, 2013. Prone positioning in severe acute respiratory distress syndrome. N. Engl. J. Med. 368, 2159–2168. doi:10.1056/NEJMoa1214103

Guervilly, C., Lacroix, R., Forel, J.-M., Roch, A., Camoin-Jau, L., Papazian, L., Dignat-George, F., 2011. High levels of circulating leukocyte microparticles are associated with better outcome in acute respiratory distress syndrome. Crit. Care Lond. Engl. 15, R31. doi:10.1186/cc9978

Haase, K., Al-Rekabi, Z., Pelling, A.E., 2014. Mechanical cues direct focal adhesion dynamics. Prog. Mol. Biol. Transl. Sci. 126, 103–134. doi:10.1016/B978-0-12-394624-9.00005-1

Hamanaka, K., Jian, M.-Y., Townsley, M.I., King, J.A., Liedtke, W., Weber, D.S., Eyal, F.G., Clapp, M.M., Parker, J.C., 2010. TRPV4 channels augment macrophage activation and ventilator-induced lung injury. Am. J. Physiol. Lung Cell. Mol. Physiol. 299, L353-362. doi:10.1152/ajplung.00315.2009

Hamanaka, K., Jian, M.-Y., Weber, D.S., Alvarez, D.F., Townsley, M.I., Al-Mehdi, A.B., King, J.A., Liedtke, W., Parker, J.C., 2007. TRPV4 initiates the acute calcium-dependent permeability increase during ventilator-induced lung injury in isolated mouse lungs. Am. J. Physiol. Lung Cell. Mol. Physiol. 293, L923-932. doi:10.1152/ajplung.00221.2007

Hannah, R.M., Dunn, K.M., Bonev, A.D., Nelson, M.T., 2011. Endothelial SK(Ca) and IK(Ca) channels regulate brain parenchymal arteriolar diameter and cortical cerebral blood flow. J. Cereb. Blood Flow Metab. Off. J. Int. Soc. Cereb. Blood Flow Metab. 31, 1175–1186. doi:10.1038/jcbfm.2010.214

Hartmannsgruber, V., Heyken, W.-T., Kacik, M., Kaistha, A., Grgic, I., Harteneck, C., Liedtke, W., Hoyer, J., Köhler, R., 2007. Arterial response to shear stress critically depends on endothelial TRPV4 expression. PloS One 2, e827. doi:10.1371/journal.pone.0000827

Hartzell, H.C., Yu, K., Xiao, Q., Chien, L.-T., Qu, Z., 2009. Anoctamin/TMEM16 family members are Ca2+-activated Cl- channels. J. Physiol. 587, 2127–2139. doi:10.1113/jphysiol.2008.163709

He, J., Qi, D., Wang, D.-X., Deng, W., Ye, Y., Feng, L.-H., Zhu, T., Zhao, Y., Zhang, C.-R., 2015. Insulin upregulates the expression of epithelial sodium channel in vitro and in a mouse model of acute lung injury: role of mTORC2/SGK1 pathway. Exp. Cell Res. 331, 164–175. doi:10.1016/j.yexcr.2014.09.024

Hellwig, N., Albrecht, N., Harteneck, C., Schultz, G., Schaefer, M., 2005. Homo- and heteromeric assembly of TRPV channel subunits. J. Cell Sci. 118, 917–928. doi:10.1242/jcs.01675

Hilfiker, M.A., Hoang, T.H., Cornil, J., Eidam, H.S., Matasic, D.S., Roethke, T.J., Klein, M., Thorneloe, K.S., Cheung, M., 2013. Optimization of a Novel Series of TRPV4 Antagonists with In Vivo Activity in a Model of Pulmonary Edema. ACS Med. Chem. Lett. 4, 293–296. doi:10.1021/ml300449k

Hirschberg, B., Maylie, J., Adelman, J.P., Marrion, N.V., 1998. Gating of recombinant small-conductance Ca-activated K+ channels by calcium. J. Gen. Physiol. 111, 565–581.

Huai, J., Zhang, Y., Liu, Q.-M., Ge, H.-Y., Arendt-Nielsen, L., Jiang, H., Yue, S.-W., 2012. Interaction of transient receptor potential vanilloid 4 with annexin A2 and tubulin beta 5. Neurosci. Lett. 512, 22–27. doi:10.1016/j.neulet.2012.01.048

Humphrey, J.D., Dufresne, E.R., Schwartz, M.A., 2014. Mechanotransduction and extracellular matrix homeostasis. Nat. Rev. Mol. Cell Biol. 15, 802–812. doi:10.1038/nrm3896

Imai, S., Okayama, N., Shimizu, M., Itoh, M., 2003. Increased intracellular calcium activates serum and glucocorticoid-inducible kinase 1 (SGK1) through a calmodulin-calcium calmodulin dependent kinase kinase pathway in Chinese hamster ovary cells. Life Sci. 72, 2199–2209.

Inal, J.M., Kosgodage, U., Azam, S., Stratton, D., Antwi-Baffour, S., Lange, S., 2013. Blood/plasma secretome and microvesicles. Biochim. Biophys. Acta 1834, 2317–2325. doi:10.1016/j.bbapap.2013.04.005

Ingber, D.E., 2002. Mechanical signaling and the cellular response to extracellular matrix in angiogenesis and cardiovascular physiology. Circ. Res. 91, 877–887.

Ishii, T.M., Silvia, C., Hirschberg, B., Bond, C.T., Adelman, J.P., Maylie, J., 1997. A human intermediate conductance calcium-activated potassium channel. Proc. Natl. Acad. Sci. U. S. A. 94, 11651–11656.

Jeske, N.A., Diogenes, A., Ruparel, N.B., Fehrenbacher, J.C., Henry, M., Akopian, A.N., Hargreaves, K.M., 2008. A-kinase anchoring protein mediates TRPV1 thermal hyperalgesia through PKA phosphorylation of TRPV1. Pain 138, 604–616. doi:10.1016/j.pain.2008.02.022

Jia, Y., Wang, X., Varty, L., Rizzo, C.A., Yang, R., Correll, C.C., Phelps, P.T., Egan, R.W., Hey, J.A., 2004. Functional TRPV4 channels are expressed in human airway smooth muscle cells. Am. J. Physiol. Lung Cell. Mol. Physiol. 287, L272-278. doi:10.1152/ajplung.00393.2003

Jian, M.-Y., King, J.A., Al-Mehdi, A.-B., Liedtke, W., Townsley, M.I., 2008. High vascular pressure-induced lung injury requires P450 epoxygenase-dependent activation of TRPV4. Am. J. Respir. Cell Mol. Biol. 38, 386–392. doi:10.1165/rcmb.2007-0192OC

Jiang, B., Deng, Y., Suen, C., Taha, M., Chaudhary, K.R., Courtman, D.W., Stewart, D.J., 2015. Marked Strain-specific Differences in the SU5416 Rat Model of Severe Pulmonary Arterial Hypertension. Am. J. Respir. Cell Mol. Biol. doi:10.1165/rcmb.2014-0488OC

Jo, A.O., Ryskamp, D.A., Phuong, T.T.T., Verkman, A.S., Yarishkin, O., MacAulay, N., Križaj, D., 2015. TRPV4 and AQP4 Channels Synergistically Regulate Cell Volume and Calcium Homeostasis in Retinal Müller Glia. J. Neurosci. Off. J. Soc. Neurosci. 35, 13525–13537. doi:10.1523/JNEUROSCI.1987-15.2015

Joiner, W.J., Khanna, R., Schlichter, L.C., Kaczmarek, L.K., 2001. Calmodulin regulates assembly and trafficking of SK4/IK1 Ca2+-activated K+ channels. J. Biol. Chem. 276, 37980–37985. doi:10.1074/jbc.M104965200

Joiner, W.J., Wang, L.Y., Tang, M.D., Kaczmarek, L.K., 1997. hSK4, a member of a novel subfamily of calcium-activated potassium channels. Proc. Natl. Acad. Sci. U. S. A. 94, 11013–11018.

Kahlfuß, S., Simma, N., Mankiewicz, J., Bose, T., Lowinus, T., Klein-Hessling, S., Sprengel, R., Schraven, B., Heine, M., Bommhardt, U., 2014. Immunosuppression by N-methyl-D-aspartate receptor antagonists is mediated through inhibition of Kv1.3 and KCa3.1 channels in T cells. Mol. Cell. Biol. 34, 820–831. doi:10.1128/MCB.01273-13

Kang, S.S., Shin, S.H., Auh, C.-K., Chun, J., 2012. Human skeletal dysplasia caused by a constitutive activated transient receptor potential vanilloid 4 (TRPV4) cation channel mutation. Exp. Mol. Med. 44, 707–722. doi:10.3858/emm.2012.44.12.080

Kanju, P., Chen, Y., Lee, W., Yeo, M., Lee, S.H., Romac, J., Shahid, R., Fan, P., Gooden, D.M., Simon, S.A., Spasojevic, I., Mook, R.A., Liddle, R.A., Guilak, F., Liedtke, W.B., 2016. Small molecule dual-inhibitors of TRPV4 and TRPA1 for attenuation of inflammation and pain. Sci. Rep. 6, 26894. doi:10.1038/srep26894

Kása, A., Csortos, C., Verin, A.D., 2015. Cytoskeletal mechanisms regulating vascular endothelial barrier function in response to acute lung injury. Tissue Barriers 3, e974448. doi:10.4161/21688370.2014.974448

Kim, S., Barry, D.M., Liu, X.-Y., Yin, S., Munanairi, A., Meng, Q.-T., Cheng, W., Mo, P., Wan, L., Liu, S.-B., Ratnayake, K., Zhao, Z.-Q., Gautam, N., Zheng, J., Karunarathne, W.K.A., Chen, Z.-F., 2016. Facilitation of TRPV4 by TRPV1 is required for itch transmission in some sensory neuron populations. Sci Signal 9, ra71-ra71. doi:10.1126/scisignal.aaf1047

Komarova, Y., Malik, A.B., 2010. Regulation of endothelial permeability via paracellular and transcellular transport pathways. Annu. Rev. Physiol. 72, 463–493. doi:10.1146/annurev-physiol-021909-135833

Komarova, Y.A., Mehta, D., Malik, A.B., 2007. Dual regulation of endothelial junctional permeability. Sci. STKE Signal Transduct. Knowl. Environ. 2007, re8. doi:10.1126/stke.4122007re8

Koshy, S., Wu, D., Hu, X., Tajhya, R.B., Huq, R., Khan, F.S., Pennington, M.W., Wulff, H., Yotnda, P., Beeton, C., 2013. Blocking KCa3.1 channels increases tumor cell killing by a subpopulation of human natural killer lymphocytes. PloS One 8, e76740. doi:10.1371/journal.pone.0076740

Köttgen, M., Buchholz, B., Garcia-Gonzalez, M.A., Kotsis, F., Fu, X., Doerken, M., Boehlke, C., Steffl, D., Tauber, R., Wegierski, T., Nitschke, R., Suzuki, M., Kramer-Zucker, A., Germino, G.G., Watnick, T., Prenen, J., Nilius, B., Kuehn, E.W., Walz, G., 2008. TRPP2 and TRPV4 form a polymodal sensory channel complex. J. Cell Biol. 182, 437–447. doi:10.1083/jcb.200805124

Koval, M., Bhattacharya, J., 2005. Vascular Gap junctions. In: Microvascular Research: Biology And Pathology, edited by Shepro D. Elsevier.

Kuebler, W.M., 2009. Effects of Pressure and Flow on the Pulmonary Endothelium, in: Voelkel, N.F., Chief, S.R. (Eds.), The Pulmonary Endothelium. John Wiley & Sons, Ltd, pp. 309–335.

Kuebler, W.M., Abels, C., Schuerer, L., Goetz, A.E., 1996. Measurement of neutrophil content in brain and lung tissue by a modified myeloperoxidase assay. Int. J. Microcirc. Clin. Exp. Spons. Eur. Soc. Microcirc. 16, 89–97.

Lacroix, R., Dubois, C., Leroyer, A.S., Sabatier, F., Dignat-George, F., 2013. Revisited role of microparticles in arterial and venous thrombosis. J. Thromb. Haemost. JTH 11 Suppl 1, 24–35. doi:10.1111/jth.12268

Laemmli, U.K., 1970. Cleavage of structural proteins during the assembly of the head of bacteriophage T4. Nature 227, 680–685.

Lang, F., Cohen, P., 2001. Regulation and physiological roles of serum- and glucocorticoid-induced protein kinase isoforms. Sci. STKE Signal Transduct. Knowl. Environ. 2001, re17. doi:10.1126/stke.2001.108.re17

Lang, P.A., Graf, D., Boini, K.M., Lang, K.S., Klingel, K., Kandolf, R., Lang, F., 2011. Cell volume, the serum and glucocorticoid inducible kinase 1 and the liver. Z. Für Gastroenterol. 49, 713–719. doi:10.1055/s-0031-1273425

Lau, S.-Y., Procko, E., Gaudet, R., 2012. Distinct properties of Ca2+-calmodulin binding to N- and C-terminal regulatory regions of the TRPV1 channel. J. Gen. Physiol. 140, 541–555. doi:10.1085/jgp.201210810

Lee, E.J., Shin, S.H., Hyun, S., Chun, J., Kang, S.S., 2011. Mutation of a putative S-nitrosylation site of TRPV4 protein facilitates the channel activates. Anim. Cells Syst. 15, 95–106. doi:10.1080/19768354.2011.555183

Lee, H., Iida, T., Mizuno, A., Suzuki, M., Caterina, M.J., 2005. Altered thermal selection behavior in mice lacking transient receptor potential vanilloid 4. J. Neurosci. Off. J. Soc. Neurosci. 25, 1304–1310. doi:10.1523/JNEUROSCI.4745.04.2005

Lee, W.-S., Ngo-Anh, T.J., Bruening-Wright, A., Maylie, J., Adelman, J.P., 2003. Small conductance Ca2+-activated K+ channels and calmodulin: cell surface expression and gating. J. Biol. Chem. 278, 25940–25946. doi:10.1074/jbc.M302091200

Levitt, J.E., Matthay, M.A., 2012. Clinical review: Early treatment of acute lung injury--paradigm shift toward prevention and treatment prior to respiratory failure. Crit. Care Lond. Engl. 16, 223. doi:10.1186/cc11144

Liedtke, W., Choe, Y., Martí-Renom, M.A., Bell, A.M., Denis, C.S., Sali, A., Hudspeth, A.J., Friedman, J.M., Heller, S., 2000. Vanilloid receptor-related osmotically activated channel (VR-OAC), a candidate vertebrate osmoreceptor. Cell 103, 525–535.

Liedtke, W., Friedman, J.M., 2003a. Abnormal osmotic regulation in trpv4-/- mice. Proc. Natl. Acad. Sci. U. S. A. 100, 13698–13703. doi:10.1073/pnas.1735416100

Liedtke, W., Friedman, J.M., 2003b. Abnormal osmotic regulation in trpv4-/- mice. Proc. Natl. Acad. Sci. U. S. A. 100, 13698–13703. doi:10.1073/pnas.1735416100

Lin, D.-H., Yue, P., Yarborough, O., Scholl, U.I., Giebisch, G., Lifton, R.P., Rinehart, J., Wang, W.-H., 2015. Src-family protein tyrosine kinase phosphorylates WNK4 and modulates its inhibitory effect on KCNJ1 (ROMK). Proc. Natl. Acad. Sci. U. S. A. 112, 4495–4500. doi:10.1073/pnas.1503437112

Lin, M.T., Jian, M.-Y., Taylor, M.S., Cioffi, D.L., Yap, F.C., Liedtke, W., Townsley, M.I., 2015. Functional coupling of TRPV4, IK, and SK channels contributes to Ca(2+)-dependent endothelial injury in rodent lung. Pulm. Circ. 5, 279–290. doi:10.1086/680166

Liou, J., Kim, M.L., Heo, W.D., Jones, J.T., Myers, J.W., Ferrell, J.E., Meyer, T., 2005. STIM is a Ca2+ sensor essential for Ca2+-store-depletion-triggered Ca2+ influx. Curr. Biol. CB 15, 1235–1241. doi:10.1016/j.cub.2005.05.055

Lorenzo, I.M., Liedtke, W., Sanderson, M.J., Valverde, M.A., 2008. TRPV4 channel participates in receptor-operated calcium entry and ciliary beat frequency regulation in mouse airway epithelial cells. Proc. Natl. Acad. Sci. U. S. A. 105, 12611–12616. doi:10.1073/pnas.0803970105

Loukin, S., Zhou, X., Su, Z., Saimi, Y., Kung, C., 2010. Wild-type and brachyolmia-causing mutant TRPV4 channels respond directly to stretch force. J. Biol. Chem. 285, 27176–27181. doi:10.1074/jbc.M110.143370

Lu, M., Wang, J., Jones, K.T., Ives, H.E., Feldman, M.E., Yao, L., Shokat, K.M., Ashrafi, K., Pearce, D., 2010. mTOR complex-2 activates ENaC by phosphorylating SGK1. J. Am. Soc. Nephrol. JASN 21, 811–818. doi:10.1681/ASN.2009111168

Lu, P., Boros, S., Chang, Q., Bindels, R.J., Hoenderop, J.G., 2008. The beta-glucuronidase klotho exclusively activates the epithelial Ca2+ channels TRPV5 and TRPV6. Nephrol. Dial. Transplant. Off. Publ. Eur. Dial. Transpl. Assoc. - Eur. Ren. Assoc. 23, 3397–3402. doi:10.1093/ndt/gfn291

Lukacs, V., Rives, J.-M., Sun, X., Zakharian, E., Rohacs, T., 2013. Promiscuous activation of transient receptor potential vanilloid 1 (TRPV1) channels by negatively charged intracellular lipids: the key role of endogenous phosphoinositides in maintaining channel activity. J. Biol. Chem. 288, 35003–35013. doi:10.1074/jbc.M113.520288

Luscinskas, F.W., Lawler, J., 1994. Integrins as dynamic regulators of vascular function. FASEB J. Off. Publ. Fed. Am. Soc. Exp. Biol. 8, 929–938.

Ma, X., Cao, J., Luo, J., Nilius, B., Huang, Y., Ambudkar, I.S., Yao, X., 2010a. Depletion of intracellular Ca2+ stores stimulates the translocation of vanilloid transient receptor potential 4-c1 heteromeric channels to the plasma membrane. Arterioscler. Thromb. Vasc. Biol. 30, 2249–2255. doi:10.1161/ATVBAHA.110.212084

Ma, X., Cheng, K.-T., Wong, C.-O., O'Neil, R.G., Birnbaumer, L., Ambudkar, I.S., Yao, X., 2011a. Heteromeric TRPV4-C1 channels contribute to store-operated Ca(2+) entry in vascular endothelial cells. Cell Calcium 50, 502–509. doi:10.1016/j.ceca.2011.08.006

Ma, X., Cheng, K.-T., Wong, C.-O., O'Neil, R.G., Birnbaumer, L., Ambudkar, I.S., Yao, X., 2011b. Heteromeric TRPV4-C1 channels contribute to store-operated Ca(2+) entry in vascular endothelial cells. Cell Calcium 50, 502–509. doi:10.1016/j.ceca.2011.08.006

Ma, X., Qiu, S., Luo, J., Ma, Y., Ngai, C.-Y., Shen, B., Wong, C., Huang, Y., Yao, X., 2010b. Functional role of vanilloid transient receptor potential 4-canonical transient receptor potential 1 complex in flow-induced Ca2+ influx. Arterioscler. Thromb. Vasc. Biol. 30, 851–858. doi:10.1161/ATVBAHA.109.196584

Ma, X., Qiu, S., Luo, J., Ma, Y., Ngai, C.-Y., Shen, B., Wong, C., Huang, Y., Yao, X., 2010c. Functional role of vanilloid transient receptor potential 4-canonical transient receptor potential 1 complex in flow-induced Ca2+ influx. Arterioscler. Thromb. Vasc. Biol. 30, 851–858. doi:10.1161/ATVBAHA.109.196584

MacKenzie, A., Wilson, H.L., Kiss-Toth, E., Dower, S.K., North, R.A., Surprenant, A., 2001. Rapid secretion of interleukin-1beta by microvesicle shedding. Immunity 15, 825–835.

Maiyar, A.C., Leong, M.L.L., Firestone, G.L., 2003. Importin-alpha mediates the regulated nuclear targeting of serum- and glucocorticoid-inducible protein kinase (Sgk) by recognition of a nuclear localization signal in the kinase central domain. Mol. Biol. Cell 14, 1221–1239. doi:10.1091/mbc.E02-03-0170

Marshall, I.C.B., Owen, D.E., Cripps, T.V., Davis, J.B., McNulty, S., Smart, D., 2003. Activation of vanilloid receptor 1 by resiniferatoxin mobilizes calcium from inositol 1,4,5-trisphosphate-sensitive stores. Br. J. Pharmacol. 138, 172–176. doi:10.1038/sj.bjp.0705003

Matthews, B.D., Thodeti, C.K., Tytell, J.D., Mammoto, A., Overby, D.R., Ingber, D.E., 2010. Ultra-rapid activation of TRPV4 ion channels by mechanical forces applied to cell surface beta1 integrins. Integr. Biol. Quant. Biosci. Nano Macro 2, 435–442. doi:10.1039/c0ib00034e

Matute-Bello, G., Downey, G., Moore, B.B., Groshong, S.D., Matthay, M.A., Slutsky, A.S., Kuebler, W.M., Acute Lung Injury in Animals Study Group, 2011. An official American Thoracic Society workshop report: features and measurements of experimental acute lung injury in animals. Am. J. Respir. Cell Mol. Biol. 44, 725–738. doi:10.1165/rcmb.2009-0210ST

McGillem, L.L., Garcia, J.G.N., 2005. Role of the Endothelial Cell cytoskeleton in Microvascular Function. In: Microvascular Research: Biology And Pathology, edited by Shepro D. Elsevier.

McHugh, J., Keller, N.R., Appalsamy, M., Thomas, S.A., Raj, S.R., Diedrich, A., Biaggioni, I., Jordan, J., Robertson, D., 2010. Portal osmopressor mechanism linked to transient receptor potential vanilloid 4 and blood pressure control. Hypertension 55, 1438–1443. doi:10.1161/HYPERTENSIONAHA.110.151860

McVey, M., Tabuchi, A., Kuebler, W.M., 2012. Microparticles and acute lung injury. Am. J. Physiol. Lung Cell. Mol. Physiol. 303, L364-381. doi:10.1152/ajplung.00354.2011

McVey, M.J., Spring, C.M., Semple, J.W., Maishan, M., Kuebler, W.M., 2016. Microparticles as biomarkers of lung disease: enumeration in biological fluids using lipid bilayer microspheres. Am. J. Physiol. Lung Cell. Mol. Physiol. 310, L802-814. doi:10.1152/ajplung.00369.2015

Mead, J., Takishima, T., Leith, D., 1970. Stress distribution in lungs: a model of pulmonary elasticity. J. Appl. Physiol. 28, 596–608.

Meade, M.O., Cook, D.J., Guyatt, G.H., Slutsky, A.S., Arabi, Y.M., Cooper, D.J., Davies, A.R., Hand, L.E., Zhou, Q., Thabane, L., Austin, P., Lapinsky, S., Baxter, A., Russell, J., Skrobik, Y., Ronco, J.J., Stewart, T.E., Lung Open Ventilation Study Investigators, 2008. Ventilation strategy using low tidal volumes, recruitment maneuvers, and high positive end-expiratory pressure for acute lung injury and acute respiratory distress syndrome: a randomized controlled trial. JAMA 299, 637–645. doi:10.1001/jama.299.6.637

Mehta, D., Malik, A.B., 2006. Signaling mechanisms regulating endothelial permeability. Physiol. Rev. 86, 279–367. doi:10.1152/physrev.00012.2005

Mercado, J., Baylie, R., Navedo, M.F., Yuan, C., Scott, J.D., Nelson, M.T., Brayden, J.E., Santana, L.F., 2014. Local control of TRPV4 channels by AKAP150-targeted PKC in arterial smooth muscle. J. Gen. Physiol. 143, 559–575. doi:10.1085/jgp.201311050

Michalick, L., Erfinanda, L., Weichelt, U., van der Giet, M., Liedtke, W., Kuebler, W.M., 2017. Transient Receptor Potential Vanilloid 4 and Serum Glucocorticoid-regulated Kinase 1 Are Critical Mediators of Lung Injury in Overventilated Mice In Vivo. Anesthesiology 126, 300–311. doi:10.1097/ALN.0000000000001443

Michalick, L., Giet, M. van der, Liedtke, W., Kuebler, W., 2014. Ca2+ entry via transient receptor potential vanilloid channel 4 mediates ventilation-induced lung vascular barrier failure (1176.3). FASEB J. 28, 1176.3.

Montell, C., 2005. The TRP superfamily of cation channels. Sci. STKE Signal Transduct. Knowl. Environ. 2005, re3. doi:10.1126/stke.2722005re3

Morenilla-Palao, C., Planells-Cases, R., García-Sanz, N., Ferrer-Montiel, A., 2004. Regulated exocytosis contributes to protein kinase C potentiation of vanilloid receptor activity. J. Biol. Chem. 279, 25665–25672. doi:10.1074/jbc.M311515200

Müller, H.C., Hellwig, K., Rosseau, S., Tschernig, T., Schmiedl, A., Gutbier, B., Schmeck, B., Hippenstiel, S., Peters, H., Morawietz, L., Suttorp, N., Witzenrath, M., 2010. Simvastatin attenuates ventilator-induced lung injury in mice. Crit. Care Lond. Engl. 14, R143. doi:10.1186/cc9209

Müller-Marschhausen, K., Waschke, J., Drenckhahn, D., 2008. Physiological hydrostatic pressure protects endothelial monolayer integrity. Am. J. Physiol. Cell Physiol. 294, C324-332. doi:10.1152/ajpcell.00319.2007

Na, T., Wu, G., Zhang, W., Dong, W.-J., Peng, J.-B., 2013. Disease-causing R1185C mutation of WNK4 disrupts a regulatory mechanism involving calmodulin binding and SGK1 phosphorylation sites. Am. J. Physiol. Renal Physiol. 304, F8–F18. doi:10.1152/ajprenal.00284.2012

Nakamura, S.-I., Yamamura, H., 2010. Yasutomi Nishizuka: father of protein kinase C. J. Biochem. (Tokyo) 148, 125–130. doi:10.1093/jb/mvq066

Narita, K., Sasamoto, S., Koizumi, S., Okazaki, S., Nakamura, H., Inoue, T., Takeda, S., 2015. TRPV4 regulates the integrity of the blood-cerebrospinal fluid barrier and modulates transepithelial protein transport. FASEB J. Off. Publ. Fed. Am. Soc. Exp. Biol. 29, 2247–2259. doi:10.1096/fj.14-261396

Nayak, P.S., Wang, Y., Najrana, T., Priolo, L.M., Rios, M., Shaw, S.K., Sanchez-Esteban, J., 2015. Mechanotransduction via TRPV4 regulates inflammation and differentiation in fetal mouse distal lung epithelial cells. Respir. Res. 16, 60. doi:10.1186/s12931-015-0224-4

Nilius, B., Owsianik, G., Voets, T., 2008. Transient receptor potential channels meet phosphoinositides. EMBO J. 27, 2809–2816. doi:10.1038/emboj.2008.217

Nilius, B., Voets, T., 2013. The puzzle of TRPV4 channelopathies. EMBO Rep. 14, 152–163. doi:10.1038/embor.2012.219

O'Neil, R.G., Heller, S., 2005. The mechanosensitive nature of TRPV channels. Pflüg. Arch. Eur. J. Physiol. 451, 193–203. doi:10.1007/s00424-005-1424-4

Park, S.Y., Kim, H.J., Yoo, K.H., Park, Y.B., Kim, S.W., Lee, S.J., Kim, E.K., Kim, J.H., Kim, Y.H., Moon, J.-Y., Min, K.H., Park, S.S., Lee, J., Lee, C.-H., Park, J., Byun, M.K., Lee, S.W., Rlee, C., Jung, J.Y., Sim, Y.S., 2015. The efficacy and safety of prone positioning in adults patients with acute respiratory distress syndrome: a meta-analysis of randomized controlled trials. J. Thorac. Dis. 7, 356–367. doi:10.3978/j.issn.2072-1439.2014.12.49

Parker, J.C., Hashizumi, M., Kelly, S.V., Francis, M., Mouner, M., Meyer, A.L., Townsley, M.I., Wu, S., Cioffi, D.L., Taylor, M.S., 2013. TRPV4 calcium entry and surface expression attenuated by inhibition of myosin light chain kinase in rat pulmonary microvascular endothelial cells. Physiol. Rep. 1, e00121. doi:10.1002/phy2.121

Parpaite, T., Cardouat, G., Mauroux, M., Gillibert-Duplantier, J., Robillard, P., Quignard, J.-F., Marthan, R., Savineau, J.-P., Ducret, T., 2016. Effect of hypoxia on TRPV1 and TRPV4 channels in rat pulmonary arterial smooth muscle cells. Pflugers Arch. 468, 111–130. doi:10.1007/s00424-015-1704-6

Pasquet, J.M., Dachary-Prigent, J., Nurden, A.T., 1996. Calcium influx is a determining factor of calpain activation and microparticle formation in platelets. Eur. J. Biochem. 239, 647–654.

Peng, G., Lu, W., Li, X., Chen, Y., Zhong, N., Ran, P., Wang, J., 2010. Expression of store-operated Ca2+ entry and transient receptor potential canonical and vanilloid-related proteins in rat distal pulmonary venous smooth muscle. Am. J. Physiol. Lung Cell. Mol. Physiol. 299, L621-630. doi:10.1152/ajplung.00176.2009

Peng, H., Lewandrowski, U., Müller, B., Sickmann, A., Walz, G., Wegierski, T., 2010. Identification of a Protein Kinase C-dependent phosphorylation site involved in sensitization of TRPV4 channel. Biochem. Biophys. Res. Commun. 391, 1721–1725. doi:10.1016/j.bbrc.2009.12.140

Perret, B., Chap, H.J., Douste-Blazy, L., 1979. Asymmetric distribution of arachidonic acid in the plasma membrane of human platelets. A determination using purified phospholipases and a rapid method for membrane isolation. Biochim. Biophys. Acta 556, 434–446.

Piccardoni, P., Manarini, S., Federico, L., Bagoly, Z., Pecce, R., Martelli, N., Piccoli, A., Totani, L., Cerletti, C., Evangelista, V., 2004. SRC-dependent outside-in signalling is a key step in the process of autoregulation of beta2 integrins in polymorphonuclear cells. Biochem. J. 380, 57–65. doi:10.1042/BJ20040151

Plantavid, M., Perret, B.P., Chap, H., Simon, M.F., Douste-Blazy, L., 1982. Asymmetry of arachidonic acid metabolism in the phospholipids of the human platelet membrane as studied with purified phospholipases. Biochim. Biophys. Acta 693, 451–460.

Prasain, N., Stevens, T., 2009. The actin cytoskeleton in endothelial cell phenotypes. Microvasc. Res. 77, 53–63. doi:10.1016/j.mvr.2008.09.012

Predescu, D., Palade, G.E., 1993. Plasmalemmal vesicles represent the large pore system of continuous microvascular endothelium. Am. J. Physiol. 265, H725-733.

Predescu, S.A., Predescu, D.N., Malik, A.B., 2007. Molecular determinants of endothelial transcytosis and their role in endothelial permeability. Am. J. Physiol. Lung Cell. Mol. Physiol. 293, L823-842. doi:10.1152/ajplung.00436.2006

Prescott, E.D., Julius, D., 2003. A modular PIP2 binding site as a determinant of capsaicin receptor sensitivity. Science 300, 1284–1288. doi:10.1126/science.1083646

Puntorieri, V., Hiansen, J.Q., McCaig, L.A., Yao, L.-J., Veldhuizen, R.A.W., Lewis, J.F., 2013. The effects of exogenous surfactant administration on ventilation-induced inflammation in mouse models of lung injury. BMC Pulm. Med. 13, 67. doi:10.1186/1471-2466-13-67

Qadri, S.M., Su, Y., Cayabyab, F.S., Liu, L., 2014. Endothelial Na+/H+ exchanger NHE1 participates in redox-sensitive leukocyte recruitment triggered by methylglyoxal. Cardiovasc. Diabetol. 13, 134. doi:10.1186/s12933-014-0134-7

Qin, F., 2007. Regulation of TRP ion channels by phosphatidylinositol-4,5-bisphosphate. Handb. Exp. Pharmacol. 509–525. doi:10.1007/978-3-540-34891-7_30

Quesenberry, P.J., Dooner, M.S., Aliotta, J.M., 2010. Stem cell plasticity revisited: the continuum marrow model and phenotypic changes mediated by microvesicles. Exp. Hematol. 38, 581–592. doi:10.1016/j.exphem.2010.03.021

Rahaman, S.O., Grove, L.M., Paruchuri, S., Southern, B.D., Abraham, S., Niese, K.A., Scheraga, R.G., Ghosh, S., Thodeti, C.K., Zhang, D.X., Moran, M.M., Schilling, W.P., Tschumperlin, D.J., Olman, M.A., 2014. TRPV4 mediates myofibroblast differentiation and pulmonary fibrosis in mice. J. Clin. Invest. 124, 5225–5238. doi:10.1172/JCI75331

Rahman, M., Mukherjee, S., Sheng, W., Nilius, B., Janssen, L.J., 2016. Electrophysiological characterization of voltage-dependent calcium-currents and TRPV4-currents in human pulmonary fibroblasts. Am. J. Physiol. Lung Cell. Mol. Physiol. ajplung.00426.2015. doi:10.1152/ajplung.00426.2015

Ramadass, R., Becker, D., Jendrach, M., Bereiter-Hahn, J., 2007. Spectrally and spatially resolved fluorescence lifetime imaging in living cells: TRPV4-microfilament interactions. Arch. Biochem. Biophys. 463, 27–36. doi:10.1016/j.abb.2007.01.036

Raychaudhuri, S.K., Raychaudhuri, S.P., Weltman, H., Farber, E.M., 2001. Effect of nerve growth factor on endothelial cell biology: proliferation and adherence molecule expression on human dermal microvascular endothelial cells. Arch. Dermatol. Res. 293, 291–295.

Reményi, A., Good, M.C., Lim, W.A., 2006. Docking interactions in protein kinase and phosphatase networks. Curr. Opin. Struct. Biol. 16, 676–685. doi:10.1016/j.sbi.2006.10.008

Ricard, J.D., Dreyfuss, D., 2001. Cytokines during ventilator-induced lung injury: a word of caution. Anesth. Analg. 93, 251–252.

Ricard, J.-D., Dreyfuss, D., Saumon, G., 2002. Ventilator-induced lung injury. Curr. Opin. Crit. Care 8, 12–20.

Rigor, R.R., Shen, Q., Pivetti, C.D., Wu, M.H., Yuan, S.Y., 2013. Myosin light chain kinase signaling in endothelial barrier dysfunction. Med. Res. Rev. 33, 911–933. doi:10.1002/med.21270

Ring, A.M., Leng, Q., Rinehart, J., Wilson, F.H., Kahle, K.T., Hebert, S.C., Lifton, R.P., 2007. An SGK1 site in WNK4 regulates Na+ channel and K+ channel activity and has implications for aldosterone signaling and K+ homeostasis. Proc. Natl. Acad. Sci. U. S. A. 104, 4025–4029. doi:10.1073/pnas.0611728104

Rong, W., Hillsley, K., Davis, J.B., Hicks, G., Winchester, W.J., Grundy, D., 2004. Jejunal afferent nerve sensitivity in wild-type and TRPV1 knockout mice. J. Physiol. 560, 867–881. doi:10.1113/jphysiol.2004.071746

Roos, J., DiGregorio, P.J., Yeromin, A.V., Ohlsen, K., Lioudyno, M., Zhang, S., Safrina, O., Kozak, J.A., Wagner, S.L., Cahalan, M.D., Veliçelebi, G., Stauderman, K.A., 2005. STIM1, an essential and conserved component of store-operated Ca2+ channel function. J. Cell Biol. 169, 435–445. doi:10.1083/jcb.200502019

Saliez, J., Bouzin, C., Rath, G., Ghisdal, P., Desjardins, F., Rezzani, R., Rodella, L.F., Vriens, J., Nilius, B., Feron, O., Balligand, J.-L., Dessy, C., 2008. Role of caveolar compartmentation in endothelium-derived hyperpolarizing factor-mediated relaxation: Ca2+ signals and gap junction function are regulated by caveolin in endothelial cells. Circulation 117, 1065–1074. doi:10.1161/CIRCULATIONAHA.107.731679

Samapati, R., Yang, Y., Yin, J., Stoerger, C., Arenz, C., Dietrich, A., Gudermann, T., Adam, D., Wu, S., Freichel, M., Flockerzi, V., Uhlig, S., Kuebler, W.M., 2012. Lung endothelial Ca2+ and permeability response to platelet-activating factor is mediated by acid sphingomyelinase and transient receptor potential classical 6. Am. J. Respir. Crit. Care Med. 185, 160–170. doi:10.1164/rccm.201104-0717OC

Sartori, C., Matthay, M.A., 2002. Alveolar epithelial fluid transport in acute lung injury: new insights. Eur. Respir. J. 20, 1299–1313.

Schaefer, M., 2005. Homo- and heteromeric assembly of TRP channel subunits. Pflüg. Arch. Eur. J. Physiol. 451, 35–42. doi:10.1007/s00424-005-1467-6

Scheiermann, C., Kunisaki, Y., Frenette, P.S., 2013. Circadian control of the immune system. Nat. Rev. Immunol. 13, 190–198. doi:10.1038/nri3386

Schindler, A., Sumner, C., Hoover-Fong, J.E., 1993. TRPV4-Associated Disorders, in: Pagon, R.A., Adam, M.P., Ardinger, H.H., Wallace, S.E., Amemiya, A., Bean, L.J., Bird, T.D., Fong, C.-T., Mefford, H.C., Smith, R.J., Stephens, K. (Eds.), GeneReviews(®). University of Washington, Seattle, Seattle (WA).

Schmid, E., Gu, S., Yang, W., Münzer, P., Schaller, M., Lang, F., Stournaras, C., Shumilina, E., 2013. Serum- and glucocorticoid-inducible kinase SGK1 regulates reorganization of actin cytoskeleton in mast cells upon degranulation. Am. J. Physiol. Cell Physiol. 304, C49-55. doi:10.1152/ajpcell.00179.2012

Schmidt, S., Schneider, S., Yang, W., Liu, G., Schmidt, E.-M., Schmid, E., Mia, S., Brucker, S., Stournaras, C., Wallwiener, D., Brosens, J.J., Lang, F., 2014. TGFβ1 and SGK1-sensitive store-operated Ca2+ entry and Orai1 expression in endometrial Ishikawa cells. Mol. Hum. Reprod. 20, 139–147. doi:10.1093/molehr/gat066

Schnizler, K., Shutov, L.P., Van Kanegan, M.J., Merrill, M.A., Nichols, B., McKnight, G.S., Strack, S., Hell, J.W., Usachev, Y.M., 2008. Protein kinase A anchoring via AKAP150 is essential for TRPV1 modulation by forskolin and prostaglandin E2 in mouse sensory neurons. J. Neurosci. Off. J. Soc. Neurosci. 28, 4904–4917. doi:10.1523/JNEUROSCI.0233-08.2008

Senning, E.N., Collins, M.D., Stratiievska, A., Ufret-Vincenty, C.A., Gordon, S.E., 2014. Regulation of TRPV1 ion channel by phosphoinositide (4,5)-bisphosphate: the role of membrane asymmetry. J. Biol. Chem. 289, 10999–11006. doi:10.1074/jbc.M114.553180

Sheldon, R., Moy, A., Lindsley, K., Shasby, S., Shasby, D.M., 1993. Role of myosin light-chain phosphorylation in endothelial cell retraction. Am. J. Physiol. 265, L606-612.

Shen, Q., Rigor, R.R., Pivetti, C.D., Wu, M.H., Yuan, S.Y., 2010. Myosin light chain kinase in microvascular endothelial barrier function. Cardiovasc. Res. 87, 272–280. doi:10.1093/cvr/cvq144

Shen, Q., Wu, M.H., Yuan, S.Y., 2009. Endothelial contractile cytoskeleton and microvascular permeability. Cell Health Cytoskelet. 2009, 43–50.

Shin, S.H., Lee, E.J., Chun, J., Hyun, S., Kang, S.S., 2015. Phosphorylation on TRPV4 Serine 824 Regulates Interaction with STIM1. Open Biochem. J. 9, 24–33. doi:10.2174/1874091X01509010024

Shin, S.H., Lee, E.J., Hyun, S., Chun, J., Kim, Y., Kang, S.S., 2012. Phosphorylation on the Ser 824 residue of TRPV4 prefers to bind with F-actin than with microtubules to expand the cell surface area. Cell. Signal. 24, 641–651. doi:10.1016/j.cellsig.2011.11.002

Shivanna, M., Srinivas, S.P., 2009. Microtubule stabilization opposes the (TNF-alpha)-induced loss in the barrier integrity of corneal endothelium. Exp. Eye Res. 89, 950–959. doi:10.1016/j.exer.2009.08.004

Shukla, A.K., Kim, J., Ahn, S., Xiao, K., Shenoy, S.K., Liedtke, W., Lefkowitz, R.J., 2010. Arresting a transient receptor potential (TRP) channel: beta-arrestin 1 mediates ubiquitination and functional down-regulation of TRPV4. J. Biol. Chem. 285, 30115–30125. doi:10.1074/jbc.M110.141549

Sidhaye, V.K., Güler, A.D., Schweitzer, K.S., D'Alessio, F., Caterina, M.J., King, L.S., 2006. Transient receptor potential vanilloid 4 regulates aquaporin-5 abundance under hypotonic conditions. Proc. Natl. Acad. Sci. U. S. A. 103, 4747–4752. doi:10.1073/pnas.0511211103

Simionescu, N., Simionescu, M., Palade, G.E., 1978. Open junctions in the endothelium of the postcapillary venules of the diaphragm. J. Cell Biol. 79, 27–44.

Simons, K., Ikonen, E., 1997. Functional rafts in cell membranes. Nature 387, 569–572. doi:10.1038/42408

Slutsky, A.S., 2005. Ventilator-induced lung injury: from barotrauma to biotrauma. Respir. Care 50, 646–659.

Slutsky, A.S., Ranieri, V.M., 2013. Ventilator-induced lung injury. N. Engl. J. Med. 369, 2126–2136. doi:10.1056/NEJMra1208707

Smyth, J.T., Dehaven, W.I., Jones, B.F., Mercer, J.C., Trebak, M., Vazquez, G., Putney, J.W., 2006. Emerging perspectives in store-operated Ca2+ entry: roles of Orai, Stim and TRP. Biochim. Biophys. Acta 1763, 1147–1160. doi:10.1016/j.bbamcr.2006.08.050

Snyder, P.M., 2009. Down-regulating destruction: phosphorylation regulates the E3 ubiquitin ligase Nedd4-2. Sci. Signal. 2, pe41. doi:10.1126/scisignal.279pe41

Sokabe, T., Fukumi-Tominaga, T., Yonemura, S., Mizuno, A., Tominaga, M., 2010. The TRPV4 channel contributes to intercellular junction formation in keratinocytes. J. Biol. Chem. 285, 18749–18758. doi:10.1074/jbc.M110.103606

Song, S., Yamamura, A., Yamamura, H., Ayon, R.J., Smith, K.A., Tang, H., Makino, A., Yuan, J.X.-J., 2014. Flow shear stress enhances intracellular Ca2+ signaling in pulmonary artery smooth muscle cells from patients with pulmonary arterial hypertension. Am. J. Physiol. Cell Physiol. 307, C373-383. doi:10.1152/ajpcell.00115.2014

Sonkusare, S.K., Bonev, A.D., Ledoux, J., Liedtke, W., Kotlikoff, M.I., Heppner, T.J., Hill-Eubanks, D.C., Nelson, M.T., 2012. Elementary Ca2+ signals through endothelial TRPV4 channels regulate vascular function. Science 336, 597–601. doi:10.1126/science.1216283

Sonkusare, S.K., Dalsgaard, T., Bonev, A.D., Hill-Eubanks, D.C., Kotlikoff, M.I., Scott, J.D., Santana, L.F., Nelson, M.T., 2014. AKAP150-dependent cooperative TRPV4 channel gating is central to endothelium-dependent vasodilation and is disrupted in hypertension. Sci. Signal. 7, ra66. doi:10.1126/scisignal.2005052

Sorge, R.E., Martin, L.J., Isbester, K.A., Sotocinal, S.G., Rosen, S., Tuttle, A.H., Wieskopf, J.S., Acland, E.L., Dokova, A., Kadoura, B., Leger, P., Mapplebeck, J.C.S., McPhail, M., Delaney, A., Wigerblad, G., Schumann, A.P., Quinn, T., Frasnelli, J., Svensson, C.I., Sternberg, W.F., Mogil, J.S., 2014. Olfactory exposure to males, including men, causes stress and related analgesia in rodents. Nat. Methods 11, 629–632. doi:10.1038/nmeth.2935

Sostegni, S., Diakov, A., McIntyre, P., Bunnett, N., Korbmacher, C., Haerteis, S., 2015. Sensitisation of TRPV4 by PAR2 is independent of intracellular calcium signalling and can be mediated by the biased agonist neutrophil elastase. Pflugers Arch. 467, 687–701. doi:10.1007/s00424-014-1539-6

Souza, D.G., Vieira, A.T., Soares, A.C., Pinho, V., Nicoli, J.R., Vieira, L.Q., Teixeira, M.M., 2004. The essential role of the intestinal microbiota in facilitating acute inflammatory responses. J. Immunol. Baltim. Md 1950 173, 4137–4146.

Spinsanti, G., Zannolli, R., Panti, C., Ceccarelli, I., Marsili, L., Bachiocco, V., Frati, F., Aloisi, A.M., 2008. Quantitative Real-Time PCR detection of TRPV1-4 gene expression in human leukocytes from healthy and hyposensitive subjects. Mol. Pain 4, 51. doi:10.1186/1744-8069-4-51

Stocker, M., 2004. Ca(2+)-activated K+ channels: molecular determinants and function of the SK family. Nat. Rev. Neurosci. 5, 758–770. doi:10.1038/nrn1516

Stöhr, H., Heisig, J.B., Benz, P.M., Schöberl, S., Milenkovic, V.M., Strauss, O., Aartsen, W.M., Wijnholds, J., Weber, B.H.F., Schulz, H.L., 2009. TMEM16B, a novel protein with calcium-dependent chloride channel activity, associates with a presynaptic protein complex in photoreceptor terminals. J. Neurosci. Off. J. Soc. Neurosci. 29, 6809–6818. doi:10.1523/JNEUROSCI.5546-08.2009

Strotmann, R., Harteneck, C., Nunnenmacher, K., Schultz, G., Plant, T.D., 2000. OTRPC4, a nonselective cation channel that confers sensitivity to extracellular osmolarity. Nat. Cell Biol. 2, 695–702. doi:10.1038/35036318

Strotmann, R., Schultz, G., Plant, T.D., 2003. Ca2+-dependent potentiation of the nonselective cation channel TRPV4 is mediated by a C-terminal calmodulin binding site. J. Biol. Chem. 278, 26541–26549. doi:10.1074/jbc.M302590200

Stüber, F., Wrigge, H., Schroeder, S., Wetegrove, S., Zinserling, J., Hoeft, A., Putensen, C., 2002. Kinetic and reversibility of mechanical ventilation-associated pulmonary and systemic inflammatory response in patients with acute lung injury. Intensive Care Med. 28, 834–841. doi:10.1007/s00134-002-1321-7

Su, K.-H., Lee, K.-I., Shyue, S.-K., Chen, H.-Y., Wei, J., Lee, T.-S., 2014. Implication of transient receptor potential vanilloid type 1 in 14,15-epoxyeicosatrienoic acid-induced angiogenesis. Int. J. Biol. Sci. 10, 990–996. doi:10.7150/ijbs.9832

Suresh, K., Servinsky, L., Reyes, J., Baksh, S., Undem, C., Caterina, M., Pearse, D.B., Shimoda, L.A., 2015. Hydrogen peroxide-induced calcium influx in lung microvascular endothelial cells involves TRPV4. Am. J. Physiol. Lung Cell. Mol. Physiol. 309, L1467-1477. doi:10.1152/ajplung.00275.2015

Suzuki, J., Fujii, T., Imao, T., Ishihara, K., Kuba, H., Nagata, S., 2013. Calcium-dependent phospholipid scramblase activity of TMEM16 protein family members. J. Biol. Chem. 288, 13305–13316. doi:10.1074/jbc.M113.457937

Suzuki, J., Umeda, M., Sims, P.J., Nagata, S., 2010. Calcium-dependent phospholipid scrambling by TMEM16F. Nature 468, 834–838. doi:10.1038/nature09583

Suzuki, M., Hirao, A., Mizuno, A., 2003. Microtubule-associated [corrected] protein 7 increases the membrane expression of transient receptor potential vanilloid 4 (TRPV4). J. Biol. Chem. 278, 51448–51453. doi:10.1074/jbc.M308212200

Tabuchi, K., Suzuki, M., Mizuno, A., Hara, A., 2005. Hearing impairment in TRPV4 knockout mice. Neurosci. Lett. 382, 304–308. doi:10.1016/j.neulet.2005.03.035

Takahashi, N., Hamada-Nakahara, S., Itoh, Y., Takemura, K., Shimada, A., Ueda, Y., Kitamata, M., Matsuoka, R., Hanawa-Suetsugu, K., Senju, Y., Mori, M.X., Kiyonaka, S., Kohda, D., Kitao, A., Mori, Y., Suetsugu, S., 2014. TRPV4 channel activity is modulated by direct interaction of the ankyrin domain to $PI(4,5)P_2$. Nat. Commun. 5, 4994. doi:10.1038/ncomms5994

Terragni, P., Ranieri, V.M., Brazzi, L., 2015. Novel approaches to minimize ventilator-induced lung injury. Curr. Opin. Crit. Care 21, 20–25. doi:10.1097/MCC.0000000000000172

The Acute Respiratory Distress Syndrome Network, 2000. Ventilation with lower tidal volumes as compared with traditional tidal volumes for acute lung injury and the acute respiratory distress syndrome. N. Engl. J. Med. 342, 1301–1308. doi:10.1056/NEJM200005043421801

Thodeti, C.K., Matthews, B., Ravi, A., Mammoto, A., Ghosh, K., Bracha, A.L., Ingber, D.E., 2009. TRPV4 channels mediate cyclic strain-induced endothelial cell reorientation through integrin-to-integrin signaling. Circ. Res. 104, 1123–1130. doi:10.1161/CIRCRESAHA.108.192930

Thomas, S.V., Kathpalia, P.P., Rajagopal, M., Charlton, C., Zhang, J., Eaton, D.C., Helms, M.N., Pao, A.C., 2011. Epithelial sodium channel regulation by cell surface-associated serum- and glucocorticoid-regulated kinase 1. J. Biol. Chem. 286, 32074–32085. doi:10.1074/jbc.M111.278283

Thorneloe, K.S., Cheung, M., Bao, W., Alsaid, H., Lenhard, S., Jian, M.-Y., Costell, M., Maniscalco-Hauk, K., Krawiec, J.A., Olzinski, A., Gordon, E., Lozinskaya, I., Elefante, L., Qin, P., Matasic, D.S., James, C., Tunstead, J., Donovan, B., Kallal, L., Waszkiewicz, A., Vaidya, K., Davenport, E.A., Larkin, J., Burgert, M., Casillas, L.N., Marquis, R.W., Ye, G., Eidam, H.S., Goodman, K.B., Toomey, J.R., Roethke, T.J., Jucker, B.M., Schnackenberg, C.G., Townsley, M.I., Lepore, J.J., Willette, R.N., 2012. An orally active TRPV4 channel blocker prevents and resolves pulmonary edema induced by heart failure. Sci. Transl. Med. 4, 159ra148. doi:10.1126/scitranslmed.3004276

Thorneloe, K.S., Sulpizio, A.C., Lin, Z., Figueroa, D.J., Clouse, A.K., McCafferty, G.P., Chendrimada, T.P., Lashinger, E.S.R., Gordon, E., Evans, L., Misajet, B.A., Demarini, D.J., Nation, J.H., Casillas, L.N., Marquis, R.W., Votta, B.J., Sheardown, S.A., Xu, X., Brooks, D.P., Laping, N.J., Westfall, T.D., 2008. N-((1S)-1-{[4-((2S)-2-{[(2,4-dichlorophenyl)sulfonyl]amino}-3-hydroxypropanoyl)-1-piperazinyl]carbonyl}-3-methylbutyl)-1-benzothiophene-2-carboxamide (GSK1016790A), a novel and potent transient receptor potential vanilloid 4 channel agonist induces urinary bladder contraction and hyperactivity: Part I. J. Pharmacol. Exp. Ther. 326, 432–442. doi:10.1124/jpet.108.139295

Tian, Y., Ullrich, F., Xu, R., Heinemann, S.H., Hou, S., Hoshi, T., 2015. Two distinct effects of PIP2 underlie auxiliary subunit-dependent modulation of Slo1 BK channels. J. Gen. Physiol. 145, 331–343. doi:10.1085/jgp.201511363

Toldi, G., Stenczer, B., Treszl, A., Kollár, S., Molvarec, A., Tulassay, T., Rigó, J., Vásárhelyi, B., 2011. Lymphocyte calcium influx characteristics and their modulation by Kv1.3 and IKCa1 channel inhibitors in healthy pregnancy and preeclampsia. Am. J. Reprod. Immunol. N. Y. N 1989 65, 154–163. doi:10.1111/j.1600-0897.2010.00899.x

Towbin, H., Staehelin, T., Gordon, J., 1979. Electrophoretic transfer of proteins from polyacrylamide gels to nitrocellulose sheets: procedure and some applications. Proc. Natl. Acad. Sci. U. S. A. 76, 4350–4354.

Tremblay, L., Valenza, F., Ribeiro, S.P., Li, J., Slutsky, A.S., 1997. Injurious ventilatory strategies increase cytokines and c-fos m-RNA expression in an isolated rat lung model. J. Clin. Invest. 99, 944–952. doi:10.1172/JCI119259

Tschumperlin, D.J., Oswari, J., Margulies, A.S.S., 2000. Deformation-Induced Injury of Alveolar Epithelial Cells. Am. J. Respir. Crit. Care Med. 162, 357–362. doi:10.1164/ajrccm.162.2.9807003

Tsuno, N., Yukimasa, A., Yoshida, O., Ichihashi, Y., Inoue, T., Ueno, T., Yamaguchi, H., Matsuda, H., Funaki, S., Yamanada, N., Tanimura, M., Nagamatsu, D., Nishimura, Y., Ito, T., Soga, M., Horita, N., Yamamoto, M., Hinata, M., Imai, M., Morioka, Y., Kanemasa, T., Sakaguchi, G., Iso, Y., 2016. Discovery of novel 2',4'-dimethyl-[4,5'-bithiazol]-2-yl amino derivatives as orally bioavailable TRPV4 antagonists for the treatment of pain: Part 1. Bioorg. Med. Chem. Lett. 26, 4930–4935. doi:10.1016/j.bmcl.2016.09.013

Tual-Chalot, S., Guibert, C., Muller, B., Savineau, J.-P., Andriantsitohaina, R., Martinez, M.C., 2010. Circulating microparticles from pulmonary hypertensive rats induce endothelial dysfunction. Am. J. Respir. Crit. Care Med. 182, 261–268. doi:10.1164/rccm.200909-1347OC

Turner, H., Fleig, A., Stokes, A., Kinet, J.-P., Penner, R., 2003. Discrimination of intracellular calcium store subcompartments using TRPV1 (transient receptor potential channel, vanilloid subfamily member 1) release channel activity. Biochem. J. 371, 341–350. doi:10.1042/BJ20021381

Ufret-Vincenty, C.A., Klein, R.M., Hua, L., Angueyra, J., Gordon, S.E., 2011. Localization of the PIP2 sensor of TRPV1 ion channels. J. Biol. Chem. 286, 9688–9698. doi:10.1074/jbc.M110.192526

Uhlig, S., Yang, Y., Waade, J., Wittenberg, C., Babendreyer, A., Kuebler, W.M., 2014. Differential regulation of lung endothelial permeability in vitro and in situ. Cell. Physiol. Biochem. Int. J. Exp. Cell. Physiol. Biochem. Pharmacol. 34, 1–19. doi:10.1159/000362980

van de Graaf, S.F.J., Hoenderop, J.G.J., van der Kemp, A.W.C.M., Gisler, S.M., Bindels, R.J.M., 2006. Interaction of the epithelial Ca2+ channels TRPV5 and TRPV6 with the intestine- and kidney-enriched PDZ protein NHERF4. Pflüg. Arch. Eur. J. Physiol. 452, 407–417. doi:10.1007/s00424-006-0051-z

Veldhuis, N.A., Lew, M.J., Abogadie, F.C., Poole, D.P., Jennings, E.A., Ivanusic, J.J., Eilers, H., Bunnett, N.W., McIntyre, P., 2012. N-glycosylation determines ionic permeability and desensitization of the TRPV1 capsaicin receptor. J. Biol. Chem. 287, 21765–21772. doi:10.1074/jbc.M112.342022

Vergara, C., Latorre, R., Marrion, N.V., Adelman, J.P., 1998. Calcium-activated potassium channels. Curr. Opin. Neurobiol. 8, 321–329. doi:10.1016/S0959-4388(98)80056-1

Verkman, A.S., Matthay, M.A., Song, Y., 2000. Aquaporin water channels and lung physiology. Am. J. Physiol. Lung Cell. Mol. Physiol. 278, L867-879.

Vion, A.-C., Ramkhelawon, B., Loyer, X., Chironi, G., Devue, C., Loirand, G., Tedgui, A., Lehoux, S., Boulanger, C.M., 2013. Shear stress regulates endothelial microparticle release. Circ. Res. 112, 1323–1333. doi:10.1161/CIRCRESAHA.112.300818

Volpin, G., Cohen, M., Assaf, M., Meir, T., Katz, R., Pollack, S., 2014. Cytokine levels (IL-4, IL-6, IL-8 and TGFβ) as potential biomarkers of systemic inflammatory response in trauma patients. Int. Orthop. 38, 1303–1309. doi:10.1007/s00264-013-2261-2

Vriens, J., Owsianik, G., Fisslthaler, B., Suzuki, M., Janssens, A., Voets, T., Morisseau, C., Hammock, B.D., Fleming, I., Busse, R., Nilius, B., 2005. Modulation of the Ca2 permeable cation channel TRPV4 by cytochrome P450 epoxygenases in vascular endothelium. Circ. Res. 97, 908–915. doi:10.1161/01.RES.0000187474.47805.30

Vriens, J., Watanabe, H., Janssens, A., Droogmans, G., Voets, T., Nilius, B., 2004. Cell swelling, heat, and chemical agonists use distinct pathways for the activation of the cation channel TRPV4. Proc. Natl. Acad. Sci. U. S. A. 101, 396–401. doi:10.1073/pnas.0303329101

Wagner, C.A., Ott, M., Klingel, K., Beck, S., Melzig, J., Friedrich, B., Wild, K.N., Bröer, S., Moschen, I., Albers, A., Waldegger, S., Tümmler, B., Egan, M.E., Geibel, J.P., Kandolf, R., Lang, F., 2001. Effects of the serine/threonine kinase SGK1 on the epithelial Na(+) channel (ENaC) and CFTR: implications for cystic fibrosis. Cell. Physiol. Biochem. Int. J. Exp. Cell. Physiol. Biochem. Pharmacol. 11, 209–218. doi:51935

Wang, L., Yin, J., Nickles, H.T., Ranke, H., Tabuchi, A., Hoffmann, J., Tabeling, C., Barbosa-Sicard, E., Chanson, M., Kwak, B.R., Shin, H.-S., Wu, S., Isakson, B.E., Witzenrath, M., de Wit, C., Fleming, I., Kuppe, H., Kuebler, W.M., 2012. Hypoxic pulmonary vasoconstriction requires connexin 40-mediated endothelial signal conduction. J. Clin. Invest. 122, 4218–4230. doi:10.1172/JCI59176

Wang, S., Meng, F., Mohan, S., Champaneri, B., Gu, Y., 2009. Functional ENaC channels expressed in endothelial cells: a new candidate for mediating shear force. Microcirc. N. Y. N 1994 16, 276–287. doi:10.1080/10739680802653150

Wang, Y., Fu, X., Gaiser, S., Köttgen, M., Kramer-Zucker, A., Walz, G., Wegierski, T., 2007. OS-9 Regulates the Transit and Polyubiquitination of TRPV4 in the Endoplasmic Reticulum. J. Biol. Chem. 282, 36561–36570. doi:10.1074/jbc.M703903200

Wärntges, S., Friedrich, B., Henke, G., Duranton, C., Lang, P.A., Waldegger, S., Meyermann, R., Kuhl, D., Speckmann, E.J., Obermüller, N., Witzgall, R., Mack, A.F., Wagner, H.J., Wagner, A., Bröer, S., Lang, F., 2002. Cerebral localization and regulation of the cell volume-sensitive serum- and glucocorticoid-dependent kinase SGK1. Pflüg. Arch. Eur. J. Physiol. 443, 617–624. doi:10.1007/s00424-001-0737-1

Watanabe, H., Murakami, M., Ohba, T., Takahashi, Y., Ito, H., 2008. TRP channel and cardiovascular disease. Pharmacol. Ther. 118, 337–351. doi:10.1016/j.pharmthera.2008.03.008

Watanabe, H., Vriens, J., Prenen, J., Droogmans, G., Voets, T., Nilius, B., 2003. Anandamide and arachidonic acid use epoxyeicosatrienoic acids to activate TRPV4 channels. Nature 424, 434–438. doi:10.1038/nature01807

Webster, M.K., Goya, L., Ge, Y., Maiyar, A.C., Firestone, G.L., 1993. Characterization of sgk, a novel member of the serine/threonine protein kinase gene family which is transcriptionally induced by glucocorticoids and serum. Mol. Cell. Biol. 13, 2031–2040.

Wegierski, T., Hill, K., Schaefer, M., Walz, G., 2006. The HECT ubiquitin ligase AIP4 regulates the cell surface expression of select TRP channels. EMBO J. 25, 5659–5669. doi:10.1038/sj.emboj.7601429

Wen, H., Östman, J., Bubb, K.J., Panayiotou, C., Priestley, J.V., Baker, M.D., Ahluwalia, A., 2012. 20-Hydroxyeicosatetraenoic acid (20-HETE) is a novel activator of transient receptor potential vanilloid 1 (TRPV1) channel. J. Biol. Chem. 287, 13868–13876. doi:10.1074/jbc.M111.334896

Wiemuth, D., Lott, J.S., Ly, K., Ke, Y., Teesdale-Spittle, P., Snyder, P.M., McDonald, F.J., 2010. Interaction of serum- and glucocorticoid regulated kinase 1 (SGK1) with the WW-domains of Nedd4-2 is required for epithelial sodium channel regulation. PloS One 5, e12163. doi:10.1371/journal.pone.0012163

Williams, R.T., Manji, S.S., Parker, N.J., Hancock, M.S., Van Stekelenburg, L., Eid, J.P., Senior, P.V., Kazenwadel, J.S., Shandala, T., Saint, R., Smith, P.J., Dziadek, M.A., 2001. Identification and characterization of the STIM (stromal interaction molecule) gene family: coding for a novel class of transmembrane proteins. Biochem. J. 357, 673–685.

Wilson, M.R., Patel, B.V., Takata, M., 2012. Ventilation with "clinically relevant" high tidal volumes does not promote stretch-induced injury in the lungs of healthy mice. Crit. Care Med. 40, 2850–2857. doi:10.1097/CCM.0b013e31825b91ef

Wisnoskey, B.J., Sinkins, W.G., Schilling, W.P., 2003. Activation of vanilloid receptor type I in the endoplasmic reticulum fails to activate store-operated Ca2+ entry. Biochem. J. 372, 517–528. doi:10.1042/BJ20021574

Wong, R., Schlichter, L.C., 2014. PKA reduces the rat and human KCa3.1 current, CaM binding, and Ca2+ signaling, which requires Ser332/334 in the CaM-binding C terminus. J. Neurosci. Off. J. Soc. Neurosci. 34, 13371–13383. doi:10.1523/JNEUROSCI.1008-14.2014

Wu, L., Gao, X., Brown, R.C., Heller, S., O'Neil, R.G., 2007. Dual role of the TRPV4 channel as a sensor of flow and osmolality in renal epithelial cells. Am. J. Physiol. Renal Physiol. 293, F1699-1713. doi:10.1152/ajprenal.00462.2006

Wu, M.H., 2005. Endothelial focal adhesions and barrier function. J. Physiol. 569, 359–366. doi:10.1113/jphysiol.2005.096537

Wu, S., Jian, M.-Y., Xu, Y.-C., Zhou, C., Al-Mehdi, A.-B., Liedtke, W., Shin, H.-S., Townsley, M.I., 2009. Ca2+ entry via alpha1G and TRPV4 channels differentially regulates surface expression of P-selectin and barrier integrity in pulmonary capillary endothelium. Am. J. Physiol. Lung Cell. Mol. Physiol. 297, L650-657. doi:10.1152/ajplung.00015.2009

Xia, X.M., Fakler, B., Rivard, A., Wayman, G., Johnson-Pais, T., Keen, J.E., Ishii, T., Hirschberg, B., Bond, C.T., Lutsenko, S., Maylie, J., Adelman, J.P., 1998. Mechanism of calcium gating in small-conductance calcium-activated potassium channels. Nature 395, 503–507. doi:10.1038/26758

Yaron, J.R., Gangaraju, S., Rao, M.Y., Kong, X., Zhang, L., Su, F., Tian, Y., Glenn, H.L., Meldrum, D.R., 2015. K+ regulates Ca2+ to drive inflammasome signaling: dynamic visualization of ion flux in live cells. Cell Death Dis. 6, e1954. doi:10.1038/cddis.2015.277

Yin, J., Hoffmann, J., Kaestle, S.M., Neye, N., Wang, L., Baeurle, J., Liedtke, W., Wu, S., Kuppe, H., Pries, A.R., Kuebler, W.M., 2008. Negative-feedback loop attenuates hydrostatic lung edema via a cGMP-dependent regulation of transient receptor potential vanilloid 4. Circ. Res. 102, 966–974. doi:10.1161/CIRCRESAHA.107.168724

Yin, J., Kuebler, W.M., 2010. Mechanotransduction by TRP channels: general concepts and specific role in the vasculature. Cell Biochem. Biophys. 56, 1–18. doi:10.1007/s12013-009-9067-2

Yin, J., Michalick, L., Tang, C., Tabuchi, A., Goldenberg, N., Dan, Q., Awwad, K., Wang, L., Erfinanda, L., Nouailles, G., Witzenrath, M., Vogelzang, A., Lv, L., Lee, W.L., Zhang, H., Rotstein, O., Kapus, A., Szaszi, K., Fleming, I., Liedtke, W.B., Kuppe, H., Kuebler, W.M., 2016. Role of Transient Receptor Potential Vanilloid 4 in Neutrophil Activation and Acute Lung Injury. Am. J. Respir. Cell Mol. Biol. 54, 370–383. doi:10.1165/rcmb.2014-0225OC

Yin, J., Michalick, L., Tang, C., Tabuchi, A., Goldenberg, N., Dan, Q., Awwad, K., Wang, L., Erfinanda, L., Nouailles-Kursar, G., Witzenrath, M., Vogelzang, A., Lv, L., Lee, W.L., Zhang, H., Rotstein, O., Kapus, A., Szaszi, K., Fleming, I., Liedtke, W.B., Kuppe, H., Kuebler, W.M., 2015. Role of Transient Receptor Potential Vanilloid 4 in Neutrophil Activation and Acute Lung Injury. Am. J. Respir. Cell Mol. Biol. doi:10.1165/rcmb.2014-0225OC

Yoshida, T., Inoue, R., Morii, T., Takahashi, N., Yamamoto, S., Hara, Y., Tominaga, M., Shimizu, S., Sato, Y., Mori, Y., 2006. Nitric oxide activates TRP channels by cysteine S-nitrosylation. Nat. Chem. Biol. 2, 596–607. doi:10.1038/nchembio821

Yuan, S.Y., Rigor, R.R., 2010. Regulation of Endothelial Barrier Function, Integrated Systems Physiology: From Molecule to Function to Disease. Morgan & Claypool Life Sciences, San Rafael (CA).

Yue, P., Lin, D.-H., Pan, C.-Y., Leng, Q., Giebisch, G., Lifton, R.P., Wang, W.-H., 2009. Src family protein tyrosine kinase (PTK) modulates the effect of SGK1 and WNK4 on ROMK channels. Proc. Natl. Acad. Sci. U. S. A. 106, 15061–15066. doi:10.1073/pnas.0907855106

Yue, P., Zhang, C., Lin, D.-H., Sun, P., Wang, W.-H., 2013. WNK4 inhibits Ca(2+)-activated big-conductance potassium channels (BK) via mitogen-activated protein kinase-dependent pathway. Biochim. Biophys. Acta 1833, 2101–2110. doi:10.1016/j.bbamcr.2013.05.004

Zhang, F., Liu, S., Yang, F., Zheng, J., Wang, K., 2011. Identification of a tetrameric assembly domain in the C terminus of heat-activated TRPV1 channels. J. Biol. Chem. 286, 15308–15316. doi:10.1074/jbc.M111.223941

Zhang, X., Huang, J., McNaughton, P.A., 2005. NGF rapidly increases membrane expression of TRPV1 heat-gated ion channels. EMBO J. 24, 4211–4223. doi:10.1038/sj.emboj.7600893

Zhao, P., Lieu, T., Barlow, N., Sostegni, S., Haerteis, S., Korbmacher, C., Liedtke, W., Jimenez-Vargas, N.N., Vanner, S.J., Bunnett, N.W., 2015. Neutrophil Elastase Activates Protease-activated Receptor-2 (PAR2) and Transient Receptor Potential Vanilloid 4 (TRPV4) to Cause Inflammation and Pain. J. Biol. Chem. 290, 13875–13887. doi:10.1074/jbc.M115.642736

Zhao, R., Tsang, S.Y., 2016. Versatile Roles of Intracellularly Located TRPV1 Channel. J. Cell. Physiol. doi:10.1002/jcp.25704

Zheng, J., 2013. Molecular mechanism of TRP channels. Compr. Physiol. 3, 221–242. doi:10.1002/cphy.c120001

Zhou, Y., Srinivasan, P., Razavi, S., Seymour, S., Meraner, P., Gudlur, A., Stathopulos, P.B., Ikura, M., Rao, A., Hogan, P.G., 2013. Initial activation of STIM1, the regulator of store-operated calcium entry. Nat. Struct. Mol. Biol. 20, 973–981. doi:10.1038/nsmb.2625

STATEMENT OF CONTRIBUTION

My colleague Lasti Erfinanda performed measurements of myeloperoxidase activity. Geraldine Nouailles-Kursar (Department of Infectious Diseases and Pulmonary Medicine, Charité - Universitätsmedizin Berlin, Germany) provided strong support in experimental design and assistance in the generation of bone marrow chimeric mice. My colleague Mazharul Maishan (Keenan Research Centre for Biomedical Science, St. Michael's Hospital, Toronto, Canada) performed the FACS analyses for enumeration of microparticles. Manuela Schläfereit and Ramona Warnke provided extensive technical assistance with animal breeding and caring. Stefan Heller (Department of Otolaryngology, Head and Neck Surgery and Molecular & Cellular Physiology, Stanford University School of Medicine, Stanford, USA) kindly provided the antibody against TRPV4. The Advanced Medical Bioimaging Core Facility (AMBIO) of Charité provided the support in aquisition of the imaging data.

CURRICULUM VITAE

PUBLICATIONS

Publications from the work presented in this thesis.

Original peer-reviewed publications

Michalick, L., Erfinanda, L., Weichelt, U., van der Giet, M., Liedtke, W., and Kuebler, W.M. (2017). Transient Receptor Potential Vanilloid 4 and Serum Glucocorticoid-regulated Kinase 1 Are Critical Mediators of Lung Injury in Overventilated Mice *In Vivo*. Anesthesiology.

Yin J., Michalick L.*, Tang C., Tabuchi A., Goldenberg N., Dan Q., Awwad K., Wang L., Erfinanda L., Nouailles-Kursar G., Witzenrath M., Vogelzang A., Lv L., Lee W.L., Zhang H., Rotstein O., Kapus A., Szaszi K., Fleming I., Liedtke W., Kuppe H., Kuebler W.M. (2016). Role of Transient Receptor Potential Vanilloid 4 in Neutrophil Activation and Acute Lung Injury. Am. J. Respir. Cell Mol. Biol.

Chen, L., Kaßmann, M., Sendeski, M., Tsvetkov, D., Marko, L., Michalick, L., Riehle, M., Liedtke, W.B., Kuebler, W.M., Harteneck, C., et al. (2015). Functional transient receptor potential vanilloid 1 and transient receptor potential vanilloid 4 channels along different segments of the renal vasculature. Acta Physiol. Oxf. Engl. 213, 481–491.

* shared first authorship

Abstracts

Michalick, L., Mertens, M., Liedtke, W., and Kuebler, W.M. (2013). Transient receptor potential cation channel vanilloid (TRPV) 4 in ventilator-induced lung injury (VILI). FASEB J. 27, 914.12.

Michalick, L., Giet, M. van der, Liedtke, W., and Kuebler, W. (2014). Ca^{2+} entry via transient receptor potential vanilloid channel 4 mediates ventilation-induced lung vascular barrier failure. FASEB J. 28, 1176.3.

Michalick, L., Giet, M. van der, Liedtke, W., and Kuebler, W. (2015). Serum/ glucocorticoid-regulated kinase (SGK) 1 and transient receptor potential vanilloid channel (TRPV) 4 mediate ventilation-induced endothelial Ca^{2+} influx and barrier failure. FASEB J. 29, 863.8.

Conference presentations

Experimental biology 2013, Boston, USA

Poster: Michalick, L., Mertens, M., Liedtke, W., and Kuebler, W.M.: Transient receptor potential cation channel vanilloid (TRPV) 4 in ventilator-induced lung injury (VILI).

35th Annual Meeting of the German Society for Microcirulation and Vascular Biology (GfMVB) 2013, Dresden, Germany

Poster: Michalick, L., Liedtke, W., and Kuebler, W.M.: Transient receptor potential cation channel vanilloid (TRPV) mediates lung vascular barrier failure in response to mechanical stretch.

Experimental biology 2014, San Diego, USA

Poster and oral presentation at trainee highlights breakfast: Michalick, L., Giet, M. van der, Liedtke, W., and Kuebler, W.M.: Ca^{2+} entry via transient receptor potential vanilloid channel 4 mediates ventilation-induced lung vascular barrier failure.

Experimental biology 2015, Boston, USA

Poster: Michalick, L., Giet, M. van der, Liedtke, W., and Kuebler, W.M.: Serum/ glucocorticoid-regulated kinase (SGK) 1 and transient receptor potential vanilloid channel (TRPV) 4 mediate ventilation-induced endothelial Ca^{2+} influx and barrier failure.

Awards

Travel grant (2014) of the "GlaxoSmithKline-Stiftung", Germany

Research visits

01/2012 – 02/2012	Lab of Prof. Dr. Wolfgang M. Kuebler, Keenan Research Centre for Biomedical Science, St. Michael's Hospital, Toronto, Ontario, Canada
09/2014 – 09/2014	Munich International Autumn School for Respiratory Medicine (MIAS) 2014, organized by Comprehensive Pneumology Center, HelmholtzZentrum München, LMU, and Asklepios (committee members: Dr. Dr. Melanie Königshoff, Prof. Dr. Oliver Eickelberg, Prof. Dr. Jürgen Behr)
09/2015 – 11/2015	Lab of Prof. Dr. Wolfgang M. Kuebler, Keenan Research Centre for Biomedical Science, St. Michael's Hospital, Toronto, Ontario, Canada

EIDESSTATTLICHE VERSICHERUNG

Hiermit versichere ich, Laura Michalick, dass ich diese Doktorarbeit mit dem Titel „TRPV4 IN VENTILATOR-INDUCED LUNG INJURY - MECHANISMS OF ENDOTHELIAL MECHANOTRANSDUCTION AND BARRIER REGULATION IN THE LUNG“ selbständig und ohne fremde Hilfe verfasst und keine anderen als die angegebenen Hilfsmittel benutzt habe. Alle Ausführungen, die dem Wortlaut oder dem Sinne nach anderen Werken entnommen wurden, sind unter Angabe der Quellen kenntlich gemacht. Der experimentelle Teil dieser Arbeit wurde angefertigt unter der Betreuung durch Prof. Dr. Wolfgang M. Kübler von März 2011 bis Dezember 2016 am Institut für Physiologie der Charité – Universitätsmedizin Berlin, Deutschland.

Diese Arbeit wurde bisher weder im Inland noch im Ausland in gleicher oder abgewandelter Fassung einer Hochschule zur Erlangung eines akademischen Grades vorgelegt.

Laura Michalick

Berlin, den 20.12.2016

ACKNOWLEDGEMENTS

First and foremost, I would like to express my sincere thanks to my supervisor Prof. Dr. Wolfgang Kübler for his constant and patient guidance during my PhD thesis. Thank you for encouraging my research, sharing your knowledge, supporting me in successful and difficult phases during the last years and helping me to focus on the essentials and the final goal.

I extent my thanks to Prof. Dr. Petra Knaus for reviewing my PhD thesis and the organization of the PhD symposium, which was great and helpful platform for constructive discussions.

Furthermore, I thank all my collaborators Prof. Dr. Marcus van der Giet and Dr. Mirjam Schuchardt, Prof. Dr. Maik Gollasch and Dr. Lajos Markó, Prof. Dr. Witzenrath and Dr. Geraldine Nouailles-Kursar, Prof. Dr. Wolfgang Liedtke for providing the *Trpv4*$^{-/-}$ mice and Prof. Dr. Stefan Heller for the TRPV4 antibody.

I would like to thank Hannah Nickles and Julia Hoffmann for the initial guidance at the beginning of my project.

Many thanks also to all current and former members of the Institute of Physiology at the Charité for helping me in with any scientific and administrative problems and questions.

A special thanks goes to my wonderful colleagues Franziska Kohse, Lasti Erfinanda, Rudi Samapati, Sarah Weidenfeld, Arata Tabuchi, Adrienn Krauszman, Mazharul Maishan and Diana Zabini for all the help, patience and the positive and enjoyable working atmosphere during and outside working times.

I would like to thank my family for all the love, care and trust in all I did. Especially my grandparents for the little microscope as the most-promising gift to my 9. or 10. birthday.

Thanks to my beloved friends: Alex, Alex, Anja, Aron, Aurore, Ben, Bettie, Christoph, Dominik, Eva, Fiene, Franzi, Fränzn, Freya, Gerald, Josy, Jule, Lena, Marlen, Nici, Sophia, Sophie and Sophie for listening to my all problems, sometimes even without understanding them at all.

And Steffen for all his love, the outstanding support and the infinite patience during the last years.